

TRANSIENT EFFECTS IN AN ENCLOSED WATER BODY DUE TO THERMAL DISCHARGE

By

SHRAVAN KUMAR GUPTA

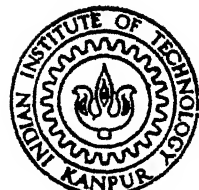
ME TH ME/1979/D

1979 G 9597

D

GUP

TRA



DEPARTMENT OF MECHANICAL ENGINEERING

INDIAN INSTITUTE OF TECHNOLOGY KANPUR

JUNE, 1979

TRANSIENT EFFECTS IN AN ENCLOSED WATER BODY DUE TO THERMAL DISCHARGE

A Thesis Submitted
in Partial Fulfilment of the Requirements
for the Degree of
DOCTOR OF PHILOSOPHY

By
SHRAVAN KUMAR GUPTA

to the

DEPARTMENT OF MECHANICAL ENGINEERING
INDIAN INSTITUTE OF TECHNOLOGY KANPUR
JUNE, 1979

111-60073
111-60458
111-62232

33 NOV 1980

ME-1978-D-GUP-TRA

To

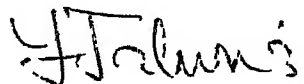
The Cherished Memory

of

My Wife

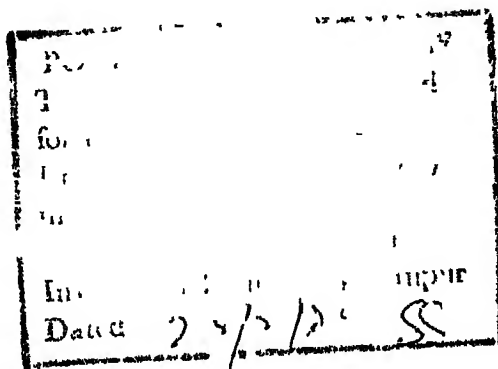
CERTIFICATE

This is to certify that this thesis entitled "Transient Effects in an Enclosed Water Body Due to Thermal Discharge", by Shri S.K. Gupta is a record of work carried out under my supervision and has not been submitted elsewhere for a degree.



(Yogesh Jaluria)
Assistant Professor
Department of Mech. Engg.
I.I.T. Kanpur

June 1979



ACKNOWLEDGEMENT

I wish to express my deep sense of gratitude and appreciation to my supervisor Prof. Y. Jaluria for his valuable and constructive guidance throughout the present work. His generous attitude has been a constant source of inspiration to me.

I am grateful to Prof. B.L. Dhoopar, Head, Department of Mechanical Engineering, I.I.T. Kanpur for his encouragement during the work.

I am thankful to Dr. S.D. Shukla, Director, and Prof. N.L. Kachhara, Head Department of Mechanical Engineering, of H.B.T.I., Kanpur, for their encouragement to carry out this research work.

I deeply appreciate the discussions and helpful comments of my friends, particularly Shri S.K. Joneja and Shri R.C. Sehgal. The facilities extended by Shri Manohar Prasad and Shri K.K. Saxena are appreciated.

I sincerely appreciate the help rendered by Shri P.N. Misra and Shri A.K. Bajpal in the fabrication of equipment and also during the experimental work.

I am thankful to Shri B.B. Srivastava and Shri B.L. Arora for preparing illustrations for the thesis. I would also like to express my appreciation for the careful typing of the manuscript by Shri J.D. Varma.

The help rendered by the staff of the Computer Centre is highly appreciated and acknowledged.

Last but not the least I am indebted to my neglected parents and children, Akash and Seema, for not expecting too much from me during my research and for keeping a cheerful environment around me.

S.K. Gupta

CONTENTS

	PAGE
LIST OF FIGURES	vii
NOMENCLATURE	xii
SYNOPSIS	xlv
CHAPTER 1 : INTRODUCTION	1
1.1 Water Body	1
1.2 Literature Survey	2
1.3 Present Work	5
CHAPTER 2 : EXPERIMENTAL STUDY	7
2.1 Experimental Arrangement	7
2.2 Experimental Results	10
2.3 Concluding Remarks	15
CHAPTER 3 : ANALYTICAL MODELS	17
3.1 Introduction	17
3.2 Isothermal Models	18
3.2.1 Constant Inflow Temperature	19
3.2.2 Constant Temperature Difference	20
3.2.3 Natural Cooling	21
3.2.4 Results of Isothermal Models	22
3.3 One Dimensional Models	23
3.3.1 Methods of Solutions and Results	26
3.3.2 Isothermal Upper Region	27
3.3.3 Discussions of Results	28

	vi
	PAGE
3.4 Recirculation in Enclosures	29
3.4.1 Governing Equations	30
3.4.2 Results and Discussions	31
3.5 The Nonlinear Problems	32
3.5.1 Governing Equations for a Two Dimensional Model	33
3.5.2 Boundary Conditions	36
3.5.3 Method of Solution and Results	36
CHAPTER 4 : SUMMARY AND CONCLUSIONS	40
4.1 Summary	40
4.2 Conclusions	41
4.3 Future Work	43
REFERENCES	45
FIGURES	49

LIST OF FIGURES

FIG. NO.	PAGE	
2.1	Photographs of the main equipment	49
2.2	Details of the tank, lid and probe	50
2.3	Schematic diagram of the experimental set-up	51
2.4	Temperature versus time in an enclosed water body with inflow located at bottom of one side and the outflow on the top of the opposite side	52
2.5	Temperature versus cooling time for an isothermal enclosed water body	53
2.6	Log T versus time for an enclosed water body	54
2.7	Outlet temperature versus time, with the intake at the centre of one side and outfall at the top of the opposite side ($Re = 5,000$; $Q_i = 1.34 \times 10^{-5} m^3/sec$ and $V = 0.1548 m^3$)	55
2.8	Transient Non-dimensional temperature profiles in an enclosed water body. The arrows indicate the directions of inflow and outflow.	56
2.9	Temperature profiles, when a stratified enclosed water body is allowed to cool in the absence of flow	57
2.10	Outfall temperature versus time when intake and outfall are located at the top of the water body on opposite sides ($Re = 4656.25$; $Q_i = 1.24 \times 10^{-5} m^3/sec$ and $V = 0.1548 m^3$)	58
2.11	Temperature profiles in an enclosed water body, with inflow and outflow located at the top on opposite sides ($Re = 4656.25$; $Q_i = 1.24 \times 10^{-5} m^3/sec$ and $V = 0.1548 m^3$)	59

FIG. NO	PAGE	
2.12	Outflow temperature versus time for various inflow locations on one side and outflow located at the top on the opposite side. ($Re = 1656.25$ and $V = 0.1548 \text{ m}^3$)	60
2.13	Outflow temperature versus time with inflow located at the centre and the outflow at the top on the same side ($Re = 2500$; $Q_i = 0.675 \times 10^{-5} \text{ m}^3/\text{sec}$ and $V = 0.1548 \text{ m}^3$)	61
2.14	Transient behaviour of the temperature profiles with the inflow and outflow located as shown ($Re = 2500$; $Q_i = 0.675 \times 10^{-5} \text{ m}^3/\text{sec}$ and $V = 0.1548 \text{ m}^3$)	62
2.15	Temperature decay of the stratified enclosed water body in absence of the flow.	63
2.16	Outflow temperature versus time with inflow and outflow located on the same side of an enclosed water body ($Re = 2,500$; $Q_i = 0.675 \times 10^{-5} \text{ m}^3/\text{sec}$ and $V = 0.1548 \text{ m}^3$)	64
2.17	Temperature profiles in an enclosed water body. The arrows indicate the direction of inflow and outflow ($Re = 2,500$; $Q_i = 0.675 \times 10^{-5} \text{ m}^3/\text{sec}$ and $V = 0.1548 \text{ m}^3$)	65
2.18	Outflow temperature versus time, with the inflow and outflow located as shown ($Re = 2,500$; $Q_i = 0.675 \times 10^{-5} \text{ m}^3/\text{sec}$ and $V = 0.1548 \text{ m}^3$)	66
2.19	Transient behaviour of the temperature profiles with inflow and outflow located at the top and at the bottom respectively, on the same side of an enclosed water body ($Re = 2,500$; $Q_i = 0.675 \times 10^{-5} \text{ m}^3/\text{sec}$ and $V = 0.1548 \text{ m}^3$)	67

FIG NO.	PAGE
2.20 Transient behaviour of the outflow temperature with inflow and outflow configuration as shown ($Re = 2,500$; $Q_i = 0.675 \times 10^{-5} m^3/sec$ and $V = 0.1548 m^3$)	68
2.21 Transient behaviour of the temperature profiles with inflow and outflow located as shown ($Re = 2,500$; $Q_i = 0.675 \times 10^{-5} m^3/sec$ and $V = 0.1548 m^3$)	69
2.22 Temperature profiles when a stratified enclosed water body is allowed to cool in the absence of flow	70
2.23 Trajectory of discharge (a) $Re = 2,500$, $\Delta T = 0 {}^\circ C$, (b) $Re = 2,500$, $\Delta T = 25 {}^\circ C$, (c) $Re = 6,250$, $\Delta T = 25 {}^\circ C$, (d) $Re = 2,500$, $\Delta T = 25 {}^\circ C$ The arrows indicate the directions of inflow and outflow	71
3.1 Isothermal Models. (a) Constant inflow temperature (b) constant energy input (c) natural cooling	72
3.2 T/CS versus θ in an isothermal water body for a constant inflow temperature or for a constant energy input	73
3.3 System constant versus loss coefficient for a constant temperature inflow into an isothermal water body	74
3.4 System constant versus loss coefficient for constant energy input into an isothermal water body	75
3.5 Transient decay of an isothermal water body in the absence of flow.	76
3.6 Comparison between theoretical and experimental results for an isothermal water body	77
3.7 One dimensional energy transport model (a) Unstable temperature profile model (b) Unstable temperature profile (c) Buoyant mixing in unstable region	78

- 3.8 Temperature profiles in an enclosed water body from a one dimensional model, with inflow and outflow located at the centre and at the top respectively 79
 $(Re = 2,500; Q_i = 0.675 \times 10^{-5} m^3/sec,$
 $V = 0.1422 m^3)$
- 3.9 Thermal profiles in an enclosed water body with inflow and outflow located at the centre and at the top respectively 80
 $(Re = 6250; Q_i = 0.1675 \times 10^{-4} m^3/sec;$
 $V = 0.1422 m^3)$
- 3.10 Thermal profiles in an enclosed water body with inflow and outflow located at the centre and at the top respectively 81
 $(Re = 1,250; Q_i = 0.335 \times 10^{-5} m^3/sec;$
 $\bar{h} = 16.1 W/m^2 ^\circ K)$
- 3.11 Thermal profiles in an enclosed water body with inflow and outflow located at the centre and at the top respectively 82
 $(Re = 6250; Q_i = 0.1675 \times 10^{-4} m^3/sec;$
 $\bar{h} = 16.1 W/m^2 ^\circ K)$
- 3.12 Transient rise in outflow (surface) temperature, for various Reynolds numbers, with inflow located at the centre and the outflow at the top 83
- 3.13 Comparison of predicted and experimental transient thermal profiles in an enclosed water body with the inflow and outflow located at the centre and at the top respectively 84
 $(Re = 2,500; Q_i = 0.675 \times 10^{-5} m^3/sec$
 $V = 0.1548 m^3, A_s = 1.03 m^2)$
- 3.14 Comparison of predicted and experimental transient outflow temperature in an enclosed water body with inflow and outflow located at the centre and at the top respectively 85
 $(Re = 2,500; Q_i = 0.675 \times 10^{-5} m^3/sec;$
 $V = 0.1548 m^3; h = 16.1 W/m^2 ^\circ K; A_s = 1.03 m^2)$

<u>FIG. NO.</u>	<u>PAGE</u>
3.15 Flow pattern in two-dimensional vertical flow, with intake and outfall on the same side of an enclosed water body, (a) inviscid flow (b) creeping flow	86
3.16 Streamlines in a two dimensional vertical creeping flow with intake and outfall located at the same side of the water body	87
3.17 Vertical flow pattern for typical two flow circuit. The arrows indicate the directions of inflow and outflow	88
3.18 Velocity distribution at the central plane (a) Z plane (b) X plane	89
3.19 Flow pattern in two dimensional vertical flow in an enclosed water body, with the inflow and outflow located as shown ($Re = 100$; $\tau = 0.495$)	90
3.20 Streamlines for rectangular tank with aspect ratio two. The arrows indicate the directions of the inflow and outflow ($Re = 100$; $\tau = 0.396$)	91
3.21 Two dimensional vertical flow pattern, with inflow and outflow located as shown ($Re' = 50$; $Gr/Re'^2 = 1$; $\tau = 0.99$)	92
3.22 Isotherms in an enclosed water body, with inflow and outflow located as shown ($Re' = 50$; $Gr/Re'^2 = 1$; $\tau = 0.99$)	93
3.23 Contours of streamlines for a two dimensional vertical flow. The arrows indicate the directions of inflow and outflow ($Re' = 50$; $Gr/Re'^2 = 1$; $\tau = 2.8712$)	94
3.24 Contours of temperature. The arrows indicate the direction of inflow and outflow ($Re' = 50$; $Gr/Re'^2 = 1$; $\tau = 2.8712$)	95

NOMENCLATURE

A	Cross-sectional area of the water body
A_s	Outer surface area of the water body
A_1, A_2 & A_3	Constants in the nonlinear model
Bi	Biot number
C_p	Specific heat of the fluid
CS	System constant for isothermal models
d	Depth of the water body
D_m	Depth of isothermally mixed layer
dx	Thickness of the wall of the tank
g	Gravitational acceleration
Gr	Grashof number
h	Heat transfer coefficient
\bar{h}	Average heat transfer coefficient
H	Dimensionless heat loss parameter
K_{eff}	Effective thermal conductivity of the wall of the tank
m	Mass flow rate of the water
L_c	Loss coefficient
P	Perimeter of the tank
Pr	Prandtl number
Q_i	Volume flow rate of the water
Q_L	Total heat loss from the surface of the tank
Re	Reynolds number <ul style="list-style-type: none"> i) Inflow Reynolds number, Re, based on inflow tube diameter ii) Tank Reynolds number, Re', based on tank depth

t	Temperature
T	Non dimensional temperature
u	Dimensional velocity in x direction
u_o	Reference velocity
U	Non-dimensional velocity in X direction
V	Volume of water in the enclosed water body
w	Dimensional velocity in z direction
W	Non-dimensional velocity in z direction
x, z	Coordinate axes
X, Z	Non-dimensional lengths in x and z direction respectively
z_1	Depth of isothermal layer
Z_1	Dimensionless depth of isothermal layer

Greek Symbols

α	Thermal diffusivity
β	Coefficient of thermal expansion
θ	Dimensionless decay parameter
τ	Time
ψ	Stream function
ξ	Vorticity
ν	Kinematic viscosity

Subscripts

a	Ambient or reference medium
h	Temperature of isothermal water body at the beginning of cooling
i	Inflow location
m	Isothermally mixed layer
o	Outflow location

SYNOPSIS

TRANSIENT EFFECTS IN AN ENCLOSED WATER BODY
DUE TO THERMAL DISCHARGE

JUNE, 1979

The study of storage of thermal energy in enclosed water bodies and the prediction of the performance under various conditions of practical interest are important aspects in the design of such systems. The aim of the present work was to study the important thermal effects of a heated discharge into an enclosed water body. Interest, obviously, lies in determining the resulting temperature field, particularly the growth and decay of thermal stratification in the water body. This study is also of relevance in heat rejection systems.

In order to study the thermal effects of a heated discharge into a water body, an experimental arrangement was designed and fabricated. The inflow rate was kept equal to the outflow so as to maintain a steady flow situation. For given inlet conditions, the transient behaviour of the water, in terms of the outflow temperature and the

temperature profiles measured in the tank, was studied at various locations, by means of thermocouples. Transient temperature profiles were obtained during the discharge of hot water. The decay in the temperature profiles was also studied in the absence of flow. It was observed that the transient response of the enclosed water body is strongly dependent on the configuration of flow circuit. The growth of thermal stratification in the tank with time was studied and the observed temperature profiles indicated strong mixing in the region above the inflow.

An analysis has also been carried out to determine the nature of the flow and temperature fields in the tank. Various mathematical models were formulated in order to evaluate the transient response of the enclosed water body, under various conditions relevant to practical systems and to the experimental arrangement.

A simplified zero dimensional model, with uniform temperature in the tank, was initially employed to predict the performance of the water body under various heat transfer conditions at the surface of the tank. The energy equation yielded the effect of thermal losses on the transient behaviour. The results obtained were found to be in reasonable agreement with the observed experimental results, under conditions which gave rise to considerable mixing in the water body.

A one dimensional model was then formulated, assuming complete mixing in the horizontal plane. The governing equation which included an averaged vertical flow was solved by finite difference techniques. The results have been compared with the temperature profiles obtained experimentally. The model was later modified to incorporate the vertical mixing due to the buoyancy effects and the flow. The modified model was found to yield results which were in good agreement with the experimental observations.

The analysis was also extended to a two-dimensional problem in order to determine the nature of flow field that arises. The cases of inviscid flow and of creeping flow were initially considered for various inflow and outflow locations. Streamlines were obtained for these various configurations. The flow field thus obtained indicates qualitatively the effectiveness of various flow configurations in energy dissipation as well as in thermal storage.

For viscous flow, normalized vorticity transport and stream-function equations were obtained. These equations were solved by means of finite difference techniques for the relevant boundary conditions. The corresponding energy equation, which is coupled to the flow through buoyancy, was also obtained and solved simultaneously. The alternating, direction implicit (ADI) method of Peaceman

and Rachford was employed. The problem could not be solved for the actual Reynolds-numbers encountered in the experiments due to convergence problems. It was observed that the computer time required to solve such a coupled system of equations is very high and the approach to the steady state is extremely slow. The streamlines and isotherms were obtained.

Several important conclusions can be drawn from the present work. The simplified zero dimensional model, which assumes uniform temperature in the water body, can easily be applied for estimating the losses and in designing the system for a well mixed water body. Although the flow in a water body is complex and depends on the geometric locations of inflow and outflow, the one dimensional model can predict, with accuracy in many cases, the temperature profiles in a thermally stratified medium. The two dimensional model allows a determination of the flow field and may often be used in conjunction with simplified one dimensional models for providing information necessary for the design of such systems. The study would help in determining the locations of the inlet and discharge points for maximum effectiveness of the system and would assist in determining the level of thermal stratification that arises in an actual system.

CHAPTER 1

INTRODUCTION

1.1 WATER BODIES

Recent years have seen a growing concern with energy, its generation, efficient utilization and the ultimate disposal of waste heat. Heat rejection is a matter of considerable concern since it affects the environment, to which the energy is rejected, and often also affects the efficiency of the basic energy generation system. An immense amount of heat is rejected to water bodies by nuclear and thermal power plants and by chemical and manufacturing industries. Thermal discharge into a water body might give rise to ecological problems. Enclosed water bodies are also used in the storage of thermal energy, as sensible heat, in solar energy systems. As a consequence, a study of the thermal effects arising due to thermal discharge to a water body is of considerable importance in heat rejection and energy storage systems.

An analysis of the system involves a study of the flow and temperature fields generated in an enclosed water body due to thermal discharge. This is a very complex problem, due to the nonlinear nature of the partial differential equations that govern the physical mechanisms. The flow and the thermal stratification that arise depend on the locations of the inflow and outflow and on various physical

variables, such as flow rates, temperature levels, dimensions of the water body, etc. The mathematical formulation of the flow and the heat transfer problem is again complicated because of generally coupled nature of the velocity and temperature fields. They are coupled through the buoyancy mechanisms that arise due to temperature differences. The present investigation is directed at determining the important thermal effects of a heated discharge into an enclosed water body. Interest lies in studying the temperature field, particularly the growth and decay of thermal stratification in the water body.

1.2 LITERATURE SURVEY

The problem of thermal discharge to a water body has been of interest to several investigations, largely because of the concern with the resulting thermal effects, in the water body, and, recently because of the interest in thermal energy storage in solar energy systems. Various mathematical models have been developed for the energy exchange mechanisms at the surface of natural water bodies, see, for instance, the work of Rafael [1962], Hindley and Miner [1972]. Henson et. al. [1961], etc., and for the convective, usually turbulent, processes within the water body. A review of the work done on heat rejection to natural water bodies, such as lakes, has been carried out by Jirka, et. al [1975] .

Moore and Jaluria [1971, 1972] considered the thermal effects of power plants on lakes, in terms of its temperature cycle. The stratification effects in lakes, during the yearly cycle, were studied by Dale and Harleman [1969]. Spalding [1977] discusses the basic mechanisms that govern the behaviour of pollutant disposal in river, bays, lakes and estuaries. Various physical and mathematical models are discussed.

Several papers on one dimensional mixing in turbulent stratified fluid flows are given in the book edited by Spalding and Afgan [1977]. The formation of an isothermal layer in a lake in Japan, the development and erosion of the thermocline, warm water spreading in cooling ponds of steam power plants and the development of the turbulent mixed region in a stratified medium have been discussed. The effect of turbulence on flow in stratified fluid is also considered.

Cabelli [1976] carried out a numerical study of the flow and temperature fields in a thermal energy storage tank for various geometric configurations. The effect of a variation in the entrance Reynolds number and the contribution of buoyancy mechanisms in promoting stratification have been examined. A comparison was also made with simple one dimensional models. The problem was solved for low Reynolds numbers, upto 200 (based on the perimeter of

the tank), although the mixed convection parameter Gr/Re^2 was in the range expected in practice.

A verification of the water temperature predictions for deep stratified reservoirs has been carried out by Burt [1974]. Numerical modelling of the thermal stratification in a reservoir with large discharge to volume ratio has been performed by Park et. al. [1973]. The predicted temperature profiles were compared with the field data for two different years. It was found that diffusion was the predominant heat transfer mechanism in the hypoliminion or middle layers, while the surface effects dominated the epiliminion or upper layers. Oberkampt and Crow [1976] have studied the velocity and temperature fields due to flow in a reservoir. The effects of inflow and outflow, wind shear and the energy loss on the reservoir are discussed.

Mollendorf and Gebhart [1973 A] considered the effect of thermal buoyancy on jet stability. Vertical buoyant jets were considered and an elaborate experimental system was designed to study the stability of the flow. The temperature field was studied by means of a Schlieren system. A perturbation analysis was also carried out by Mollendorf and Gebhart [1973 B] on the base flow to study the effect of buoyancy on the resulting flow. Fay [1973] considered buoyant plumes in detail. Jaluria and Gebhart [1973] assessed the stability of buoyancy induced flows in

a stratified medium. Extensive experimentation was carried out to obtain the desired form of stratification and to study its decay. Turner [1973] gives a review of the work done on similar buoyancy induced flows. Thermal stratification is considered in detail. These papers, along with the several others on stratification and jet flows [see, Gebhart, 1979], indicate the interest that exists in the problem of thermal discharge to water bodies. Thermal discharge is largely by means of turbulent jet flows and the water bodies are generally thermally stratified.

1.3 PRESENT WORK

Very little experimental work has been done on the thermal transient effects of an enclosed water body due to a thermal discharge. The aim of the present investigation was to carryout such an experimental study for large discharge to volume ratios and to verify the validity of the various mathematical models, in terms of the experimental results obtained. Two dimensional models, for the transport of momentum and energy in mixed convection flow, are considered, in addition to simpler isothermal and one-dimensional models.

An experimental arrangement was designed and fabricated to study the thermal performance of an enclosed water body. The inflow and outflow rates were kept the same, to maintain a fixed volume of water. The effect of

a variation in the inflow and outflow locations on the thermal stratification and on the transient behaviour of the temperature profiles in the tank have been studied in detail. The results are presented in terms of the measured temperature field. The buoyant flow has also been visually observed by means of a die injected into the tank through the inflow of water.

Mathematical models have been developed and related to the experimental results, in order to predict the performance of the water body in actual systems. An isothermal model was employed for a fully mixed water body and its energy exchange with the environment has been considered. The results obtained were found to be in agreement with the observed experimental results for the conditions which give rise to complete mixing in the tank, particularly the case when the inflow is at the bottom of the tank and outflow at the top. A one dimensional model was also developed and predictions for the temperature profiles were obtained. The model was later modified to incorporate the vertical mixing due to buoyancy effects and the flow. Very good agreement with the experimental results was obtained.

The flow fields for the two cases of inviscid and creeping flow were also obtained for various configurations in steady flow. For viscous flow the normalized vorticity transport and stream function equations were solved numerically. The coupling with the energy equation was also considered and results were obtained for various values of the Reynolds number.

CHAPTER 2

EXPERIMENTAL STUDY

2.1 EXPERIMENTAL ARRANGEMENT

In order to study the thermal effects of a heated water discharge into an enclosed water body, an experimental arrangement which incorporates the basic features involved in the study was devised. Of particular interest in the present investigation was the determination of the basic characteristics of the thermal stratification, that arises for various inflow and outflow conditions. The experiment employed an enclosed water body contained in a tank, in which hot water, heated by means of a constant water bath, was discharged. The temperature field was measured by means of thermocouples, employing a 48 channel recorder, and the flow rate was obtained from suitable flow meters.

The photographs of the main equipment used in the experimental arrangement are shown in Fig. 2.1. The water body was simulated experimentally by means of water contained in a perspex tank, of inside dimensions $0.6 \times 0.6 \times 0.44$ m, as shown in Fig. 2.1 (a). On one side of this tank, three circular holes were drilled and brass tubes of internal diameter 0.6 cm. were inserted in these holes and sealed against leakage. On the opposite side of the tank, an outflow opening was made through which the outflow was kept equal to the inflow. A thermocole sheet, of size

0.6 x 0.6 x .023 m., was used as the lid for the tank, as shown in Fig. 2.2 (b). Holes were made in the lid for the insertion of the thermocouple probes for recording the temperature profiles at various locations. The desired inflow of hot water, at various inlet temperature levels, was obtained by the flow of water through a coiled tube which was located in the constant temperature bath (ultra thermo-state, temp. range - 30 °C to 200 °C, capacity 15 litres, control accuracy ± 0.03 °C). The temperature of the hot water was varied by operating a thermoregulator valve which controls the bath temperature. In order to vary and measure the hot water flow rate, a rotameter, with a needle valve, was fitted at one end of the tube which carries the water through the bath. The flow rate was also checked by collecting the outlet water in a measuring flask several times during the experiment. The water level was kept unaltered.

A Honeywell forty-eight point temperature recorder was used to obtain the temperature at any point in the water body. Standard copper-constantan thermocouples, made from wires of diameter 0.125 mm., were calibrated and used in the measurement of the temperature field. The recorder had an accuracy of the order of 0.15 °C. A thermocouple probe as shown in Fig. 2.2 (c) was prepared. A scale was fixed with the probe and holes 1 cm. apart were drilled along its length. These holes were used for locating the thermocouples. The

probe could be positioned at any desired location in the tank and the flow could be varied over a wide range of flow rates. The transient temperature profiles were measured by means of this arrangement.

The experimental arrangement employed for the flow is shown schematically in Fig. 2.3. Water from an overhead tank enters the constant temperature bath coil at one end and the hot water leaving the coil was discharged into the enclosed water body at any one of the desired locations, a, b or c, as shown in the diagram. The outflow from the tank was taken from location d or any one of the remaining locations, designated as a, b or c. When the inflow and outflow locations were selected on the same side of the tank, the discharge from the tank was allowed to flow through a flow-meter with a needle valve. This arrangement facilitated the regulation of flow.

Thermocouples were fitted at each inlet and outlet location. Temperatures at other desired locations were obtained from the thermocouple probes described above. The inflow and outflow water temperatures and the temperature at various other locations were recorded at different time intervals. Experiments were conducted for various geometric configurations, different flow rates and various inlet temperatures. Extensive experimentation was also carried out to check the repeatability and accuracy of the

experiments. A very high level of accuracy, within a few percent, in the temperature data was obtained. The results obtained indicate the transient thermal behaviour of the water body to the energy input, through a heated discharge. Some of the important and characteristic results are presented in the next section.

2.2 EXPERIMENTAL RESULTS

In the present investigation, transient temperature distribution in the enclosed water body has been studied for various flow rates, with particular interest in the basic characteristics of the thermal stratification that arises for different inflow outflow locations. The heated, isothermal or stratified, water body was also allowed to cool in the absence of flow and the temperature decay was studied. The following dimensionless variables are employed in presenting the results:

$$T = \frac{t - t_a}{t_i - t_a} ; \quad z = \frac{z}{d} ; \quad \bar{\tau} = \frac{\alpha \tau}{d^2}$$

where t is the water temperature at any point in the tank, t_a is the ambient temperature and t_i is the inlet hot water temperature. Also, z is the vertical distance of the location where measurements are taken, from the top of the tank, d is the depth of water in the tank, α is the thermal diffusivity of water and τ is time in seconds.

The exit temperature is denoted by \bar{t}_o (where the over bars on dimensionless time has been dropped beyond this.)

The transient response of the water outlet temperature is shown in Fig. 2.4 with the hot water inlet at the bottom and the outlet located at the top of the tank on the opposite side. It was found that complete mixing occurs in the tank due to the flow and the buoyancy effects, since the water body was found to be isothermal for the flow rates considered. The value of the mixed convection parameter is of the order of 0.01, based on the inlet tube diameter, indicating dominant forced convection mechanisms.

The transient temperature decay of an initially isothermal water body is shown in Fig. 2.5. The average loss coefficient has been obtained graphically as shown in Fig. 2.6. The water body remains isothermal while cooling. The average film coefficient \bar{h} was estimated to be $16.1 \frac{W}{m^2 K}$ assuming that the top and bottom of the tank are perfectly insulated).

Figures 2.7, 2.8 and 2.9 indicate the transient thermal behaviour of the enclosed water body for the inflow and outflow conditions shown. The transient temperature response of the exit water temperature is indicated in Fig. 2.7. The temperature is seen to rise gradually to the inlet temperature level. Figure 2.8 shows the variation of the temperature profiles inside the tank during thermal discharge. It is evident from these curves that complete mixing occurs in the tank from the intake location to the top of the tank. It is due to the rise of the buoyant

fluid and the mixing due to the flow that is generated. Figure 2.9 shows the decay of the temperature profiles in the absence of thermal discharge, when the enclosed water body was allowed to cool in the natural environment of the room. Since the cooling is largely by natural convection and as water has a high thermal capacity, the cooling rate was very slow as expected. When the inlet and outlet were both located at the top of the tank, on opposite sides, the thermal behaviour of the water body was studied and is shown in Figs. 2.10 and 2.11. Figure 2.10 clearly indicates the rapid rate at which the outflow temperature approaches the temperature of the inlet water. Figure 2.11 shows the thermal stratification that arises during the thermal discharge. The enclosed water body is obviously strongly stratified. The bottom remains largely unaltered and a strong temperature gradient is generated, which becomes steeper with time. Figure 2.12 compares the transient response of the outlet water temperature obtained for various flow configurations. As expected, the inflow at the top gives the fastest response.

Figures 2.13 to 2.22 indicate the thermal behaviour of the enclosed water body due to heated discharge, when the inflow and outflow are both located on the same side of the water body. The Reynolds number based on inflow tube diameter is equal to 2500. Figure 2.13 shows the transient behaviour of the outlet water temperature.

Again the temperature is seen to rise at a decreasing rate to the inlet temperature value. It takes about 6 hours to reach within 67 percent of the inlet temperature. Figure 2.14 shows the temperature profiles during thermal discharge. It is seen from these curves that the water body temperature at the bottom is essentially unaltered by the heated effluent for a fairly long time, about seven hours. The bottom layers gain energy by thermal diffusion and, as such, the rate of energy transfer is low compared to the top layers. The upper layers are found to be largely isothermal due to the mixing that arises. Figure 2.15 shows the decay of temperature in a stratified water body in the absence of flow. The profiles are very interesting. Again a slow decay is observed, with the water body indicating an isothermal upper layer and a decaying stratification level with time. The surface temperature decreases sharply and the bottom temperature increases due to thermal diffusion. The variation in the outflow, water temperature and in the temperature profiles with time are shown in Figs. 2.16 and 2.17 respectively, for inflow located at the center (location b) of one side and the outflow at the bottom of the same side (location c). The outflow temperature is not affected by the thermal discharge for 160 minutes. The stratified temperature profiles are set up at a very fast rate, again with an isothermal upper layer. The bottom temperature rises more gradually with time.

Figures 2.18 to 2.22 show the effect of various other geometric configurations, of the inflow and outflow, commonly encountered in heat rejection systems. Figure 2.18 clearly shows that, for a long time the outflow temperature is not affected by the heated effluent but as time progresses it is seen to increase. This observation is of relevance to the design of a heat rejection system, employing a water body, since the outflow is generally employed in the heat rejection process and a higher temperature of outflow will reduce the efficiency of the system.

The temperature profiles at eight time levels are shown in Fig. 2.19. It is evident that the exit temperature is not affected for five hours but is significantly affected as time progresses. The profiles are also strongly time dependent.

For inflow located at the top of one side and the outflow at the center on the same side the response of the enclosed water body is seen in Figs. 2.20, 2.21 and 2.22. The variation in the exit water temperature is indicated in Fig. 2.20. The rise in the exit water temperature is slow up to 150 minutes beyond which the trend of the curve completely changes. After eight hours the exit temperature was found to be only 65% of the highest temperature (i.e. inlet water temperature). It is evident from Fig. 2.21 that the bottom temperature of the water body is not

significantly affected by heated affluents even after eight hours. This indicates the slow rate of energy transfer to the bottom layers. Figure 2.2 exhibits the cooling of the stratified enclosed water body in the absence of flow, when it was allowed to lose energy in the natural environment of the room. The bottom temperature of the water body rises due to thermal diffusion but at a very slow rate as expected. The surface temperature falls gradually.

Photographs for the heated discharge have also been taken by injecting dye tracer at the inflow. Figure 2.23 shows these photographs, as obtained from the side of the tank, for various inflow and outflow locations. Figure 2.23 (a) depicts the trajectory of the discharged water jet when the inflow and the enclosed water body are at the same temperature, i.e. without buoyancy. Figures 2.23 (b), (c), and (d) have been taken for different inflow and outflow configurations. The vertical rise of the heated fluid due to buoyancy and the resulting mixing is clearly seen.

2.3 CONCLUDING REMARKS

For the flow under study, turbulent mixing is expected to have a significant effect on the energy exchange in the water body. In the present case, the buoyancy force is vertical and the thermal discharge is horizontal. As such, a horizontal homogeneity in the water body was seen to arise. Mixing due to flow also

causes the region above the inlet to be isothermal. The flow in this region is complex and three dimensional. However, the thermal effects are found to be mainly one dimensional for the flow rates encountered in the experiment. The experimental study indicates that, for the conditions encountered in the experiments, it may be possible to estimate the thermal performance of the enclosed water body by suitable one dimensional mathematical models.

CHAPTER 3

ANALYTICAL MODELS

3.1 INTRODUCTION

The thermal behaviour of a water body depends on the shape and dimensions of the water body, configuration of the flow circuit, temperature and flow rate of discharge and energy loss to the environment. The buoyancy driven fluid flow and energy exchange mechanisms, which arise in the water body, are very complex in nature and the resulting processes have, therefore, not been studied in desired detail so far. The relevant equations which govern the flow are difficult to solve without considerable simplifying assumptions. The basic problem is a three dimensional one, in which the flow is coupled to the energy equation, through buoyancy. The partial non-linear nature of these equations makes an analytical solution possible only for very simplified circumstances, which are often physically unrealistic. Even the numerical solution is fairly involved for the general problem. Therefore, some simplified models are developed here. Their applicability to actual systems is considered in terms of the experimental results given earlier.

3.2 ISOTHERMAL MODELS

In certain circumstances, complete mixing in the horizontal and vertical planes of the water body is obtained. In the experimental study undertaken for the present work also, it was observed that for inflow at the bottom of the tank, with outflow at the top, an unstratified water body was obtained. Similarly for small tanks with large mixing effects due to buoyancy and the flow, an isothermal assumption may be made. It is then possible to predict the thermal performance and to study the effect of losses on the temperature of the water body, without considering the detailed mechanism of the flow.

The equations which govern the performance of an isothermal water body arise simply from the conservation of energy. The following assumptions are made:

1. There is complete mixing in the water body and the volume of water remains constant.
2. The heat capacity of the fluid is much larger compared to that of the tank material.
3. The physical properties of the fluid are constant.
4. The ambient temperature and the film coefficient are taken as constant.

3.2.1 Constant Inflow Temperature

Consider a water body as shown in Fig. 3.1 (a).

Let the temperature of water and that at the inside surface of the container wall be t at time τ . Water enters the tank at a constant temperature t_i and leaves it at the temperature of the water body. An energy balance of the water body gives:

$$\rho C_p V \frac{dt}{d\tau} = m C_p (t_i - t) - Q_1 \quad (3.1)$$

where m is the mass flow rate, C_p is the specific heat and ρ is the density of water. Also Q_1 is the total heat loss from the surface. A convenient and efficient way for expressing Q_1 from the outer surface of the water body is given by the steady heat loss expression:

$$Q_1 = h \left(\frac{1}{1 + Bi} \right) A_s (t - t_a)$$

where A_s is surface area for heat loss. Here it has been assumed that energy loss is proportional to the temperature difference $(t - t_a)$ and the Biot number $Bi = h dx / K_{eff}$, where dx is the thickness of the wall material and K_{eff} is its effective thermal conductivity. This expression takes into account the heat loss by conduction from the walls of the water body.

$$\text{Let } T = \frac{t - t_a}{t_i - t_a}$$

The mass flow $m = \rho Q_1$; where Q_1 is volume flow rate.

Inserting the above values in Equation (3.1),

$$\frac{dT}{d\tau} = \frac{Q_1}{V} + \left\{ \frac{Q_1}{V} + \frac{h A_s}{\rho V C_p} \left(\frac{1}{1 + Bi} \right) \right\} T \quad (3.2)$$

Equation (3.2) is an ordinary differential equation with constant coefficients and can, therefore, be solved conveniently, for the initial condition $T = 0$ at $\tau = 0$. The solution of Equation (3.2) can be written in the form

$$T = CS (1 - e^{-\theta}) \quad (3.3)$$

where $CS = 1 / (1 + \frac{h A_s L_c}{\rho Q_1 C_p})$ and

$$\theta = \left(\frac{h A_s L_c}{\rho V C_p} + \frac{Q_1}{V} \right) \tau , \text{ such that}$$

$$0.5 \leq CS \leq 1 , \text{ and Loss Coefficient}$$

$$L_c = \frac{1}{1 + Bi} = \frac{1}{1 + \frac{h dx}{K_{eff}}} , \text{ such that}$$

$$0 \leq L_c \leq 1 , \text{ and } \bar{h} = h \cdot L_c$$

3.2.2 Constant Temperature Difference

In this case, the water is supplied at a constant temperature difference Δt above the outlet water temperature, as shown in Fig. 3.1 (b). This implies a constant energy input into the system, by means of, say, solar energy or an electrical heating system. The rest of the specifications are the same as before and the governing equation is obtained as

$$\rho C_p V \frac{dt}{d\tau} = \rho Q_1 C_p \Delta t - \bar{h} A_s (t - t_a) \quad (3.4)$$

where $\bar{h} = h \cdot L_e$

$$\text{Let } T = \frac{t - t_a}{\Delta t}$$

Inserting the dimensionless variable T for t , Eq. (3.4) reduces to

$$\frac{dT}{d\tau} = \frac{Q_1}{V} - \frac{\bar{h} A_s}{\rho V C_p} T \quad (3.5)$$

For the initial condition $T = 0$ at $\tau = 0$, the solution is

$$T = CS (1 - \text{Exp}^{-\theta}) \quad (3.6)$$

where $CS = \frac{\rho Q_1 C_p}{\bar{h} A_s}$ and $\theta = \frac{\bar{h} A_s}{\rho V C_p} \tau$, such that $1 \leq CS \leq \infty$

3.2.3 Natural Cooling

Consider a water body which is at a temperature t_h at $\tau = 0$. There is no flow in the tank and the water body is allowed to cool in the natural environment, as shown in Fig. 3.1 (c). This circumstance is of relevance in the determination of temperature decay for energy storage systems, such as those employed in chemical and allied industries. The governing equation is

$$\rho V C_p \frac{dt}{d\tau} = -\bar{h} A_s (t - t_a) \quad (3.7)$$

Nondimensionalizing by $T = \frac{t - t_a}{t_h - t_a}$, the equation reduces to

$$\frac{dT}{d\tau} = - \frac{\bar{h} A_s}{\rho V C_p} T \quad (3.8)$$

For the initial condition $T = 1$ at $\tau = 0$, the solution is

$$T = \text{Exp}^{-\theta} \quad (3.9)$$

where

$$\theta = \frac{\bar{h} A_s}{\rho V C_p} \tau$$

3.2.4 Results of the Isothermal Models

Figure 3.2 indicates the variation of temperature T/CS with time θ . From this graph, the time required to attain a certain temperature level for a given thermal discharge can be determined. The time required to attain 99% of the maximum temperature is obtained as $\theta = 4.6$.

The system constant CS versus the loss coefficient for a given inflow is shown in Fig. 3.3 for various values of the heat transfer coefficient \bar{h} ($Q_1 = 0.1 \times 10^{-3}$ m^3/sec and $A_s = 6.0 m^2$). It is seen that for $h = 10 W/m^2 K$, system constant reduces to 0.87, whereas for $\bar{h} = 100 W/m^2 K$, it attains the minimum value 0.5 at loss coefficient equal to 0.7. System constant versus the loss coefficient for a constant temperature difference Δt is indicated in Fig. 3.4, for flow rate equal to 0.1×10^{-3} m^3/sec . In this case, system constant is directly proportional to the flow rate and inversely proportional to the loss coefficient.

In Fig. 3.5, the transient decay of an isothermal water body is considered. It is an exponential decay. For any given system, the decrease in temperature during a certain time interval can be estimated from this graph.

In Fig. 3.6, the experimentally measured temperature rise in an isothermal enclosed water body is compared with the theoretically determined values for a constant inflow temperature. A fairly good comparison between the two is obtained, for $\bar{h} = 16.1 \text{ W/m}^2 \text{ }^\circ\text{C}$, leading support to this model for systems where complete mixing arises.

3.3 ONE DIMENSIONAL MODELS

The experimental study indicated that, despite the flow in the water body being three dimensional, the measured temperature profiles that arise are essentially one dimensional, for the various geometric configurations and the flow rates considered. Cabelli [1976] carried out a numerical study of a storage tank and he also concluded that the thermal performance of the tank can be easily approximated by simple one dimensional models. In this section, suitable one dimensional models have been considered and analyzed.

Consider the water body as shown in Fig. 3.7 (a), in which the inflow is located at a certain depth and outflow is at the top. The energy equation is obtained for

a vertical one-dimensional model as

$$\frac{\partial t}{\partial \tau} + w \frac{\partial t}{\partial z} = \alpha \frac{\partial^2 t}{\partial z^2} - \frac{\bar{h} P}{A \rho C_p} (t - t_a) \quad (3.10)$$

where w is the average vertical velocity, α the molecular thermal diffusivity, P the perimeter of the water body and A its cross-sectional area. Here loss at the sides is considered in terms of \bar{h} , which may as before be taken equal to $\bar{h} = h(1/1 + Bi)$. In writing the expression for the heat loss from the sides of the water body, it has been assumed that the film coefficient \bar{h} also takes into account the radiative heat loss. In general, however, the convective and radiative terms may be employed in full.

The equation (3.10) can be non-dimensionalized by defining

$$T = \frac{t - t_a}{t_i - t_a}, \quad Z = \frac{z}{d}, \quad \bar{\tau} = \frac{\alpha \tau}{d^2}$$

$$w = \frac{w d}{\alpha}$$

where d is the depth of the tank.

The nondimensional equation therefore becomes:

$$\frac{\partial T}{\partial \tau} + W \frac{\partial T}{\partial Z} = \frac{\partial^2 T}{\partial Z^2} - HT \quad (3.11)$$

where the overbar on dimensionless time has been dropped for convenience. Also,

$$H = \frac{\bar{h} P d^2}{A K_f} = \frac{\bar{h} P d^2}{A \alpha e C_p}$$

where K_f is the thermal conductivity of the fluid

If we assume an initial condition of uniform temperature and a step change in the inflow water temperature, the boundary conditions are

$$T(Z, 0) = 0$$

$$T(Z_i, \tau) = 1$$

$$\frac{\partial T}{\partial Z} = 0 \text{ at } Z = 0 \text{ and } Z = 1$$

In section II, vertically below the inlet, heat transfer is largely by diffusion, convective mixing being essentially negligible. For a one dimensional model, of course, no velocity exists below the inlet point, the flow being above the inlet to the exit at the top. The above equation, therefore, reduces to the following, in the region below the inlet.

$$\frac{\partial T}{\partial \tau} = - \frac{\partial^2 T}{\partial Z^2} - HT \quad (3.12)$$

The initial and the boundary conditions are

$$T(Z, 0) = 0$$

$$T(Z_i, \tau) = 1$$

$$\frac{\partial T}{\partial Z} = 0 \text{ at } Z = 1 \text{ and } Z = 0$$

Here, it has been assumed that the top and bottom of the body of water is perfectly insulated. The gradient may be obtained from energy transfer, if heat loss is considered.

3.3.1: Method of Solution and Results

Equations (3.11) and (3.12), with the given boundary conditions, were solved numerically by finite difference techniques by employing an implicit method. The tank was divided into 45 sections, each of uniform temperature. This produced a tridiagonal system of equations which was solved by a tridiagonal algorithm, described by Carnahan, et. al. [1969] .

For inflow at the mid point and the exit at the top, the numerically obtained temperature profiles, for the flow rates of $0.67 \times 10^{-5} \text{ m}^3/\text{sec}$ and $0.1675 \times 10^{-4} \text{ m}^3/\text{sec}$, are shown in Figs. 3.8 and 3.9. The predicted temperature distribution is clearly unstable, since a temperature increase with depth is observed. This causes denser fluid to be above the lighter fluid and is, therefore, expected to be thermally unstable. In practical situations, this type of a temperature profile will generally cause mixing. It may exist only when the losses from the surface are at a very high rate,* as indicated by Drake and Harleman [1963] . However, they pointed out that a slight disturbance will cause vertical mixing. This vertical mixing will take place up to a finite depth D_m and can be determined by making an energy balance (Refer. Fig. 3.7 (b)) as

* Author also observed this experimentally with the water body uncovered at the top.

$$\int_0^{D_m} \{ (T(z, \tau) - T_m) \} dz = 0 \quad (3.13)$$

$$\text{at } z = D_m, \quad T(D_m, \tau) = T_m \quad (3.14)$$

where T_m is the temperature of isothermally mixed layer.

From Equations (3.13) and (3.14), the depth of the unstratified mixed layer near the surface of the water body, caused due to the mixing arising from the unstable thermal stratification, can be determined. In a buoyant flow, as in plumes, a higher temperature is expected at greater depth. However, in the experiments carried out here, buoyancy induced mixing and that due to the flow was seen to give rise to an isothermal upper layer.

3.3.2 Isothermal Upper Region

The experimental results showed that, for the range of flow rates studied, if the outlet is situated at the top and inflow at any other height, then complete mixing is observed from the inflow to the top of the tank. Thermal energy is transported by the convective process, which also includes the buoyancy mechanisms. Below the inlet, the convective flow is absent and conductive mechanisms dominate.

Consider the water body as shown in Fig. 3.7 (c). From the inflow to the outlet at the top, the water body is assumed to be isothermal at any instant. The overall

energy balance for the isothermal region, for unit horizontal area, gives

$$\frac{\partial t}{\partial \tau} = \frac{w}{z_1} (t_i - t) - \frac{\alpha}{z_1} \frac{\partial t}{\partial z} - \frac{\bar{h}_p}{\rho C_p A} (t - t_a) \quad (3.15)$$

where z_1 is the depth of the isothermal region and $\frac{\partial t}{\partial z}$ is evaluated at the interface of the two regions.

If we nondimensionalize as before, the equation becomes

$$\frac{\partial T}{\partial \tau} = \frac{W}{Z_1} (1 - T) - \frac{1}{Z_1} \frac{\partial T}{\partial Z} - HT \quad (3.16)$$

where

$$Z_1 = \frac{z_1}{d}, \quad W = \frac{w d}{\alpha}$$

$$H = \frac{\bar{h}_p d^2}{A K_f}$$

Equation (3.16) is used to determine the temperature of the isothermal section. The temperature profile of the section II is determined by using Eq. (3.12). An explicit finite difference sequence was used to solve Eq. (3.16) along with Eqn. (3.12).

3.3.3 Discussion of Results

The temperature profiles predicted from the above model are shown in Figs. 3.10 and 3.11, for the flow rates of $0.335 \times 10^{-5} \text{ m}^3/\text{sec}$ and $1.675 \times 10^{-5} \text{ m}^3/\text{sec}$ respectively. It can be seen in Fig. 3.10 that the bottom temperature

remains essentially unaffected for about 10 hours and that the increase of the temperature of the top section is at a very slow rate. However, for $Re = 6250$, the temperature of top section builds up at a much faster rate. Figure 3.12 indicates the transient rise in the surface temperature of the enclosed water body for Reynolds numbers 1250, 2500 and 6250. Figures 3.13 and 3.14 indicate the discrepancy between the theoretically predicted and the experimentally measured temperature profiles. From these figures, it is obvious that, although the one dimensional model is an approximate one and does not allow a consideration of the flow, it can approximate the temperature profile of an actual system quite closely, in the ranges under consideration. Therefore, in several systems, the one dimensional model, as developed in this section, would be adequate in predicting the thermal behaviour. This observation is supported by the several studies of natural water bodies, employing the one dimensional model, as discussed earlier.

3.4 RECIRCULATION IN ENCLOSURES

The nature of mixing in bodies of water due to flow depends mainly on the recirculation pattern. The experimental study of the flow pattern in water bodies due to inflow-outflow is very difficult, due to its three dimensional nature. A numerical study is carried out here. The two limiting cases of inviscid and creeping flow have

been considered initially for various geometric configurations. The results also indicate the dependence of the flow on the aspect ratio of the tank. In general, the flow is viscous and the Reynolds number is large so that creeping flow may not be employed. However, averaging in one direction, for the 2D model, particularly for low flow rates does bring Reynolds number low enough so that creeping flow may give realistic results in several cases. The results here are presented only as an indication of the nature of the flow. The actual viscous transient problem is considered later, with coupling due to buoyancy.

3.4.1 Governing Equations

For a two dimensional, irrotational, inviscid flow in an enclosure, the basic governing equation, which has been solved by the finite difference technique, is the standard Laplace equation:

$$\frac{\partial^2 \psi}{\partial X^2} + \frac{\partial^2 \psi}{\partial Z^2} = 0 \quad (3.17)$$

where ψ is stream function. If U and W are velocities in X and Z directions respectively, then $U = \frac{\partial \psi}{\partial Z}$ and $W = -\frac{\partial \psi}{\partial X}$. ψ is constant at the boundaries and a constant inflow and outflow velocity gives a linear variation in ψ at these locations.

The basic equation for flow at low Re , indicative of low velocity or high viscosity and often called

creeping motion, is the standard biharmonic equation

$$\nabla^4 \psi = 0 \quad (3.18)$$

The boundary conditions are obtained from the no-slip conditions at the walls, so that ψ is constant and $\frac{\partial \psi}{\partial n} = 0$ at the boundaries, where n represents the direction normal to the wall. The above linear equation is also the basic equation for the hydrodynamic theory of lubrication. These equations are solved numerically by means of finite difference methods, as discussed by Gupta and Jaluria [1978].

3.4.2 Results and Discussions

Figure 3.15 shows the streamlines for the inviscid and creeping flow, with the outflow positioned on the same side as the inflow, the former being at the bottom. In the case of inviscid flow, the streamlines are uniformly spaced, whereas in the case of creeping flow the stream lines are concentrated near the plane of the intake and outlet. Figure 3.16 shows the streamlines for creeping flow in a rectangular tank of aspect ratio 2. In the center of the tank, the motion of the fluid is slow. This flow pattern is quite different from what was obtained for a square tank.

Figure 3.17 shows the streamlines for a two flow circuit which is very common in thermal storage

systems. The inflow and outflow velocities are assumed to be constant in all the cases discussed above. Figure 3.18 shows the velocity distributions at the central plane of the tank. The velocity W in the Z plane is found to be maximum near $X = 0.25$ and the U component of the velocity is negligible. The component W in the X plane is maximum at $Z = 0.5$ and W is maximum at $Z = 0.25$ and 0.75 .

3.5 THE NONLINEAR PROBLEM

The analysis of fluid motion within bodies of water due to a heated discharge is particularly complicated because of the buoyancy effects, which generally make it a mixed convection problem. In isothermal and one dimensional models, the thermal behaviour was studied without an analysis of the flow. A good agreement between predicted and experimental results was observed. This was largely due to the mixing caused by the flow and the buoyancy mechanisms. However, at low flow rates and constant inlet temperatures, such complete mixing is not expected and the temperature and the velocity will vary in the vertical and horizontal planes. A two dimensional model, assuming uniformity in one horizontal direction, is considered in this section. This model will apply when complete mixing can be assumed in the direction normal to the inflow and outflow directions. This would be the case for an inflow

over the entire width of the water body and for narrow water bodies, so that uniformity exists across it. In several cases, a two dimensional model may be employed by averaging the flow over the width of the water body. The basic problem is, obviously, three dimensional. But the complicity involved with solving the general problem makes it desirable to analyze the flow in terms of simpler two dimensional models. In some cases, horizontal models are suitable and allow a study of the flow without considering the mixed convection effects, see, for instance, the work of Jirka, et. al. [1975] and Schgal and Jaluria [1979].

3.5.1 Governing Equations for a Two Dimensional Model

Consider a water body in which the motion of the fluid is two dimensional, as shown in Fig. 3.7 (d). The basic governing equations are those of conservation of mass, momentum and energy. The governing equations are obtained for a two dimensional flow, assuming constant properties and making the usual Boussinesq approximation [see, e.g., Schlichting, 1968] as:

$$\frac{\partial u}{\partial x} + \frac{\partial w}{\partial z} = 0 \quad (3.19)$$

$$\frac{Du}{Dt} = - \frac{1}{\rho_a} \frac{\partial P}{\partial x} + v \nabla^2 u \quad (3.20)$$

$$\frac{Dw}{Dt} = - \frac{1}{\rho_a} \frac{\partial P}{\partial z} - g \beta (t - t_a) + v \nabla^2 w \quad (3.21)$$

$$\frac{Dt}{D\tau} = \alpha v^2 t \quad (3.22)$$

where u is the horizontal velocity in x direction and w is the vertical velocity in z direction. Here, the subscript a refers to a reference value, generally the ambient medium or the initial value.

By cross-differentiating Equations (3.20) and (3.21) with respect to z and x respectively and subtracting, the pressure terms are eliminated and the vorticity equation is obtained as:

$$\frac{D\xi}{D\tau} = g \beta \frac{\partial t}{\partial x} + v \nabla^2 \xi \quad (3.23)$$

where the vorticity ξ is given by

$$\xi = \frac{\partial u}{\partial z} - \frac{\partial w}{\partial x} \quad (3.24)$$

If we define the stream function ψ by $u = \frac{\partial \psi}{\partial z}$ and $w = -\frac{\partial \psi}{\partial x}$, the continuity equation is satisfied and it is related to vorticity by

$$\xi = \nabla^2 \psi \quad (3.25)$$

Therefore, the governing equations reduce to

$$\frac{D\xi}{D\tau} = g \beta \frac{\partial t}{\partial x} + v \nabla^2 \xi \quad (3.26)$$

$$\frac{Dt}{D\tau} = \alpha v^2 t \quad (3.27)$$

$$\xi = \nabla^2 \psi \quad (3.28)$$

And $u = \frac{\partial \psi}{\partial z}$ and $w = -\frac{\partial \psi}{\partial x}$.

The equations are normalized by defining characteristic time $\tau^* = \frac{d}{u_o}$ and $\psi^* = d u_o$, where u_o is the reference velocity, taken as the inflow velocity. The following dimensionless variables are used

$$T = \frac{t - t_a}{t_1 - t_a}; \quad X = \frac{x}{d}, \quad Z = \frac{z}{d}$$

$$\bar{\tau} = \frac{\tau}{\tau^*}, \quad \bar{\psi} = \frac{\psi}{\psi^*}, \quad \bar{U} = \frac{u}{u_o}, \quad \bar{W} = \frac{w}{u_o}$$

The above governing equations can then be written as

$$\frac{D\xi}{D\tau} = A_1 \frac{\partial T}{\partial X} + A_2 \nabla^2 \xi \quad (3.29)$$

$$\frac{D T}{D \tau} = A_3 \nabla^2 T \quad (3.30)$$

$$\xi = \nabla^2 \psi \quad (3.31)$$

And $U = \frac{\partial \psi}{\partial Z}; \quad W = -\frac{\partial \psi}{\partial X}$

where the overbars have been dropped for convenience.

The parameters A_1 , A_2 and A_3 in the above equations are given by

$$A_1 = Gr/Re'^2; \quad A_2 = 1/Re'; \quad A_3 = 1/(Re' Pr)$$

where $Gr = g \beta d^3 \Delta T / \gamma^2$, $Re' = u_o d / v$ and $Pr = v/\alpha$

Cabelli [1976] has also considered the above system of equations in his analysis of flow in a solar energy storage tank.

3.5.2 Boundary Conditions

At the walls the no-slip boundary condition is employed. Therefore, $U = 0$, $W = 0$. Consequently ψ is constant and $\frac{\partial \psi}{\partial n} = 0$.

At the inflow:

$$U = 1 ; \quad W = 0$$

Therefore, the stream function was distributed linearly across the opening. It was assumed that the fluid entering the solution region was irrotational and therefore inflow vorticity was assigned a value zero. The vorticity value at the outflow was determined by using Equation (3.31).

The fluid enters the solution region at a constant temperature. The temperature gradient normal to the boundary was equal to zero since the tank was assumed to be insulated at the boundaries. However, losses can be taken into account as was done in the case of the unstratified and one dimensional models.

3.5.3 Method of Solution and Results

The energy and vorticity transport equations were both solved by alternating direction implicit (ADI) method of Peaceman and Rachford as described in Carnahan [1969]. The stream function equation was solved by using

the Gauss - Seidel iteration method. The velocity component in the solution domain was calculated by using second order centered space difference. The vorticity at walls was calculated from the streamfunction field, using the method described by Roache [1976].

Finite difference methods were used for studying the flow pattern. Equations (3.29), alongwith (3.31) , were initially solved for $A_1 = 0$, i.e. without considering the buoyancy effects, in order to get the flow pattern. Figures 3.19 and 3.20 indicate the flow patterns for $Re' = 100$. These figures indicate the effect of geometry. Figure 3.19 shows the flow pattern for a square tank, whereas Fig. 3.20 shows that for a rectangular tank, with an aspect ratio of two. It was found that the flow stabilizes very soon, although the problem could not be solved for the actual Reynolds numbers encountered, in the experiment, due to stability problems. If we reduce the mesh size, it was possible to go to higher Reynolds number, but then the computer time also becomes much higher. The flow pattern obtained is physically expected and is similar to that obtained earlier for the case of creeping flow.

Figures 3.21 and 3.22 indicate the stream line pattern and the isotherms for $\frac{Gr}{Re'^2} = 1.0$; $Re' = 50$ and $\tau = 0.99$. For the same parameters, the stream lines

pattern and isotherms are shown in Figs. 3.23 and 3.24 for a time $\tau = 2.8712$. From these figures it is again evident that for a buoyant flow also, the flow stabilizes very soon, whereas the temperature penetration is very slow. This was also seen in the experimental study, where the temperature field was found to vary over a considerable period of time.

The major problem in such a computational study is the instability that poses a limitation on the time step. The coupled natures of the equations makes the solution very slow and, even though the computer solution is sometimes necessary for certain practical problems, such as power plant heat rejection systems where the recirculation pattern is needed for the design of the system, the stability problem at higher Re would often make the numerical solution a formidable task. This study was undertaken largely to obtain the basic procedure for determining the flow in a two dimensional system and to indicate the basic features of the numerical results thus obtained.

For the experimental study carried out, it has already been shown that one dimensional models are adequate in determining the thermal behaviour. However, interest does exist in the flow field in circumstances where the recirculation is crucial to design, as in airconditioning

and heat rejection systems. In such cases, a numerical study of the flow may be undertaken as given above to determine the flow pattern and the velocity levels encountered, for steady state as well as for transient cases.

CHAPTER 4

SUMMARY AND CONCLUSIONS

4.1 SUMMARY

In several heat rejection and energy storage systems, the problem of thermal discharge to an enclosed water body arises. The thermal effects that result are often of importance in the consideration of the ecological impact of the energy rejected on the water body. The thermal stratification that frequently arises in such cases is also of significance in the study of thermal energy storage. The present work is directed at determining the transient thermal effects in an enclosed water body due to thermal discharge.

The study is carried out experimentally, followed by relevant analysis. The thermal behaviour of the water body is dependent on various variables such as inflow-outflow locations, inflow temperature and flow rate, dimensions and geometry of the water body, environmental conditions, etc. This study considers several of these in detail. The effect of the inflow-outflow locations and of the inflow temperature and flow rate are considered in detail. The temperature profiles are obtained as functions of time and the growth and decay of thermal stratification are studied in detail. Based on the experimental results, analytical models are

developed. The complex two dimensional model, with coupling due to buoyancy, was studied. However, it was found that simpler isothermal and one-dimensional models are suitable for the range of flow rates examined in the present work. Good agreement between analytical and experimental results was obtained, indicating the validity of these simplified models in the circumstances studied experimentally. For other cases, the two-dimensional model may be employed and some results are indicated. The general three dimensional problem is a very complex one and need be undertaken only in cases where the simpler models are inapplicable. This study considers these various models and the analytical results thus obtained in terms of the experimental results.

4.2 CONCLUSIONS

The experimental results, along with various suitable mathematical models, have been discussed in detail. The results from analysis have also been compared with the experimental results, indicating good agreement. The main conclusions of the present investigations are discussed below.

The experimental work indicates that for the large flow rates considered here, Reynolds numbers ranging between 2000 and 6250, complete mixing in the flow region, between the inflow and outflow, arises due to the flow and

the buoyancy effects. For such flows, the geometric location of the inflow and the outflow has an important effect on the thermal performance of the system. If the inflow and the outflow are both located at the top, but on opposite sides, the water body is stably stratified and the level of stratification increases with time. If the inflow is located at the bottom, with the outflow at the top, the water body is found to be isothermal. If the inflow is located at any other location with the outflow at the top, the enclosed water body can be divided into two distinct regions, the upper region being isothermal and the lower stratified. In addition to these, the flow configurations commonly encountered in various heat rejection systems, such as those in thermal power plants, have been studied. The effect of the flow variables on the outflow temperature and on the transient temperature profiles have been obtained and discussed in terms of the physical processes involved.

Suitable theoretical models have also been considered for determining the thermal performance of an actual system. Isothermal models were found to characterize the transient behaviour of water bodies in which complete mixing arises due to flow. These were considered for constant inflow temperature and for constant energy input. The effect of energy loss to the environment on the thermal performance was studied. For stratified water bodies,

obtained with specified locations of inflow and outflow, relevant one-dimensional models were developed and the governing equations were solved numerically. Theoretically predicted results have been compared with the experimentally observed values and a good agreement was observed.

The two dimensional vertical flow pattern has been obtained for the two limiting cases of inviscid and creeping flow. The effect of geometry on the flow has been investigated. The actual non-linear viscous problem has also been considered. It was observed that the flow pattern is established relatively fast and thermal diffusion continues more gradually. The problem could be solved only for low Reynolds number, because of numerical instability problems. A reduction in the mesh size makes it possible to go to somewhat higher Reynolds numbers. But this involves large computer times and the complexity increases as Re is increased. Since the basic mechanisms could be studied at low values also, it was decided not to pursue the work to large values. Moreover at large values, the one dimensional models were found to be quite satisfactory.

4.3 FUTURE WORK

This study has considered the thermal effects in an enclosed water body due to heated discharges at fairly high values of the inflow Reynolds numbers. The actual problem is, obviously, three dimensional. However,

for small water bodies, complete mixing may often arise leading to the isothermal approximation. Similarly, in narrow water bodies, complete mixing may exist in one or both horizontal dimensions, leading to two or more dimensional models. Future work must examine this question in detail. This would involve consideration of a very wide range of flow rates and/or water bodies of various dimensions. The one-dimensional model is a very simple one and has, therefore, been used for natural water bodies extensively. It is necessary to determine its validity. The present work indicates some of the circumstances under which it may be employed.

Another question which is of considerable significance pertains to the relative importance of buoyancy effects. The parameter Gr/Re^2 must be varied to determine how buoyancy affects the thermal behaviours. In the present work, this parameter is generally quite small. At large values, the buoyancy-induced flow will dominate and the stratification profiles may be quite different.

Considerable work needs to be done on the understanding of the flow that arises in a general three-dimensional problem. The two dimensional problem must also be studied at larger Re . With thermal stratification and dominating turbulent transport, the eddy viscosity and diffusivity will be strong functions of the depth and this must be incorporated in the analysis, as done for stratified natural water bodies.

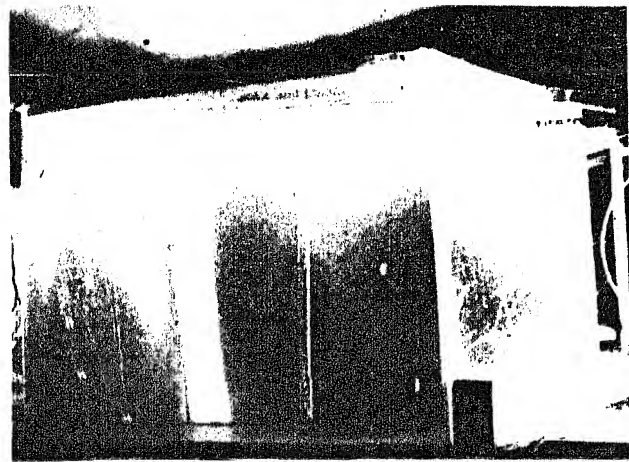
REFERENCES

1. Burt, W.V. [1974] , "Verification of Water Temperature Forecasts For Deep, Stratified Reservoirs", Water Resources Research, Vol. 10 (1), pp. 93 - 97.
2. Cabelli, A. [1977] , "Storage Tanks - A Numerical Experiment," Solar Energy, Vol. 19, pp. 45 - 54.
3. Carnahan, B., Luther, H.A. and Wilkes, J.O. [1969] , Applied Numerical Methods, John Wiley and Sons, Inc., New York.
4. Dake, J.M.K. and Harleman, D.R.F. [1969] , "Thermal Stratification in Lakes: Analytical and Laboratory Studies," Water Resources Research, Vol. 5, (2), pp. 484 - 495.
5. Fay, J.A. [1973] , "Buoyant Plumes and wakes," Ann. Rev. Fluid Mech., Vol. 5, p. 15.
6. Gebhart, B. [1979] , "Buoyancy Induced Fluid Motions Characteristics of Applications in Technology - The 1978 Freeman Scholar Lecture," J. Fluids Engg., Vol. 101, pp. 5 - 28.

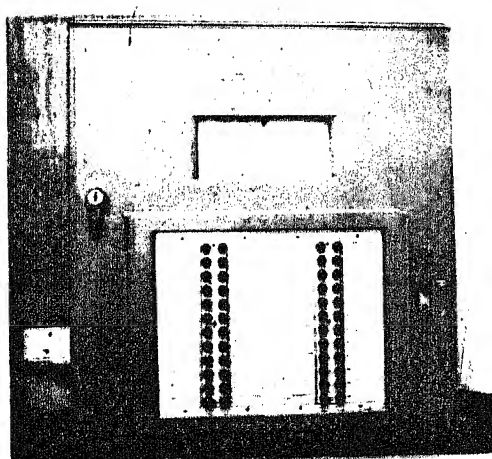
7. Gupta, S.K. and Jaluria, Y. [1978] , "A Study of Recirculation in Enclosures," Proc. 8th Nat. Conf. Fluid Mech. and Fluid Power, Coimbatore.
8. Hanson, E.B., Brandshaw, A.S. and Chandler, D.C. [1961], "The Physical Limnology of Cayuga Lake, New York," Memoir 378, Agricultural Expts. Station, Cornell Univ, U.S.A.
9. Hindley, R.D. and Miner, R.M. [1972] , "Evaluating Water Surface Heat Exchange Coefficient," ASCE (Hyd. Div.), Vol. 98, pp. 1411 - 1426.
10. Jaluria, Y. and Gebhart, B. [1973] , "An Experimental Study of Nonlinear Disturbance Behaviour in Natural Convection," J. Fluid Mech., Vol. 61 (2), pp. 337 - 365.
11. Jirka, G.H., Abraham, G. and Harleman, D.R.F. [1975] , "An Assessment of Techniques for Hydrothermal Prediction," Rep. No. PB 250509, Nat. Tech. Inf. Ser., U.S.A.
12. Mollendorf, J.C. and Gebhart, B. [1973A] , "An Experimental and Numerical Study of the Viscous Stability of a Round Laminar Vertical Jet with and without Thermal Buoyancy for Symmetric Asymmetric Disturbances," J. Fluid Mech., Vol. 61, Part 2, pp. 367 - 399.
13. Mollendorf, J.C. and Gebhart, B. [1973 B] , "Thermal Buoyancy in Round Laminar Vertical Jets," Int. J. Heat Mass Transfer, Vol. 16, pp. 735 - 745.

14. Moore, F.K. and Jaluria, Y. [1971], "Temperature Cycle of a Lake with Power Plants," Presented at the Winter Annual Meeting of ASME, Washington, 1971, and Published in "Environmental and Geophysical Heat Transfer," ASME, N.Y., 1971.
15. Moore, F.K. and Jaluria, Y. [1972], "Thermal Effects of Power Plants on Lakes," J. Heat Transfer, Vol. 94, pp. 163 - 166.
16. Oberkampf, W.F. and Crow, L. [1976], "Numerical Study of the Velocity and Temperature Fields in a Flow Through a Reservoir," J. Heat Transfer, Transactions of ASME, Series C, Vol. 98 (3), pp. 353 - 359.
17. Park, G.G. and Schmidt, P.S. [1973], "Numerical Modeling of Thermal Stratification in a Reservoir with Large Discharge to Volume Ratio," Water Resource Bull., Vol. 9 (5), pp. 932 - 941.
18. Raphael, J.M. [1962], "Prediction of Temperature in Rivers and Reservoirs," J. Power Div., ASCP, Vol. 88, pp. 157 - 180.
19. Roache, P.J. [1976], Computational Fluid Dynamics, Revised Edition, Hermosa Publishers, Albuquerque, U.S.A.

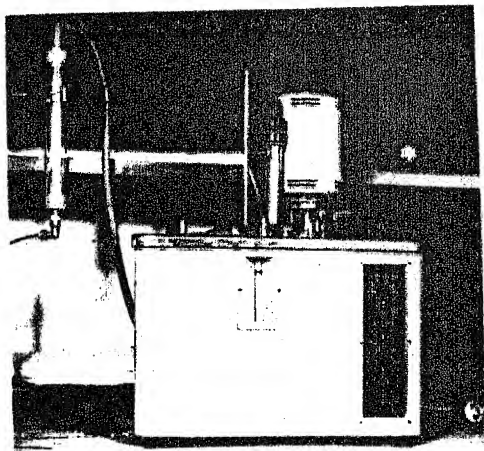
20. Schlichting, H. [1968] , Boundary Layer Theory, 6th Edition, McGraw-Hill Book Co., Inc., New York.
21. Sehgal, R.C. and Jaluria, Y. [1979] , "On the Horizontal Recirculation in Water Bodies Due to Thermal Discharge," To be Presented at National Heat and Mass Transfer Conf., San Diego, U.S.A.
22. Spalding, D.B. [1977] , 'Heat and Mass Transfer in River, Bays, Lakes and Estuaries,' Advances in Heat Transfer, Vol. 13, pp. 61 - 117, Academic Press.
23. Spalding, D.B. and Afgaw, N. [1977] , Heat Transfer and Turbulent Buoyant Convection, Vol. I, Hemisphere Publishing Corporation, Washington.
24. Turner, J.S. [1973] , "Buoyancy Effects in Fluids," Cambridge Univ. Press, England.



(a) Tank



(b) Temperature Recorder



(c) Constant Temp. Bath

Fig. 12.11. Photographs of the main equipment

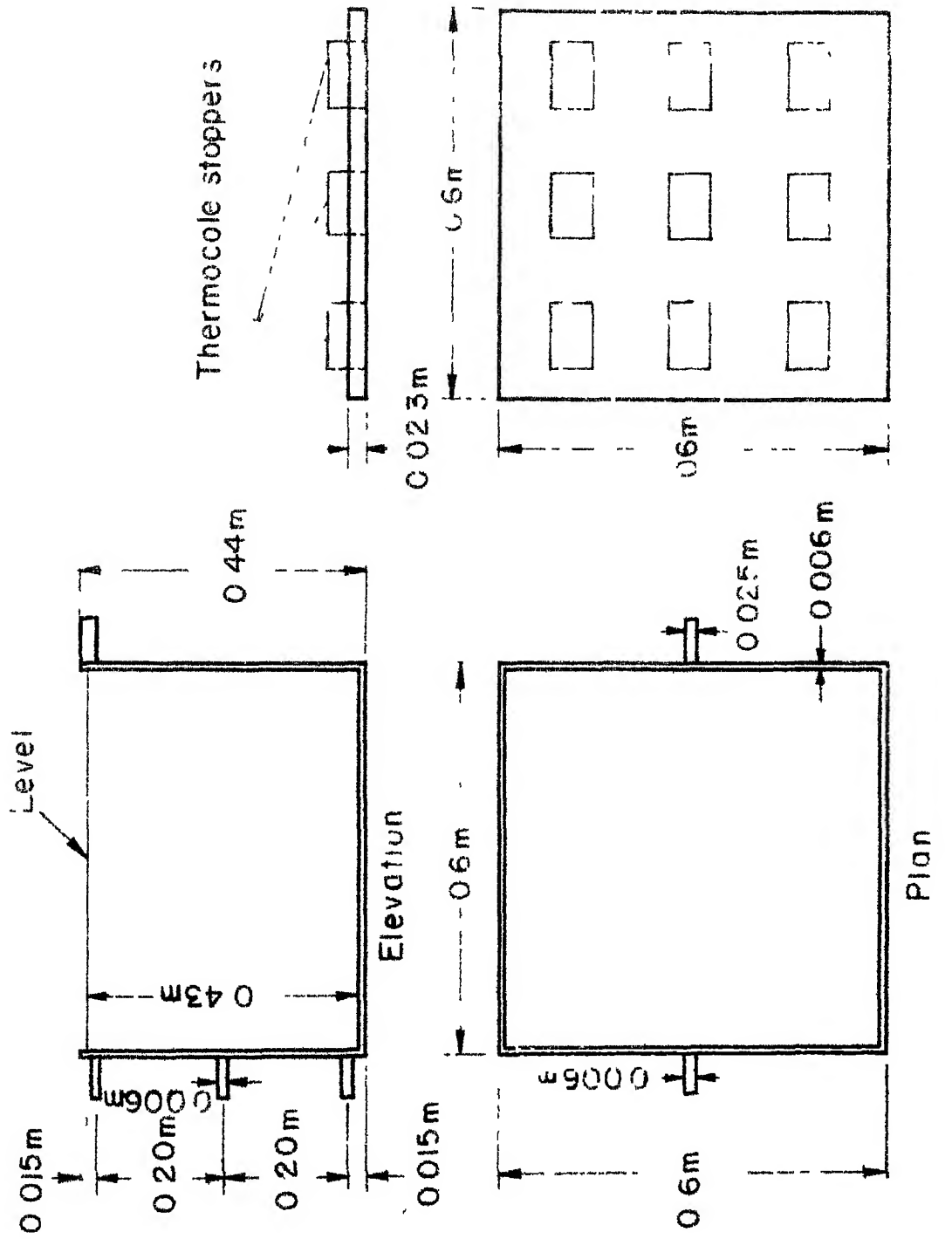
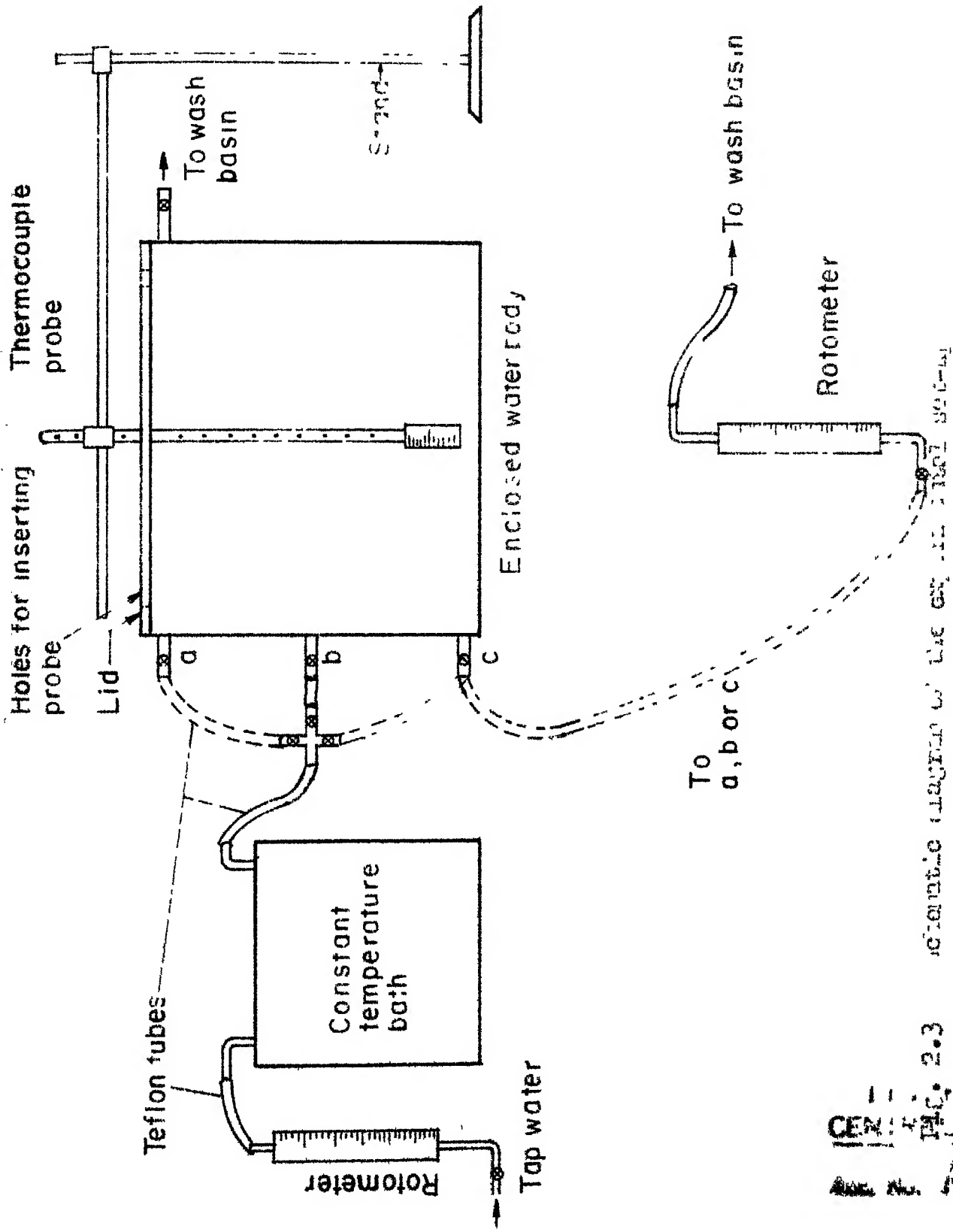


Fig. 2. Design of the Perspex tank, Thermocole lid and probe.



CEN 1
 115°C 20.3
 110°C 20.3
 105°C 20.3
 100°C 20.3
 95°C 20.3
 90°C 20.3
 85°C 20.3
 80°C 20.3
 75°C 20.3
 70°C 20.3
 65°C 20.3
 60°C 20.3
 55°C 20.3
 50°C 20.3
 45°C 20.3
 40°C 20.3
 35°C 20.3
 30°C 20.3
 25°C 20.3
 20°C 20.3
 15°C 20.3
 10°C 20.3
 5°C 20.3
 0°C 20.3
 -5°C 20.3
 -10°C 20.3
 -15°C 20.3
 -20°C 20.3
 -25°C 20.3
 -30°C 20.3
 -35°C 20.3
 -40°C 20.3
 -45°C 20.3
 -50°C 20.3
 -55°C 20.3
 -60°C 20.3
 -65°C 20.3
 -70°C 20.3
 -75°C 20.3
 -80°C 20.3
 -85°C 20.3
 -90°C 20.3
 -95°C 20.3
 -100°C 20.3
 -105°C 20.3
 -110°C 20.3
 -115°C 20.3
 -120°C 20.3
 -125°C 20.3
 -130°C 20.3
 -135°C 20.3
 -140°C 20.3
 -145°C 20.3
 -150°C 20.3
 -155°C 20.3
 -160°C 20.3
 -165°C 20.3
 -170°C 20.3
 -175°C 20.3
 -180°C 20.3
 -185°C 20.3
 -190°C 20.3
 -195°C 20.3
 -200°C 20.3
 -205°C 20.3
 -210°C 20.3
 -215°C 20.3
 -220°C 20.3
 -225°C 20.3
 -230°C 20.3
 -235°C 20.3
 -240°C 20.3
 -245°C 20.3
 -250°C 20.3
 -255°C 20.3
 -260°C 20.3
 -265°C 20.3
 -270°C 20.3
 -275°C 20.3
 -280°C 20.3
 -285°C 20.3
 -290°C 20.3
 -295°C 20.3
 -300°C 20.3
 -305°C 20.3
 -310°C 20.3
 -315°C 20.3
 -320°C 20.3
 -325°C 20.3
 -330°C 20.3
 -335°C 20.3
 -340°C 20.3
 -345°C 20.3
 -350°C 20.3
 -355°C 20.3
 -360°C 20.3
 -365°C 20.3
 -370°C 20.3
 -375°C 20.3
 -380°C 20.3
 -385°C 20.3
 -390°C 20.3
 -395°C 20.3
 -400°C 20.3
 -405°C 20.3
 -410°C 20.3
 -415°C 20.3
 -420°C 20.3
 -425°C 20.3
 -430°C 20.3
 -435°C 20.3
 -440°C 20.3
 -445°C 20.3
 -450°C 20.3
 -455°C 20.3
 -460°C 20.3
 -465°C 20.3
 -470°C 20.3
 -475°C 20.3
 -480°C 20.3
 -485°C 20.3
 -490°C 20.3
 -495°C 20.3
 -500°C 20.3
 -505°C 20.3
 -510°C 20.3
 -515°C 20.3
 -520°C 20.3
 -525°C 20.3
 -530°C 20.3
 -535°C 20.3
 -540°C 20.3
 -545°C 20.3
 -550°C 20.3
 -555°C 20.3
 -560°C 20.3
 -565°C 20.3
 -570°C 20.3
 -575°C 20.3
 -580°C 20.3
 -585°C 20.3
 -590°C 20.3
 -595°C 20.3
 -600°C 20.3
 -605°C 20.3
 -610°C 20.3
 -615°C 20.3
 -620°C 20.3
 -625°C 20.3
 -630°C 20.3
 -635°C 20.3
 -640°C 20.3
 -645°C 20.3
 -650°C 20.3
 -655°C 20.3
 -660°C 20.3
 -665°C 20.3
 -670°C 20.3
 -675°C 20.3
 -680°C 20.3
 -685°C 20.3
 -690°C 20.3
 -695°C 20.3
 -700°C 20.3
 -705°C 20.3
 -710°C 20.3
 -715°C 20.3
 -720°C 20.3
 -725°C 20.3
 -730°C 20.3
 -735°C 20.3
 -740°C 20.3
 -745°C 20.3
 -750°C 20.3
 -755°C 20.3
 -760°C 20.3
 -765°C 20.3
 -770°C 20.3
 -775°C 20.3
 -780°C 20.3
 -785°C 20.3
 -790°C 20.3
 -795°C 20.3
 -800°C 20.3
 -805°C 20.3
 -810°C 20.3
 -815°C 20.3
 -820°C 20.3
 -825°C 20.3
 -830°C 20.3
 -835°C 20.3
 -840°C 20.3
 -845°C 20.3
 -850°C 20.3
 -855°C 20.3
 -860°C 20.3
 -865°C 20.3
 -870°C 20.3
 -875°C 20.3
 -880°C 20.3
 -885°C 20.3
 -890°C 20.3
 -895°C 20.3
 -900°C 20.3
 -905°C 20.3
 -910°C 20.3
 -915°C 20.3
 -920°C 20.3
 -925°C 20.3
 -930°C 20.3
 -935°C 20.3
 -940°C 20.3
 -945°C 20.3
 -950°C 20.3
 -955°C 20.3
 -960°C 20.3
 -965°C 20.3
 -970°C 20.3
 -975°C 20.3
 -980°C 20.3
 -985°C 20.3
 -990°C 20.3
 -995°C 20.3
 -1000°C 20.3

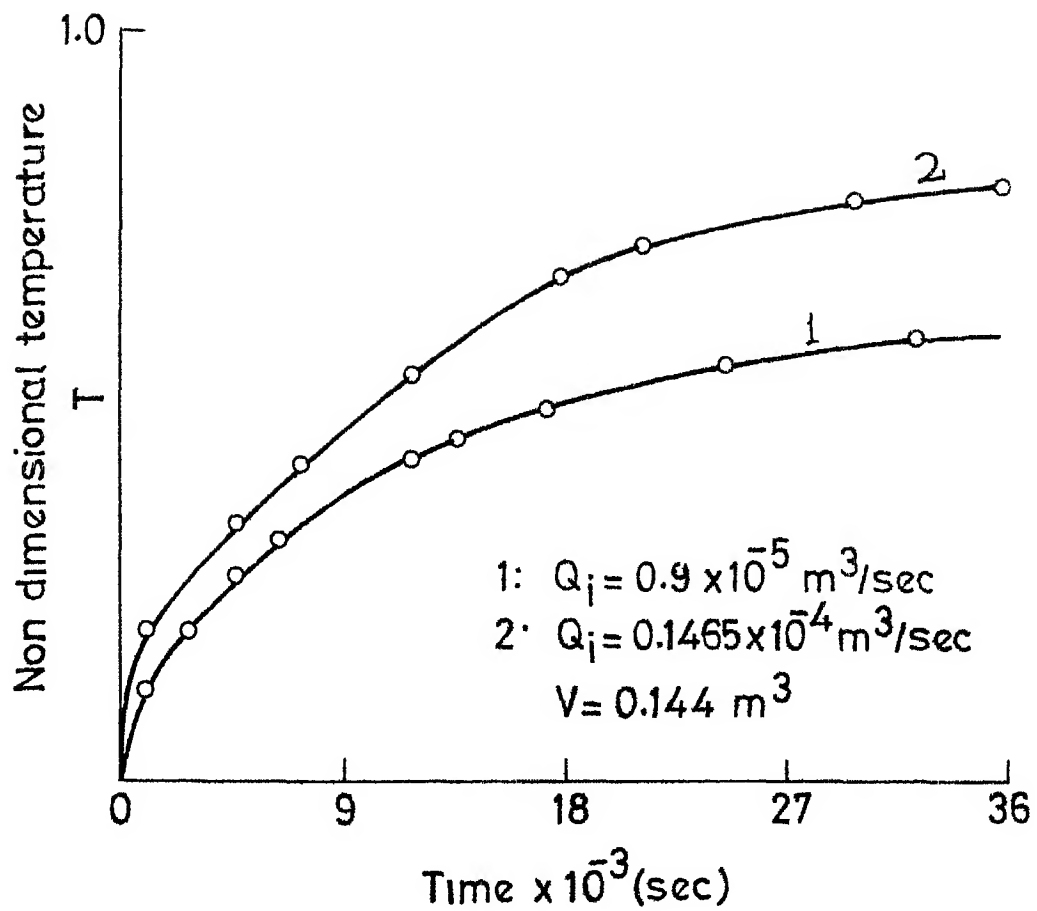


Fig. 2.4 Temperature versus time in an enclosed water body with inflow located at bottom of one side and the outflow on the top of the opposite side.

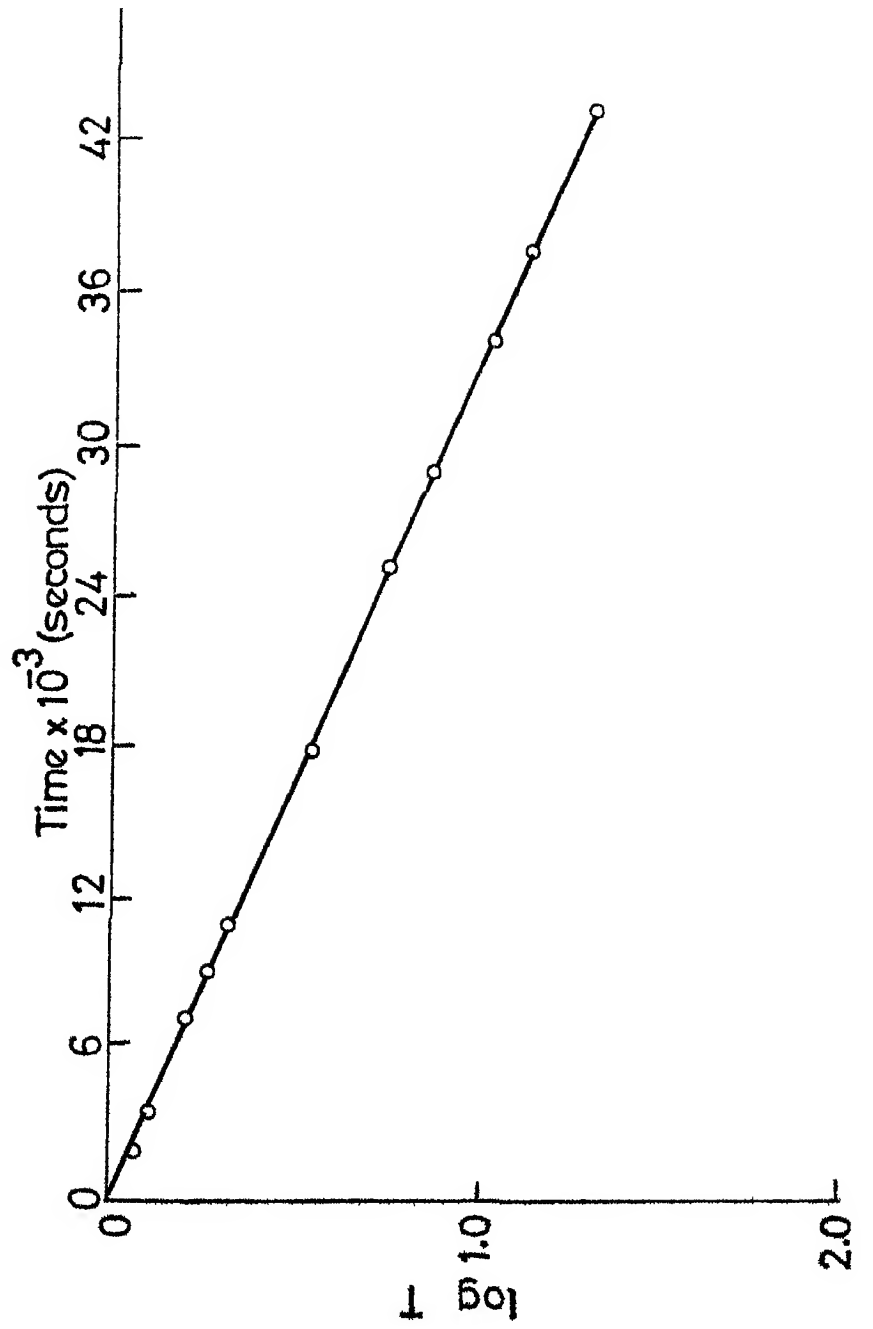


Fig. 2.6 Log T versus time for a 0.122 mol/l solution of HgCl_2 .

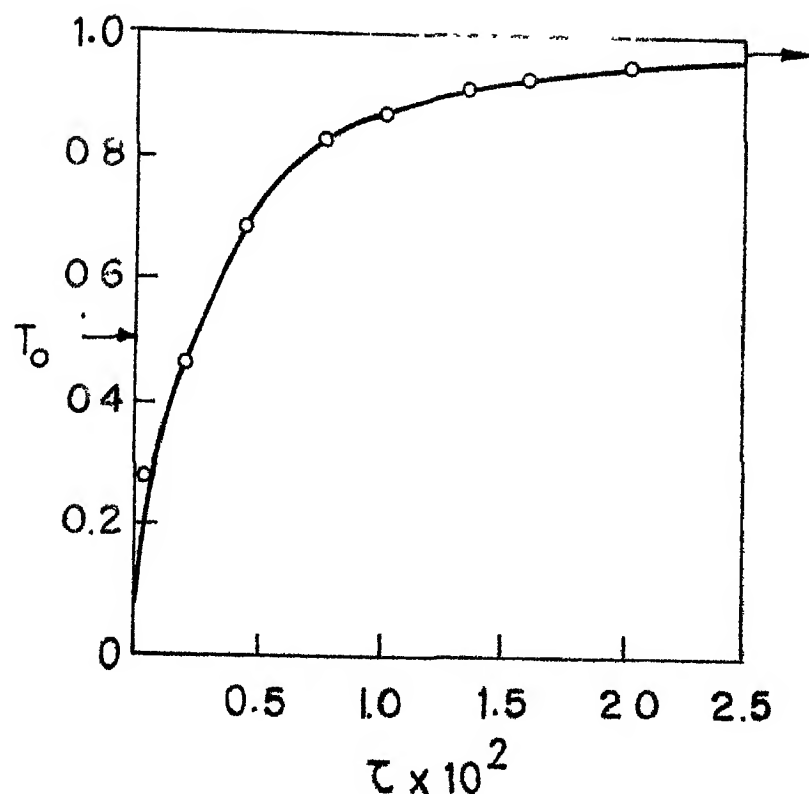


Fig. 2.7

Outlet temperature versus time, with the intake at the centre of one side and outfall at the top of the opposite side

($Re = 5,000$; $Q_1 = 1.34 \times 10^{-5} \text{ m}^3/\text{sec}$ and
 $V = 0.1548 \text{ m}^3$).

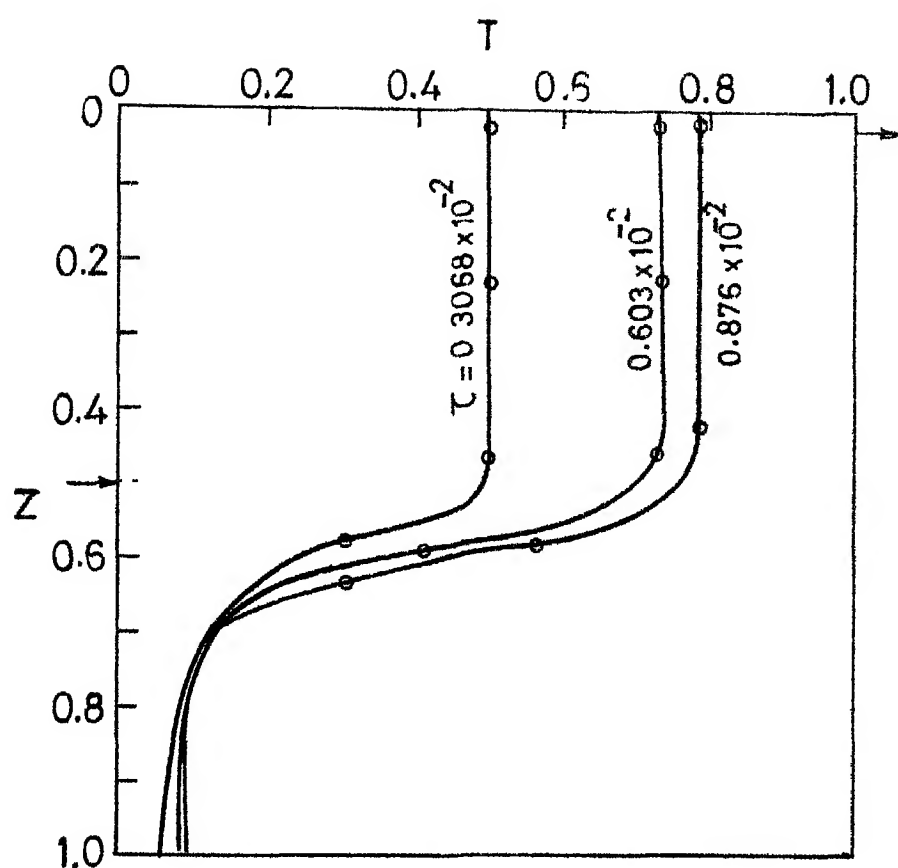


Fig. 2.8 Transient Non-dimensional temperature profiles in an enclosed water body. The arrows indicate the direction of inflow and outflow.

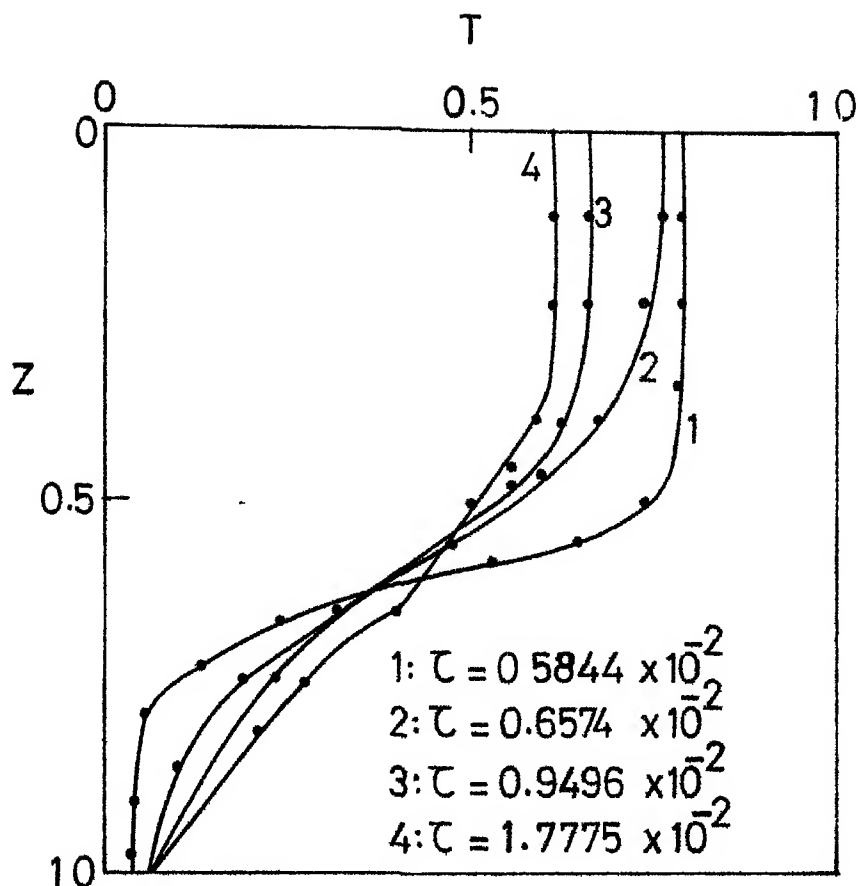
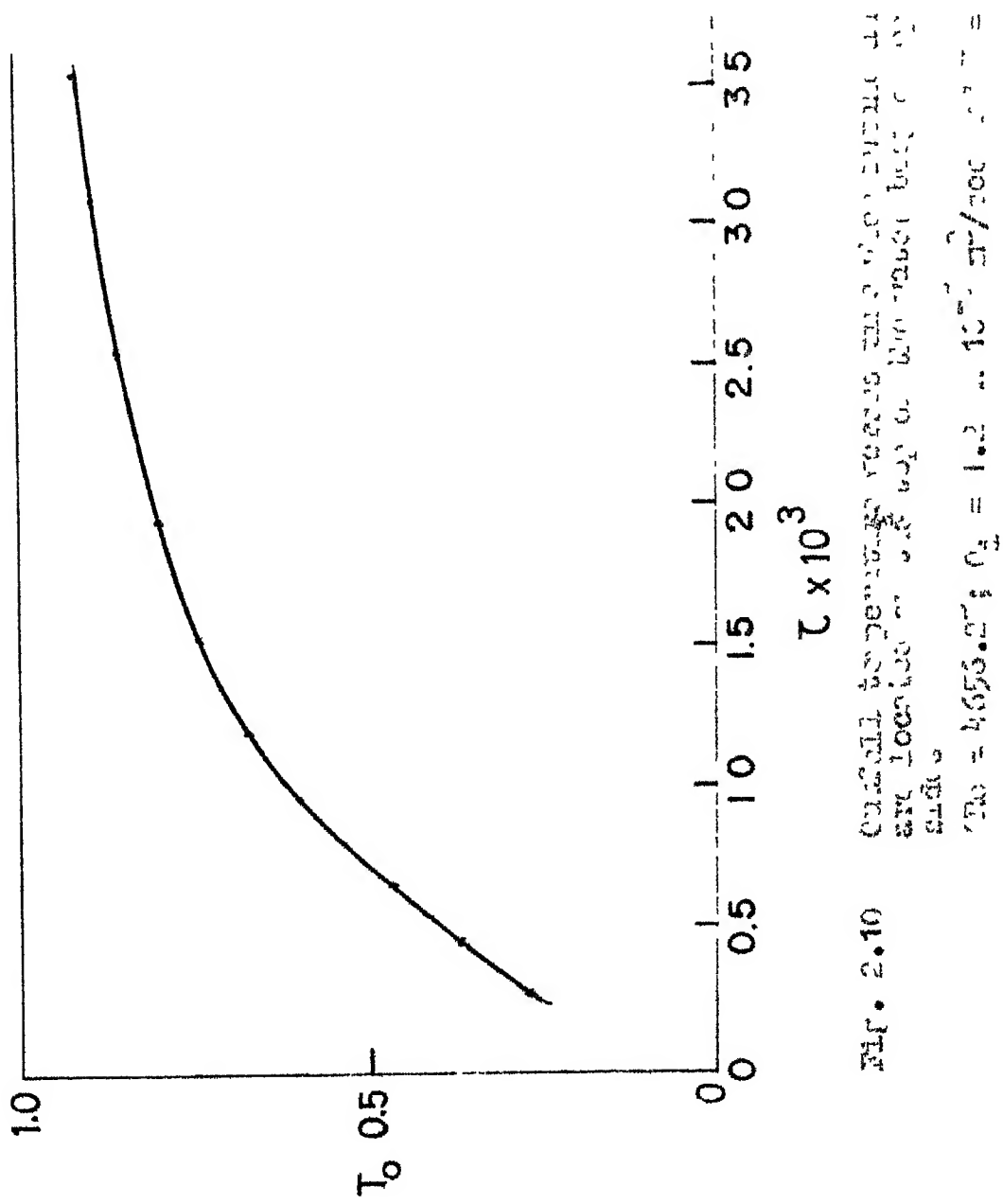


Fig. 2.9 Temperature profiles, when a stratified enclosed water body is allowed to cool in the absence of flow.



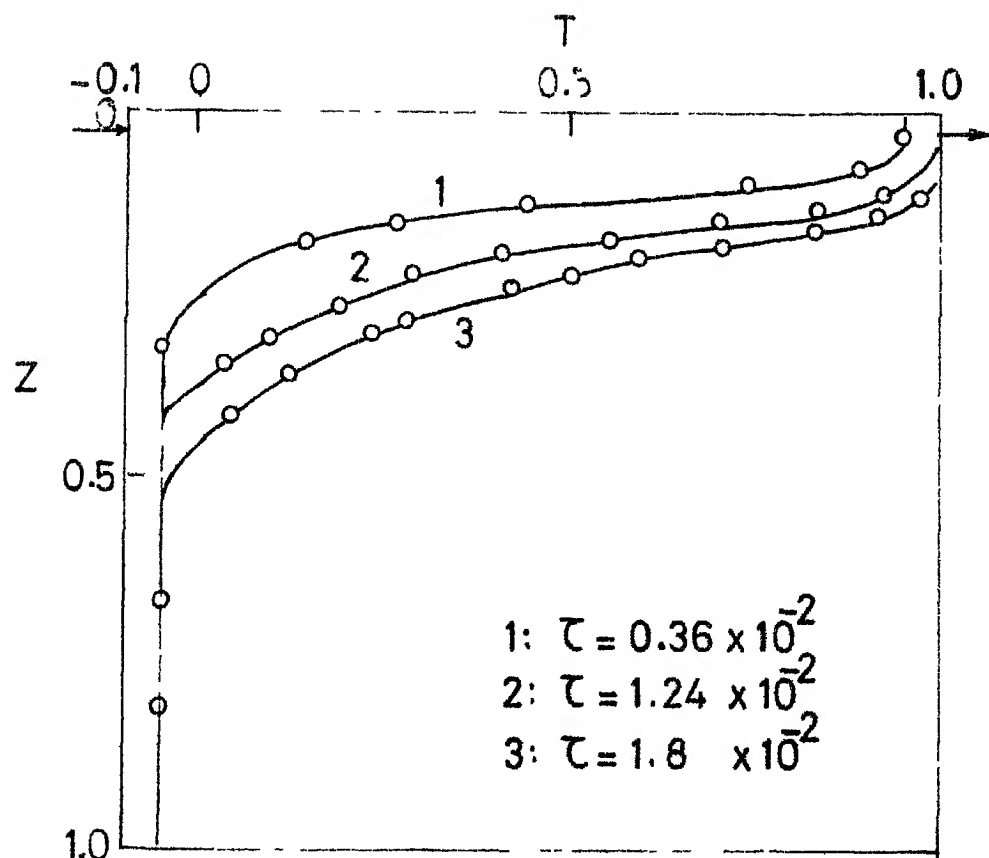


Fig. 2.11 Temperature profiles in an enclosed water body, with inflow and outflow located at the top on opposite sides
 $(Re = 4656.25; Q_1 = 1.2 \times 10^{-5} \text{ m}^3/\text{sec}$
 $\text{and } V = 0.1548 \text{ m}^3).$

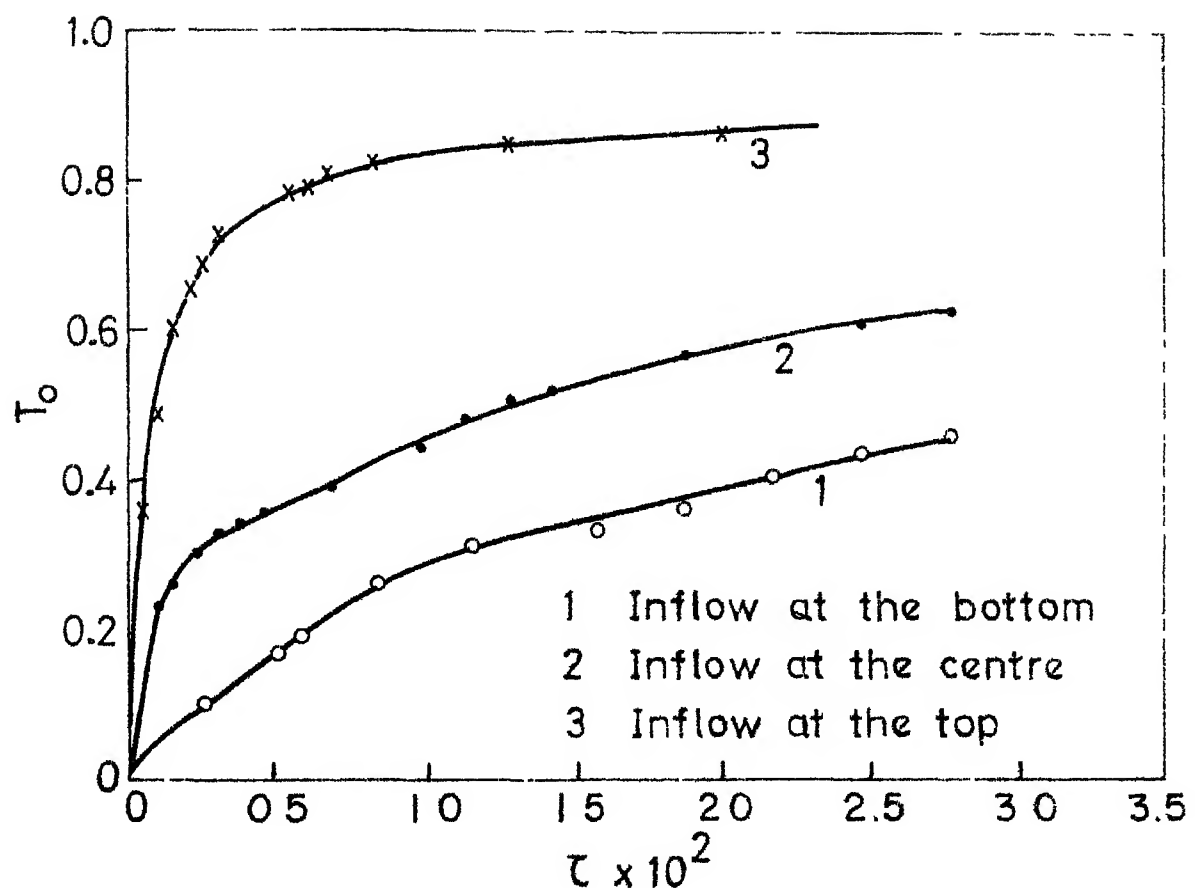


Fig. 2.12 Outflow temperature versus time for various inflow locations on one side and outflow located at the top on the opposite side.
 $(Re = 1651.75$ and $V = 6.1548 \text{ m}^3)$.

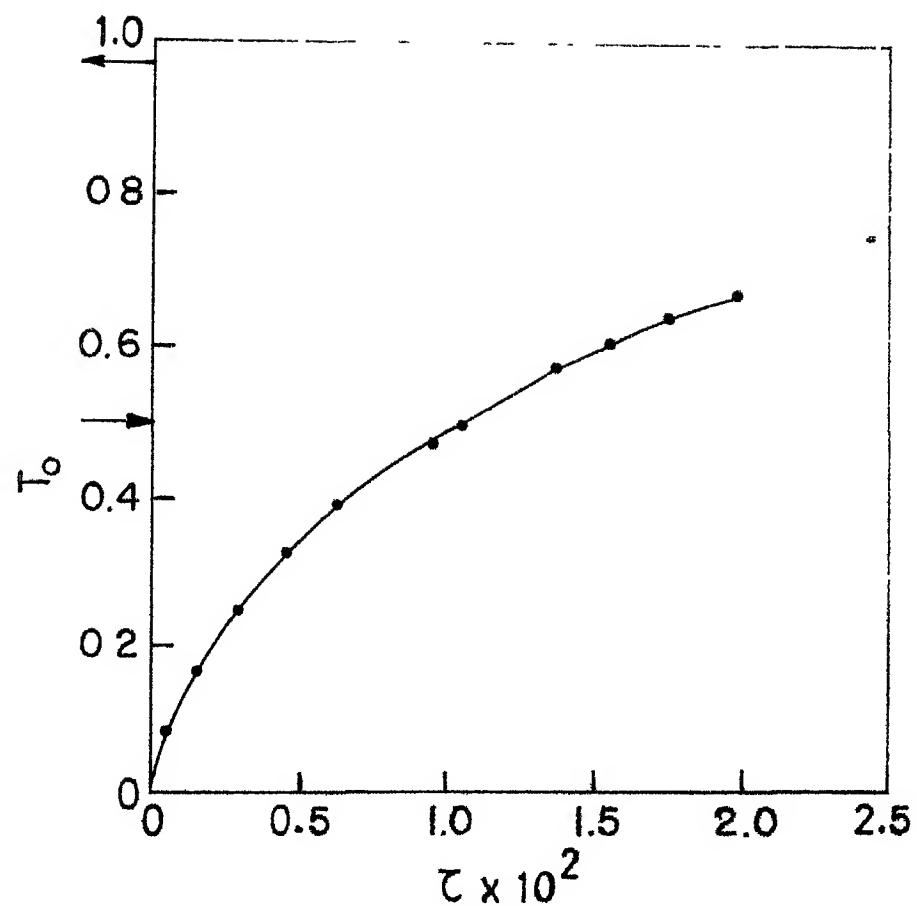


Fig. 2.13 Outflow temperature versus time with inflow located at the centre and the outflow at the top on the same side ($Re = 2500$; $Q_i = 0.675 \times 10^{-5} \text{ m}^3/\text{sec}$ and $V = 0.1548 \text{ m}^3$).

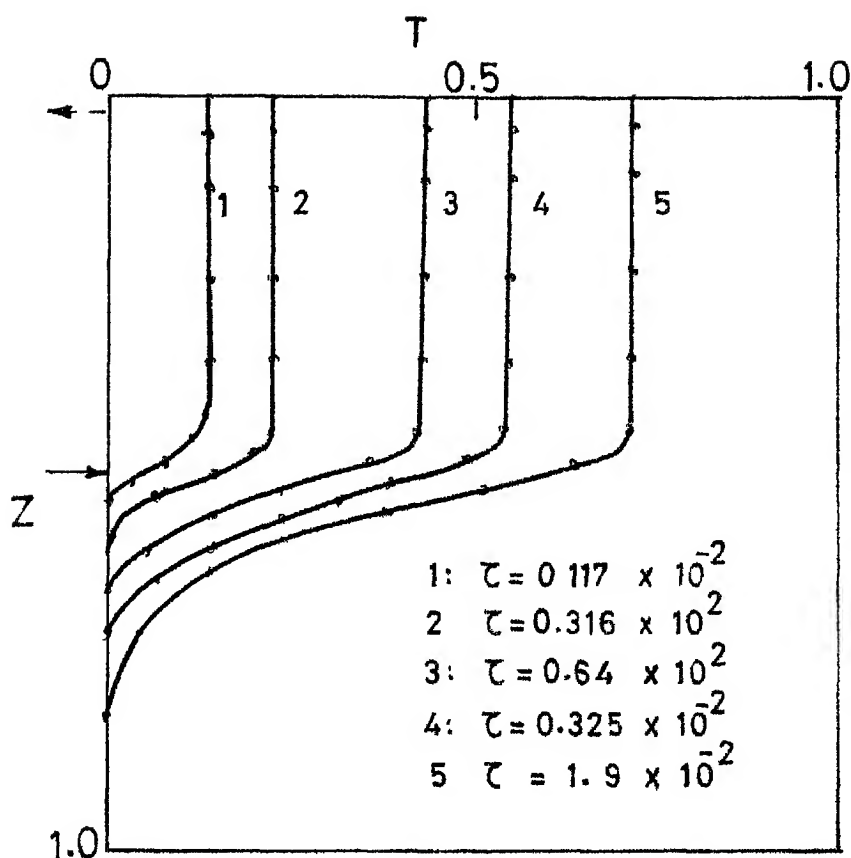


Fig. 2.14 Transient behaviour of the temperature profiles with the inflow and outflow located as shown

($Re = 2500$; $Q_1 = 0.675 \times 10^{-5} \text{ m}^3/\text{sec}$ and $V = 0.1548 \text{ m}^3$).

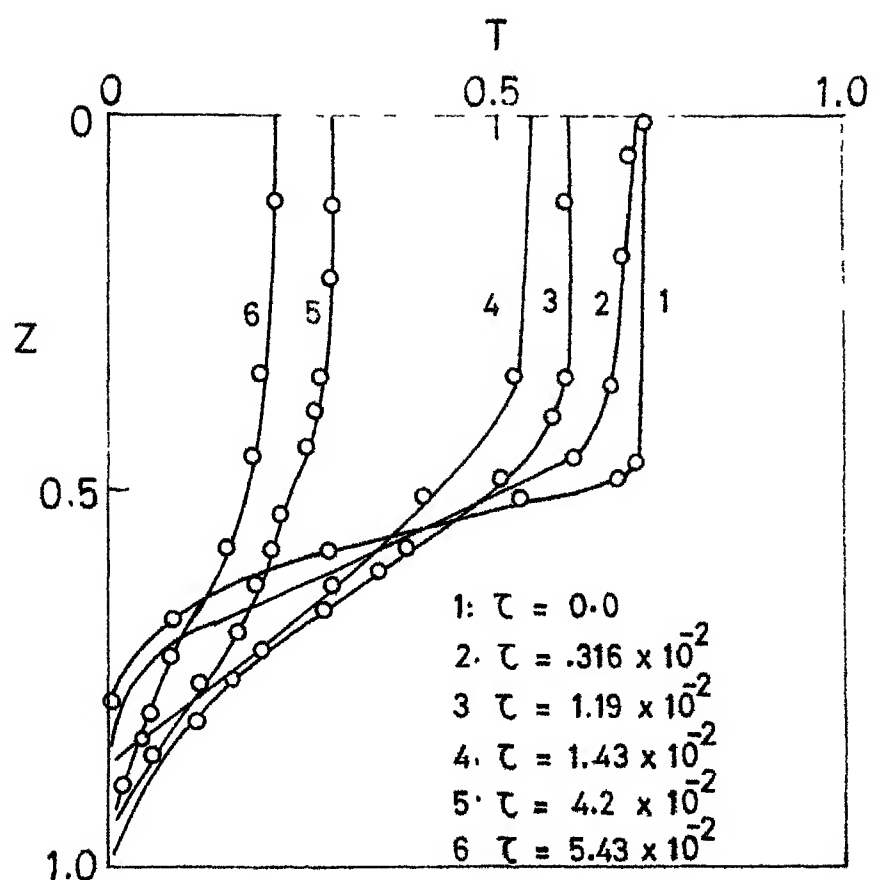


Fig. 2.15 Temperature decay of the stratified enclosed water body in absence of the flow.

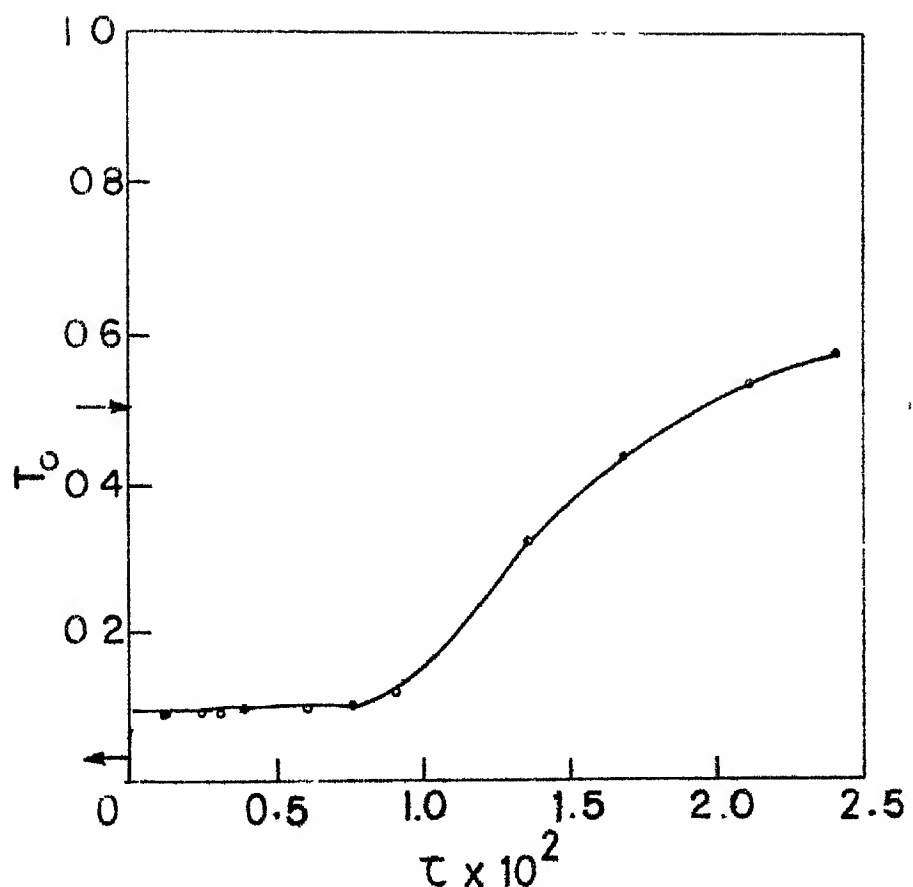


Fig. 2.16 Outflow temperature versus time with inflow and outflow located on the same side of an enclosed water body
($Re = 2,500$; $Q_1 = 0.675 \times 10^{-5} \text{ m}^3/\text{sec}$ and $V = 0.1540 \text{ m}^3$).

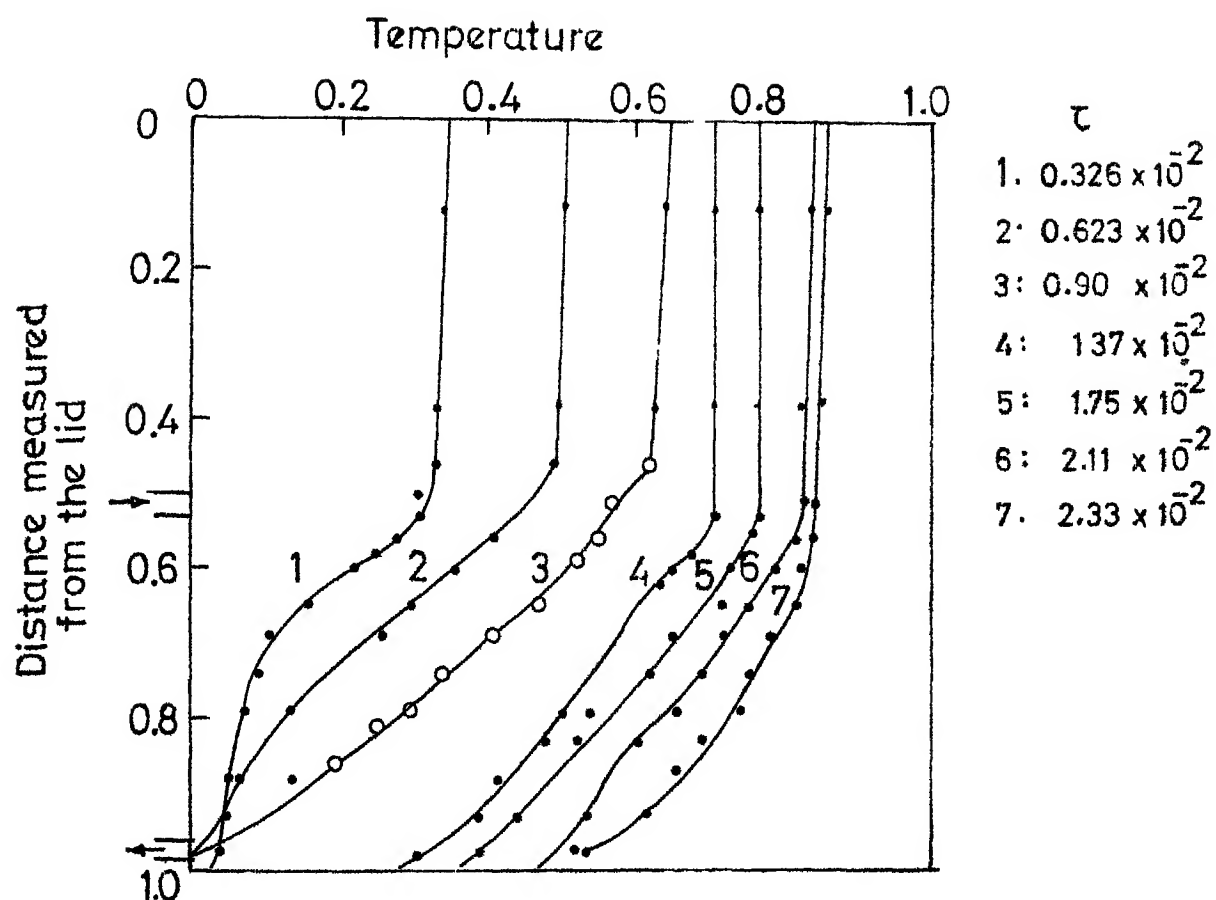


Fig. 2.17 Temperature profiles in an enclosed water body. The arrows indicate the direction of inflow and outflow ($Re = 2,500$; $Q_1 = 0.675 \times 10^{-5} \text{ m}^3/\text{sec}$ and $V = 0.1548 \text{ m}^3$).

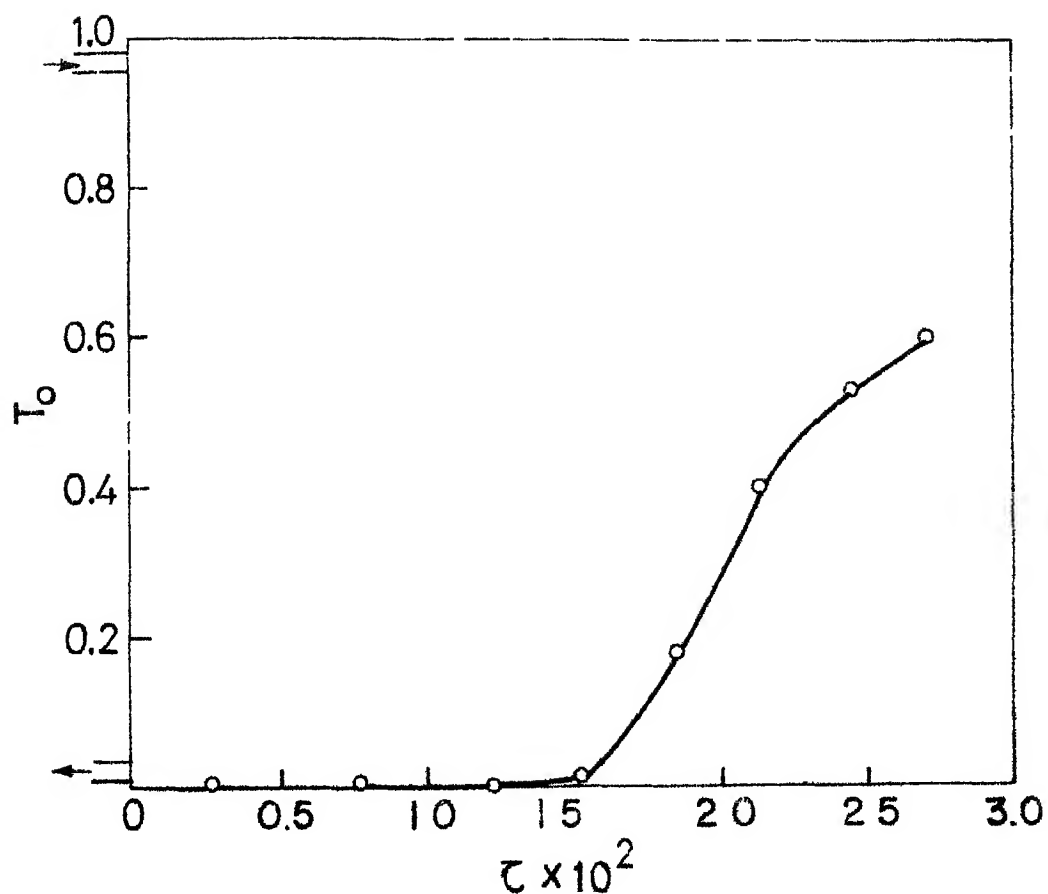


Fig. 2.18 Outflow receptacle mixture versus time, with the inflow and outflow located as shown ($Re = 2,500$; $G_1 = 0.675 \times 10^{-5} \text{ m}^3/\text{sec}$ and $V = 0.1540 \text{ m}^3$).

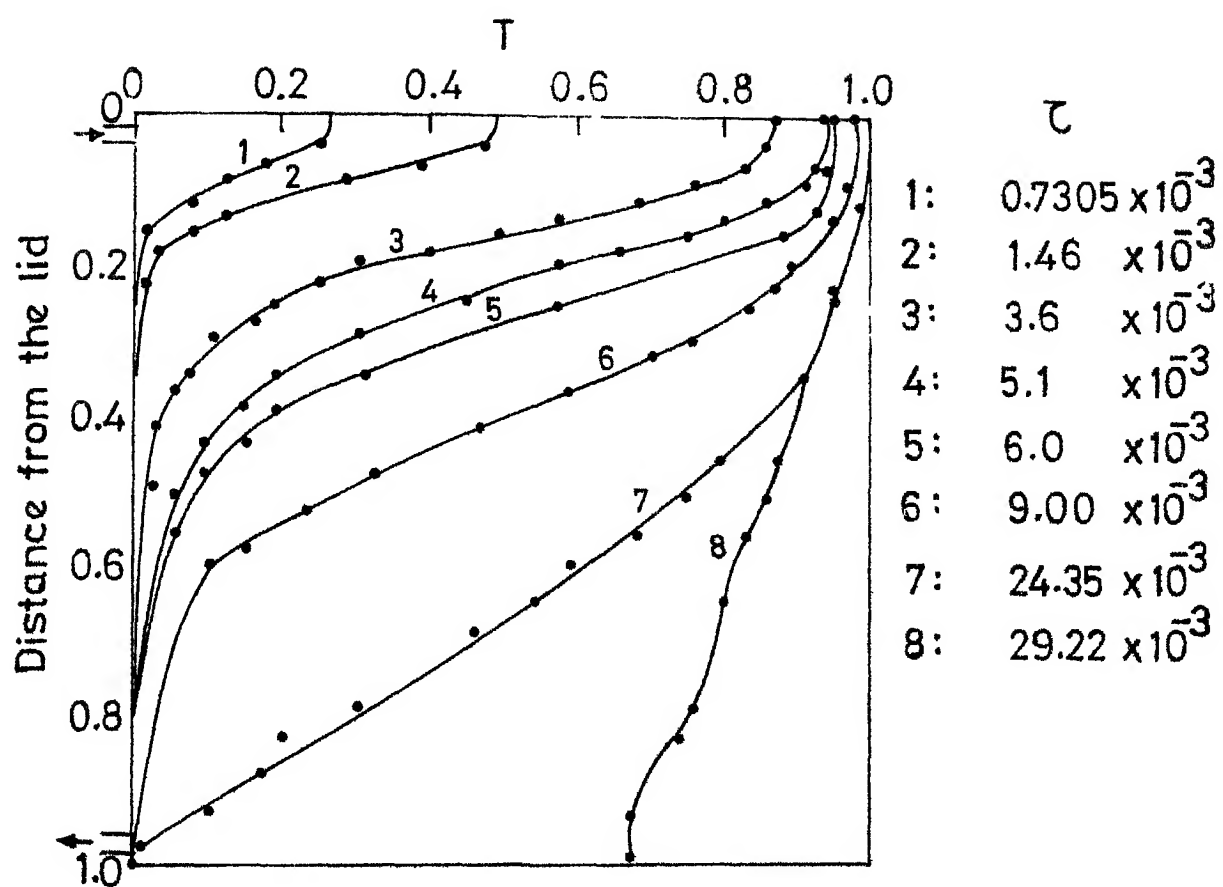


Fig. 2.19 Transient bimodal temperature profiles with inflow and outflow located at the top and at the bottom respectively, on the same side of an enclosed water body ($Re = 2,500$; $C_1 = 0.675 \times 10^{-5} \text{ m}^3/\text{sec}$ and $V = 0.1548 \text{ m}^3$).

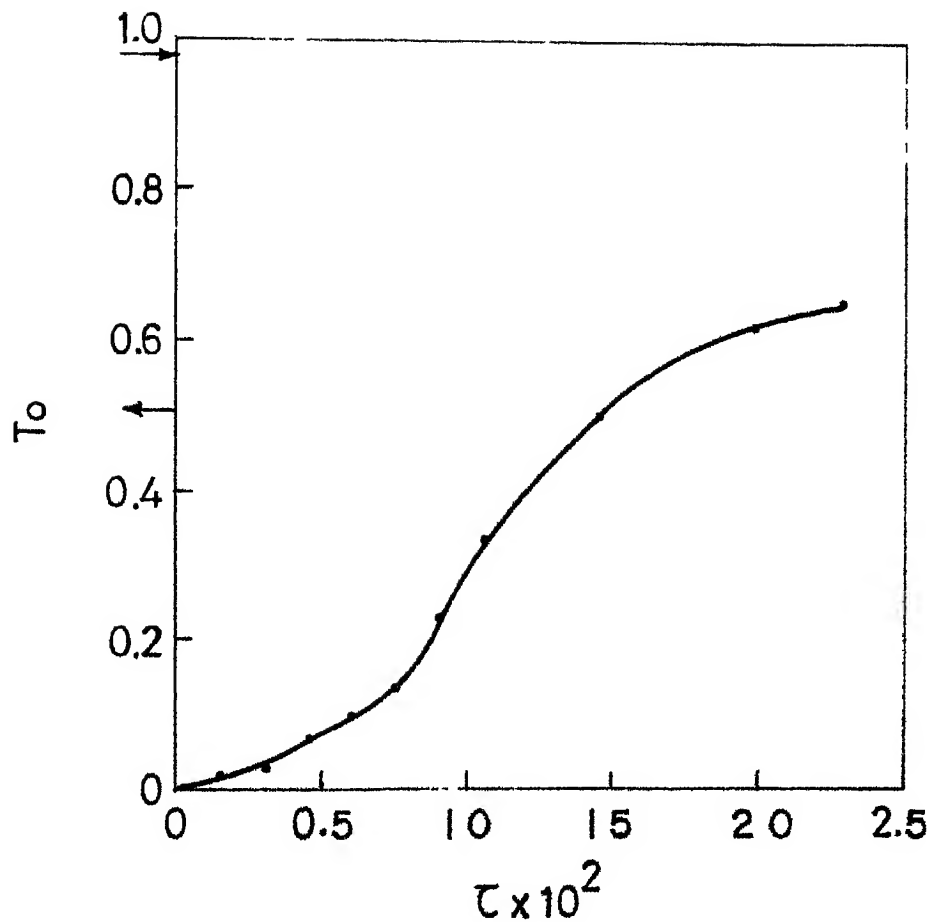


Fig. 2.20 Transient behaviour of the outflow temperature T_o with inflow and outflow configuration as in Fig. 2.16
($Re = 2,500$; $Q_1 = 0.675 \times 10^{-3} \text{ m}^3/\text{sec}$
and $V = 0.1545 \text{ m}^3$).

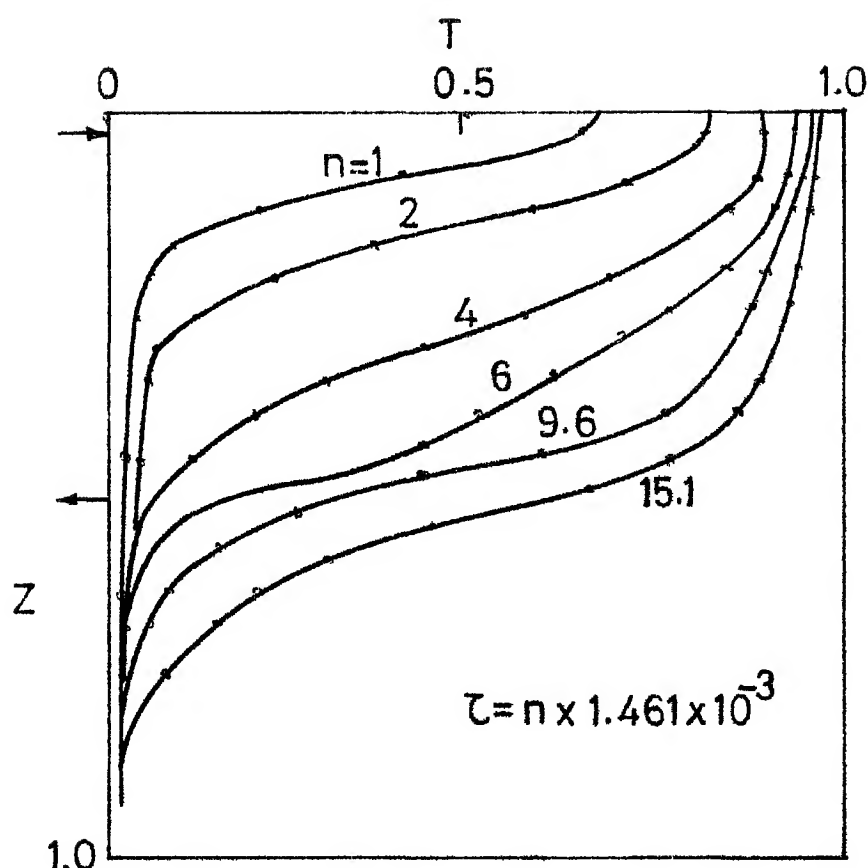
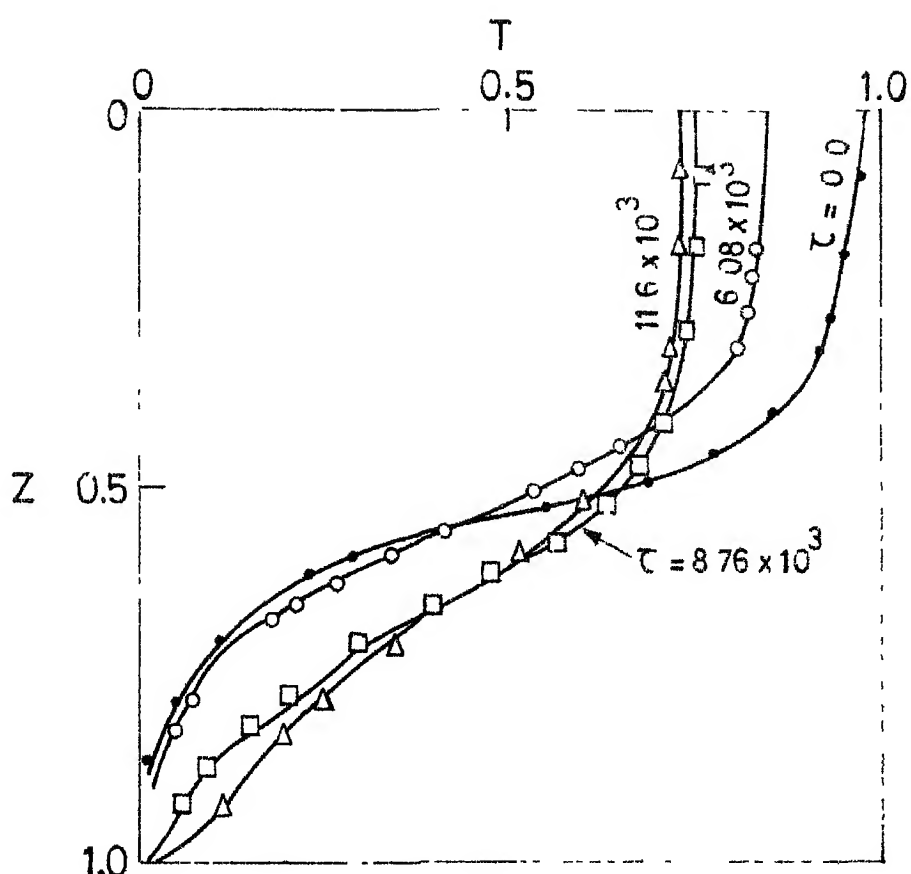


FIG. 2.21 Transient behaviour of the temperature profiles with inflow and outflow located as shown
 $(Re = 2,500; Q_1 = 0.675 \times 10^{-5} m^3/sec$
and $V = 0.1548 m^3)$.



$T_1 = 1.0^\circ\text{C}$ Temperature profiles for a semi-infinite enclosed water body in contact to cool in the absence of flow.

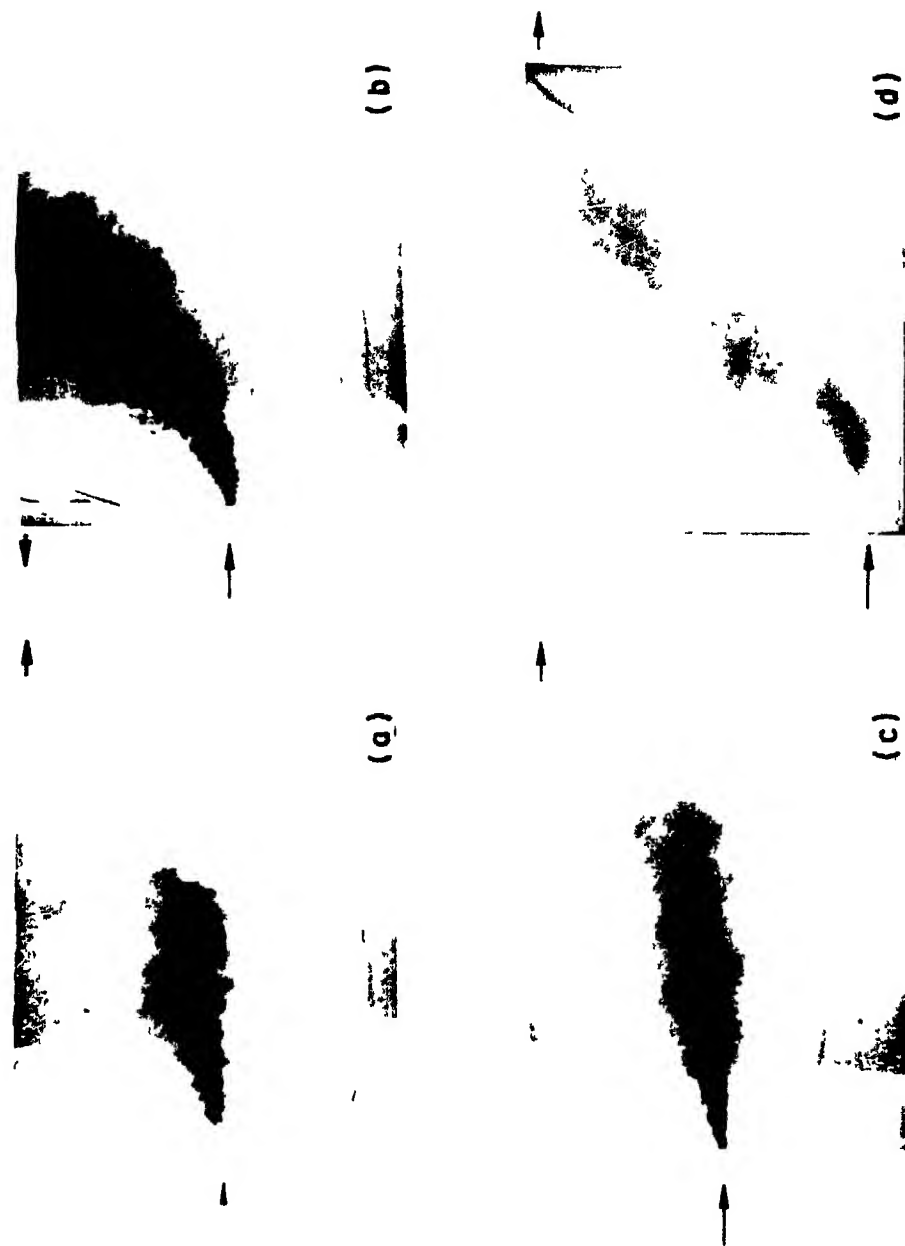


Fig 2.23 Trajectory of discharge (a) $Re = 2500, \Delta T = 0^\circ C$,
(b) $Re = 2500, \Delta T = 25^\circ C$, (c) $Re = 6250, \Delta T = 25^\circ C$,
(d) $Re = 2500, \Delta T = 25^\circ C$. The arrows indicate the direction of inflow and outflow

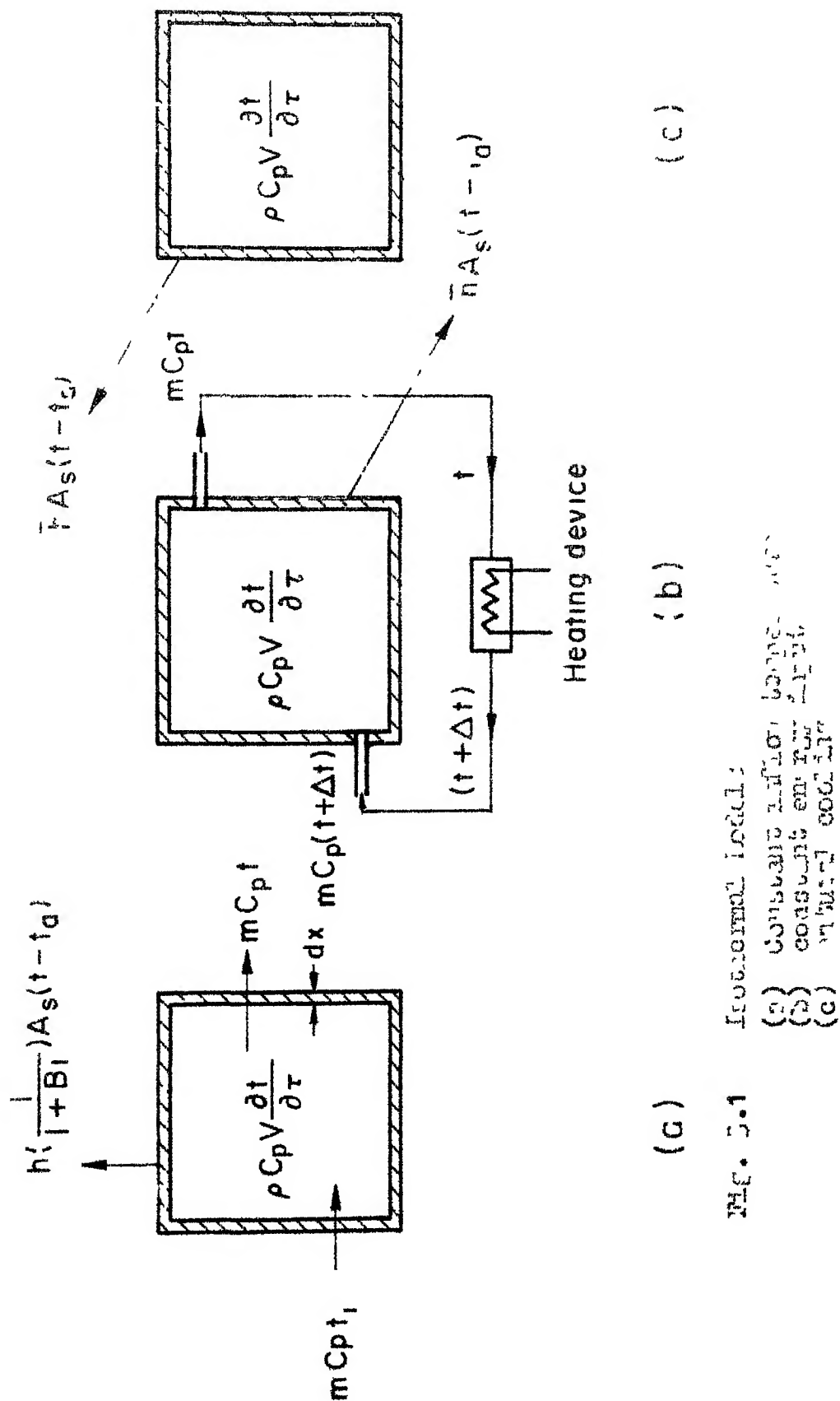
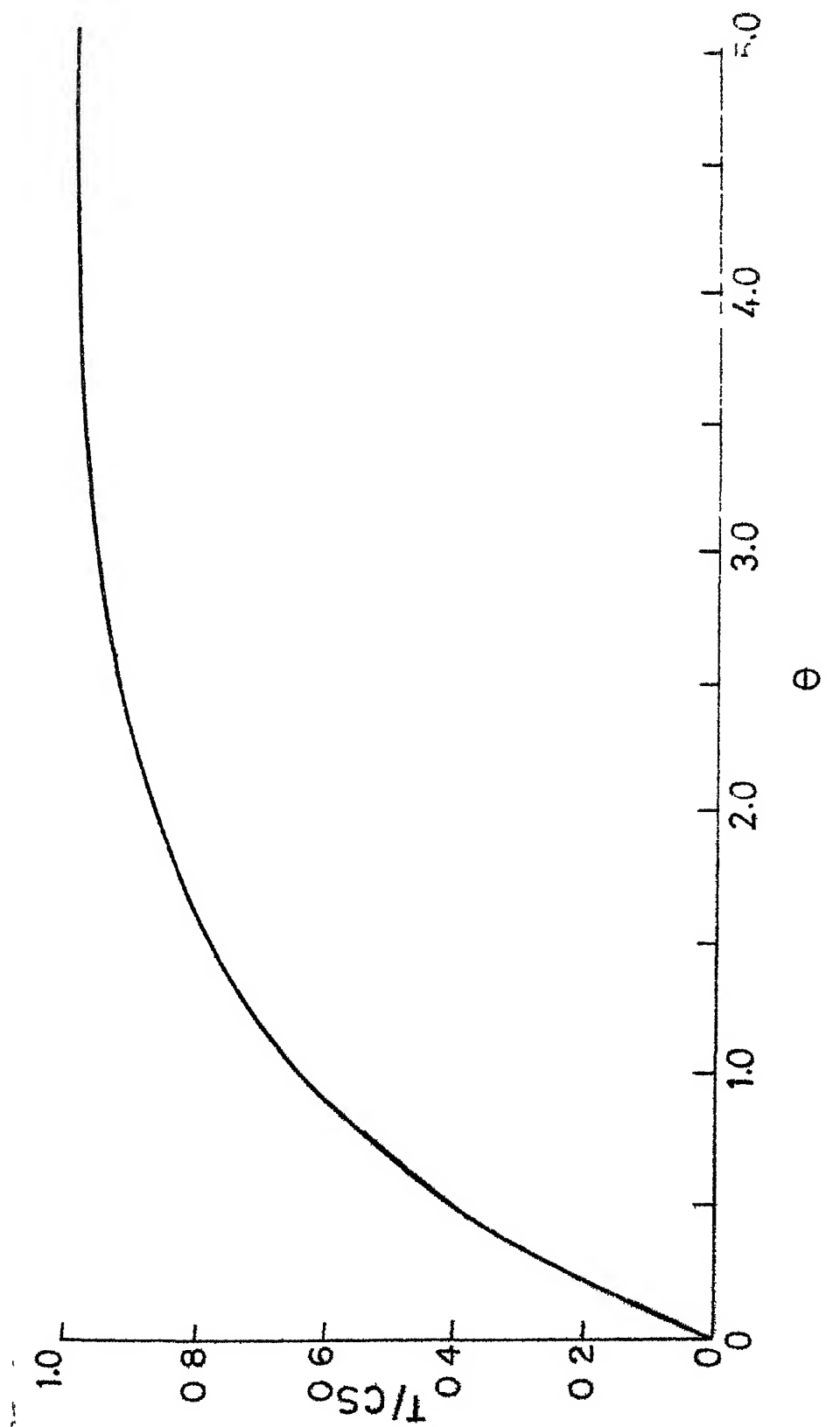


Fig. 5.1 Internal load:

- (a) Constant resistance
- (b) constant ρC_p
- (c) variable ρC_p



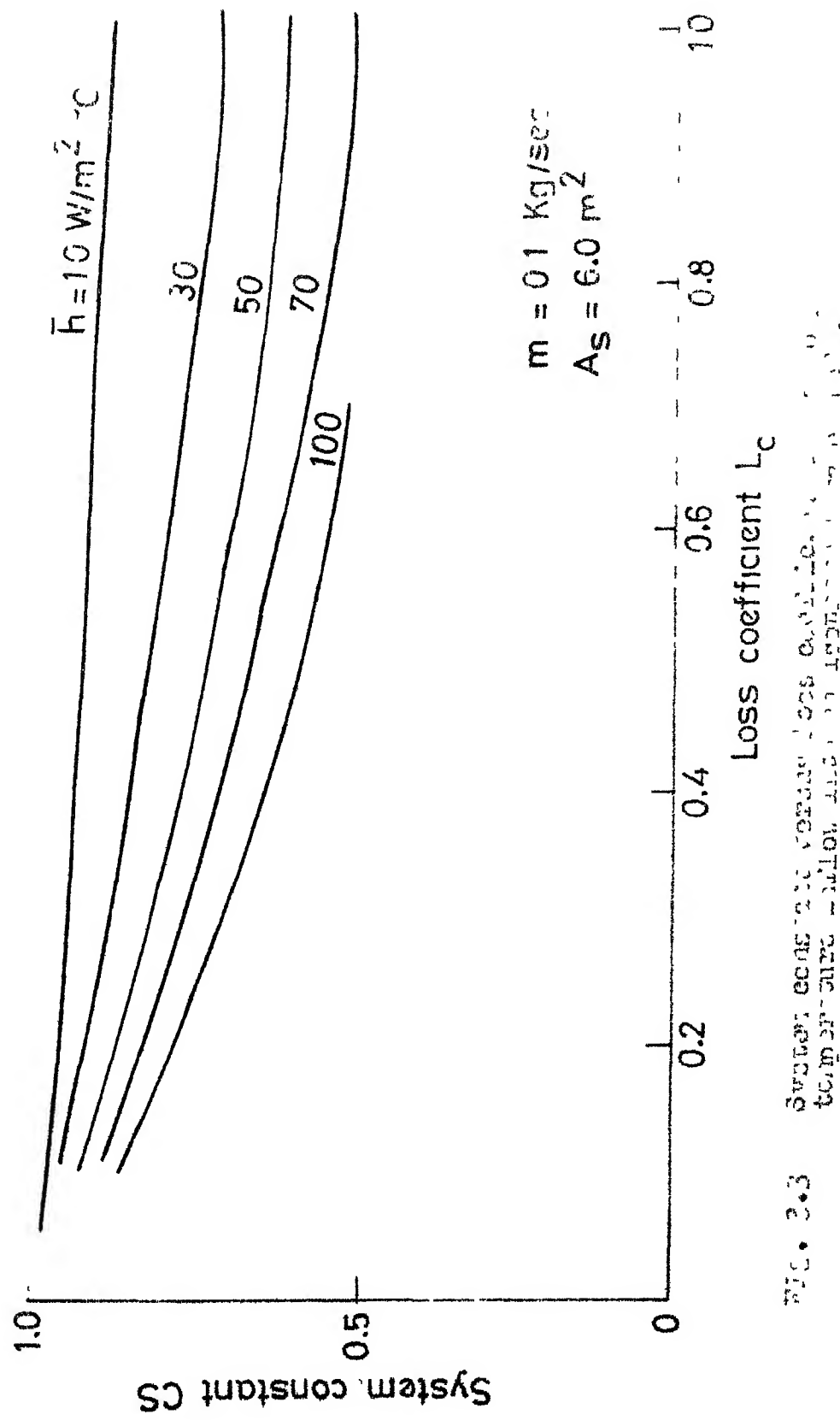


Fig. 3.3 Effect of system loss coefficient on system constant for different values of \bar{h} .

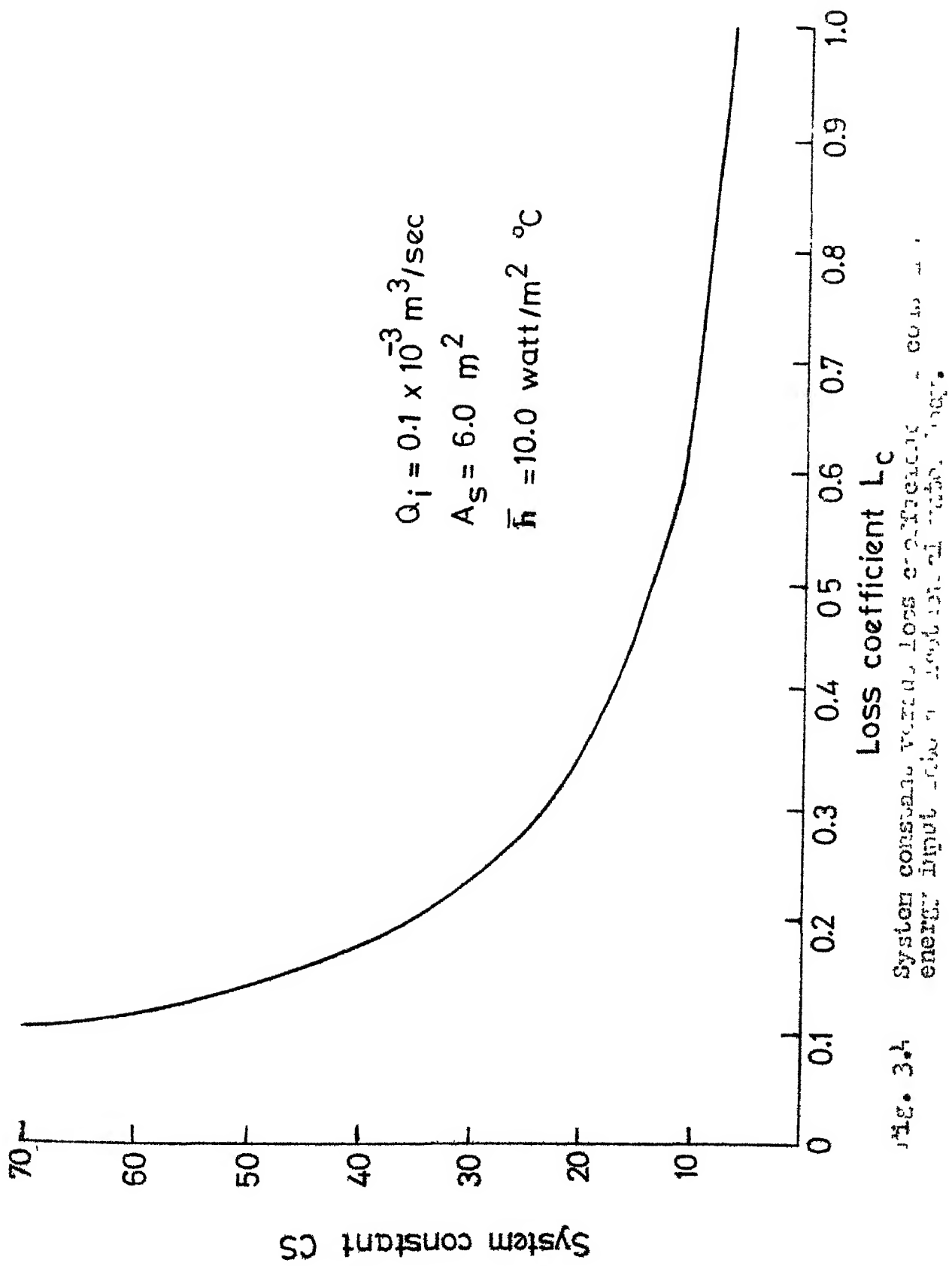


Fig. 3.4 System constant versus Loss coefficient L_C .
Input energy - r_{in} , output energy - r_{out} .

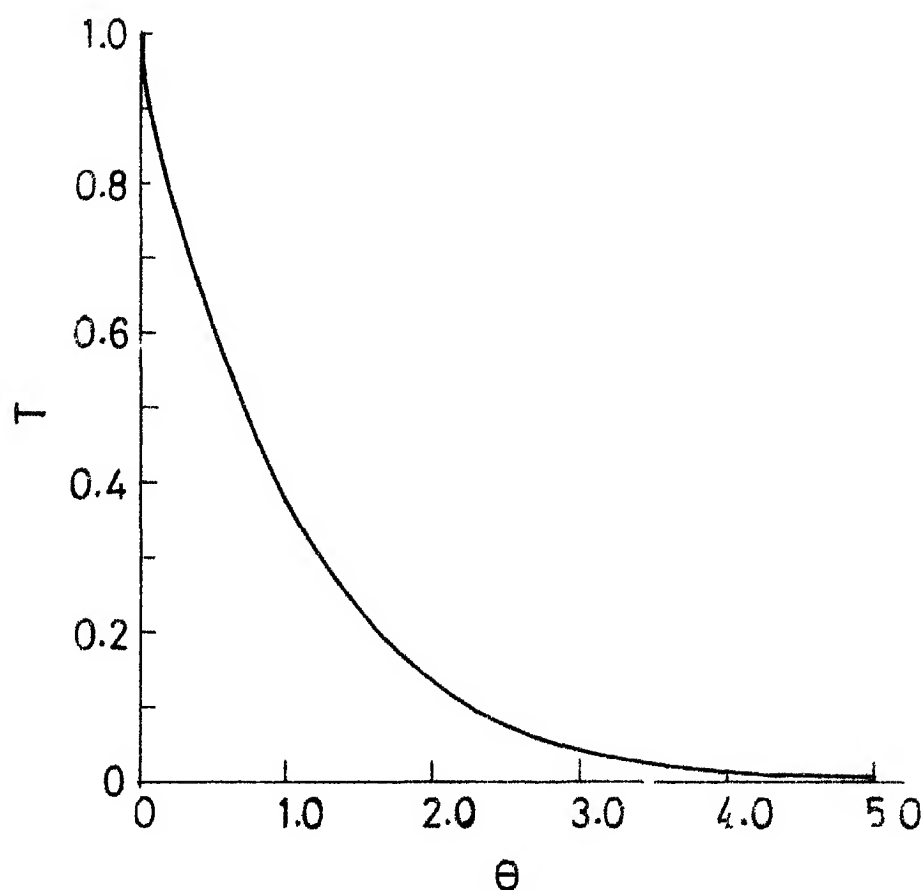


Fig. 1. The dependence of T on θ for different values of α .

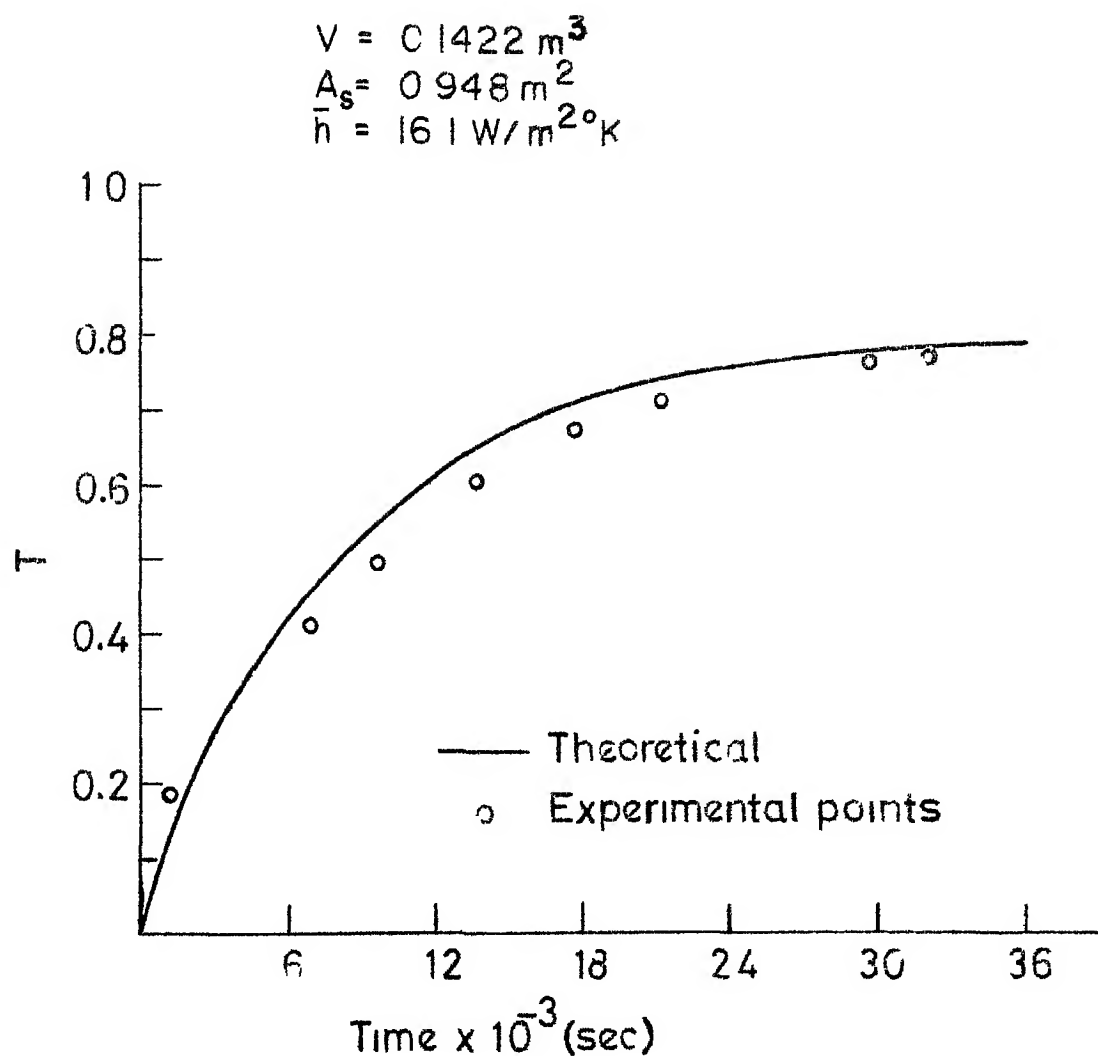
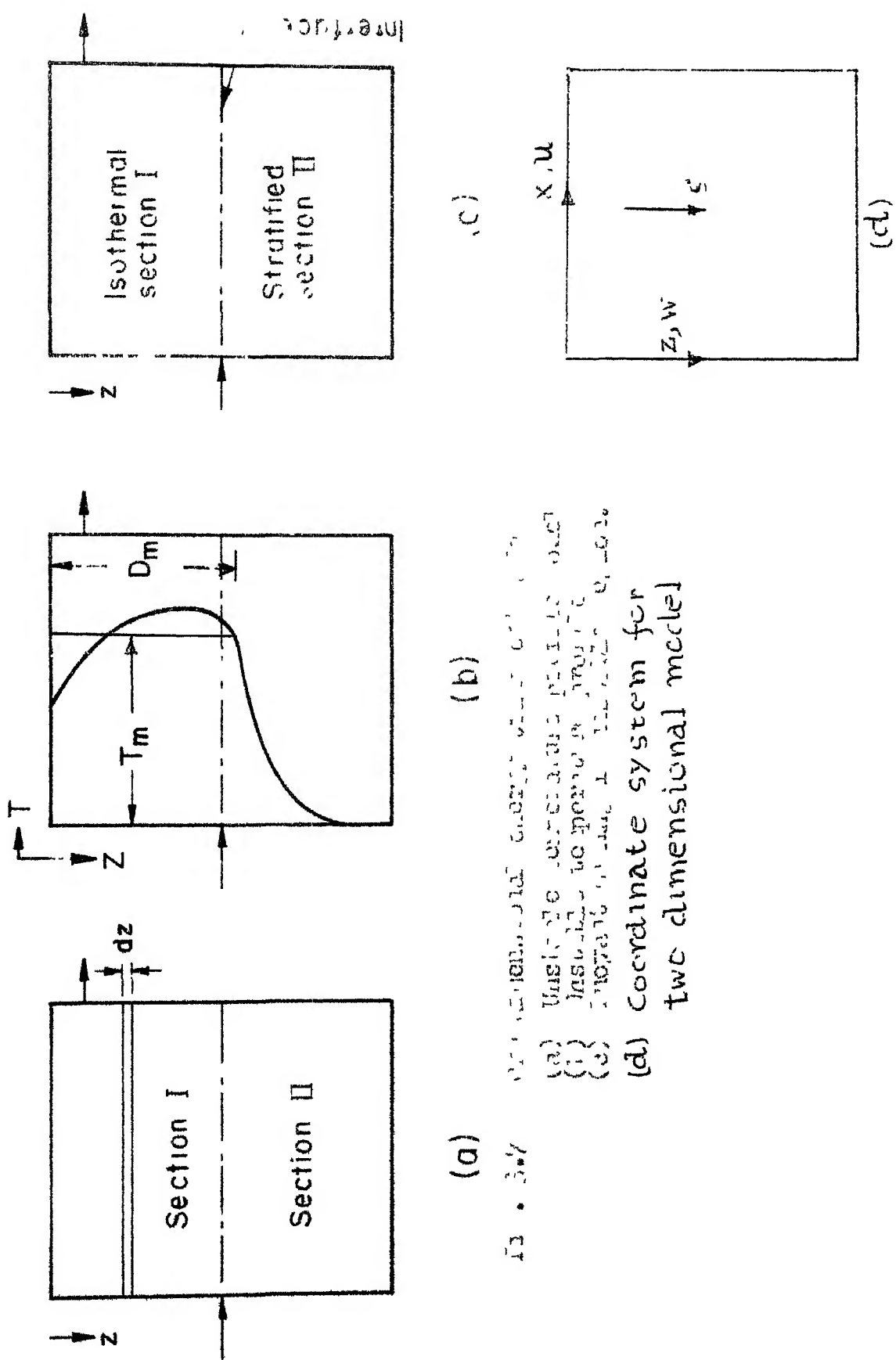


FIG. D.6 Comparison between theoretical and experimental results for a rectangular body.



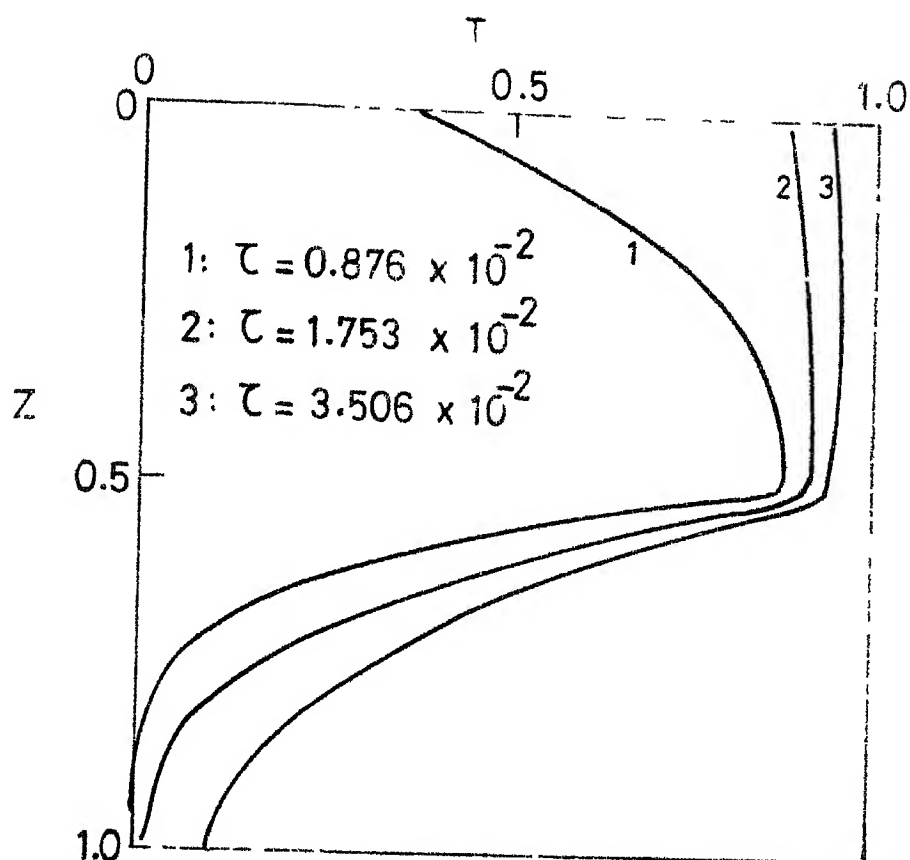


Fig. 3.3 Temperature profile in an invader body fluid due to infiltration with inflow rate $1.0 \times 10^3 \text{ sec}^{-1}$ at the centre and at the corner respectively.
 $(\rho_e = 2,500; \alpha_1 = 0.07 \times 10^{-3} \text{ m}^2/\text{sec}, V = 0.142 \text{ m}^2)$.

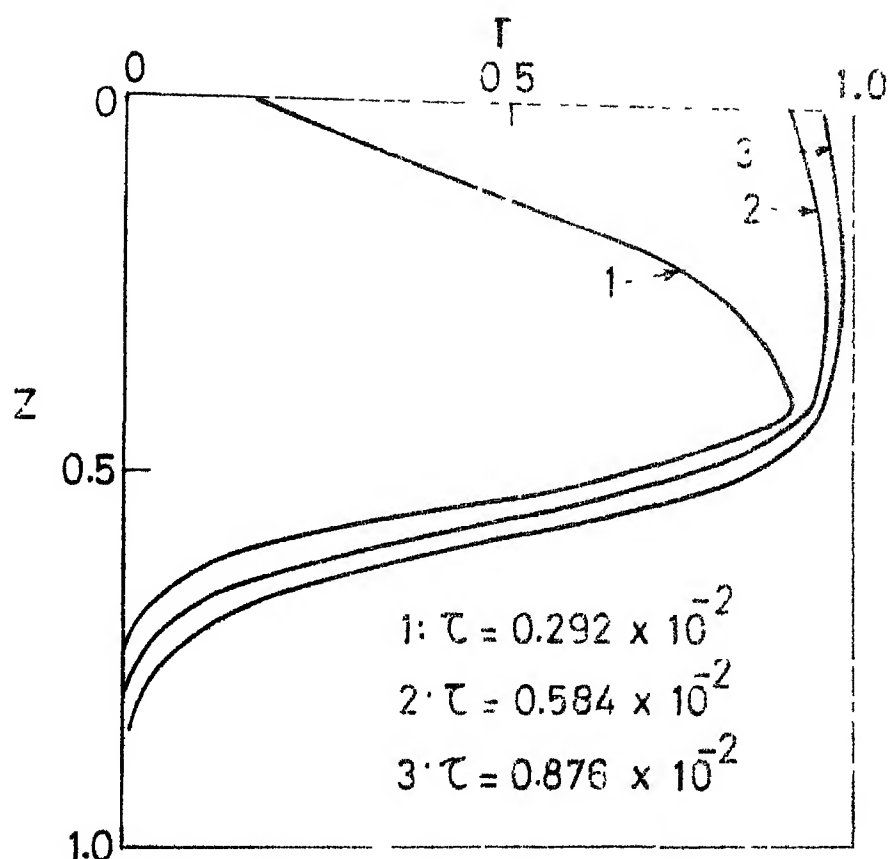


Fig. 3.9 Thermal profile in a rotating cylinder with a central heat source and a cold boundary. (Re = 6250; $L_z = 1.07 \times 10^{-2}$; $V = 0.147 \times 10^{-2}$).

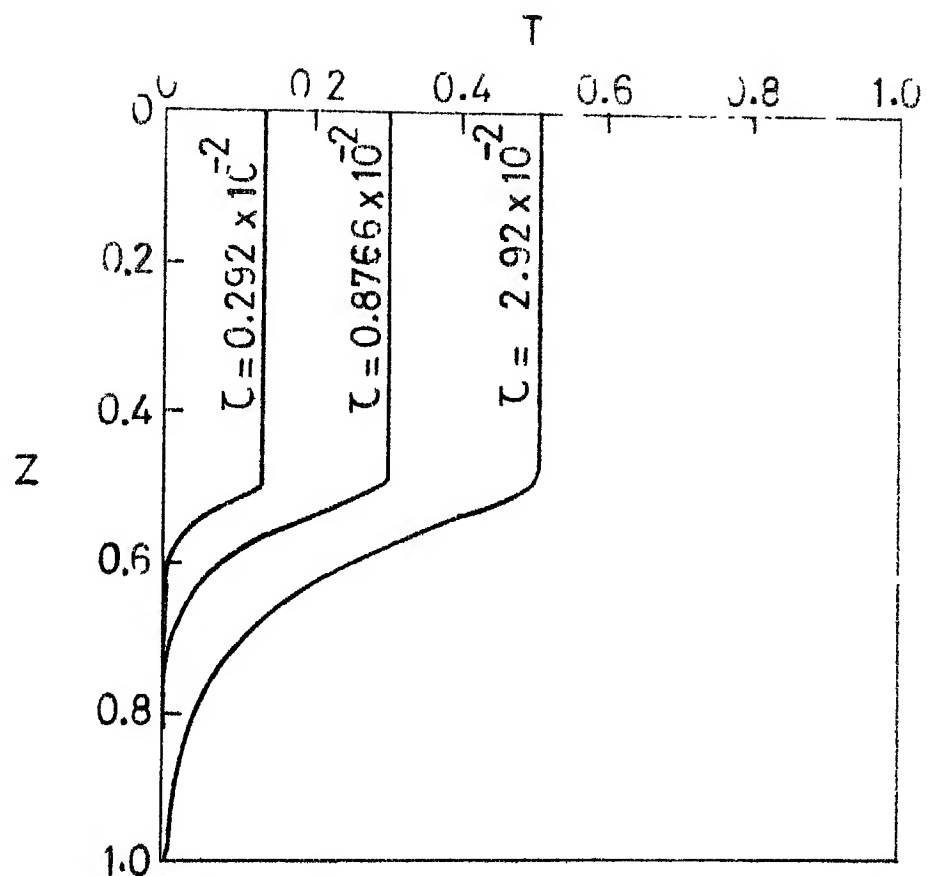


Fig. 3.10 Thermal profiles in an end-on circular cylinder with infarated outflow located at the centre and at the corner respectively ($Re = 1250$; $\alpha_1 = 0.55 \times 10^{-3} \text{ m}^3/\text{sec}$; $H = 16.1 \text{ W/m}^2 \text{ o}_1$).

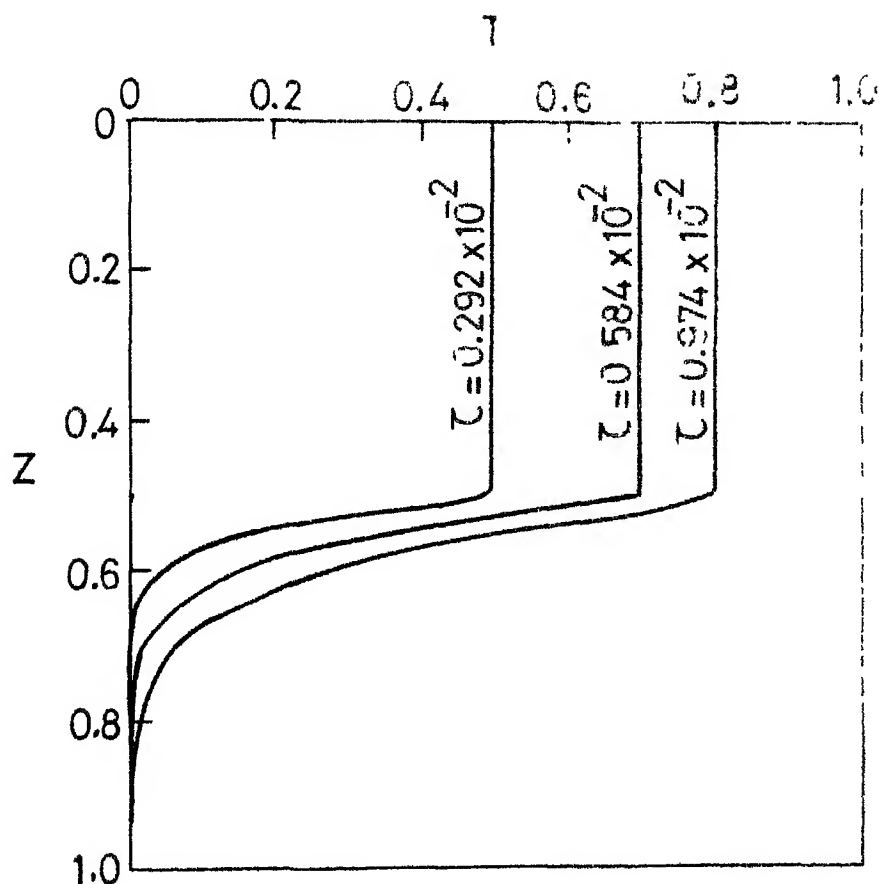


FIG. 3.11 Thermal profiles in an enclosure type body with inflow and outflow located at the centre and at the top respectively
 $(Re = 6250; C_i = 0.1675 \times 10^{-1} \text{ m}^3/\text{sec};$
 $\bar{h} = 16.1 \text{ W/m}^2 \text{ }^\circ\text{C}).$

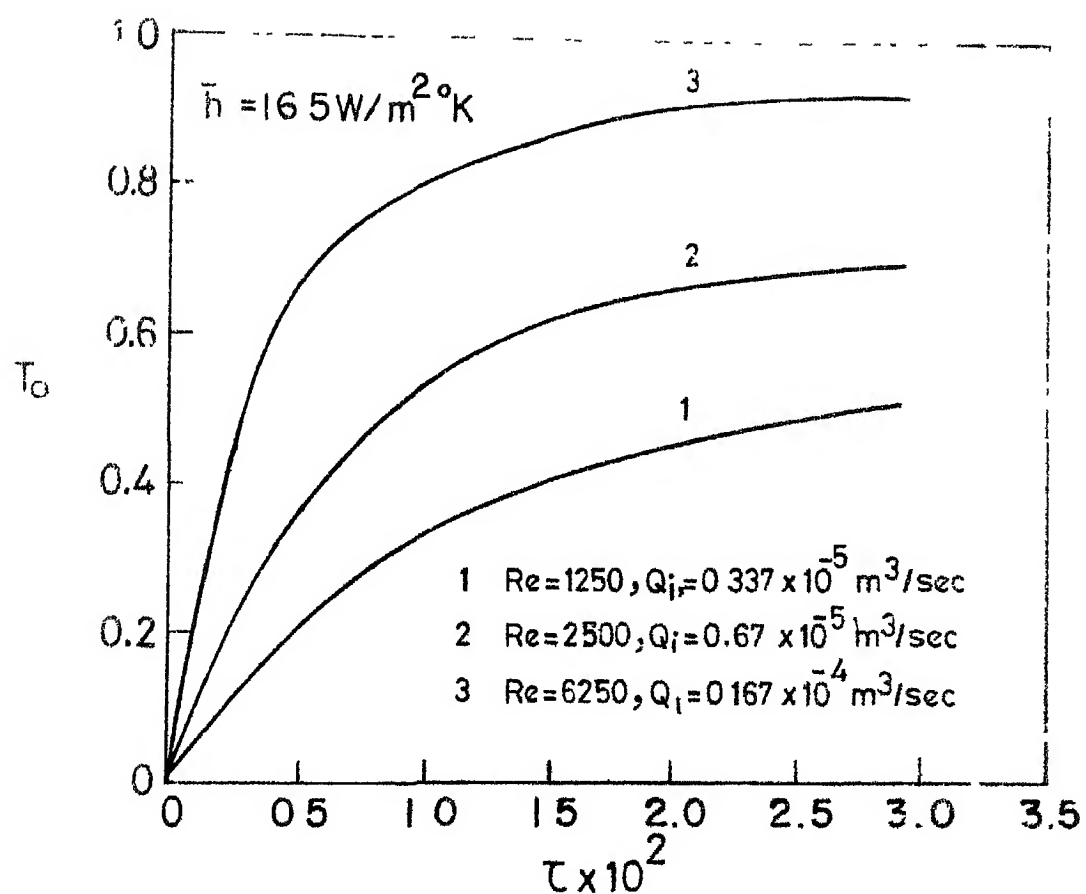


Fig. 12. Transient rise in outlet (top) temperature, top versus normalized time, with inflow localized at the centre and the outlet at the top.

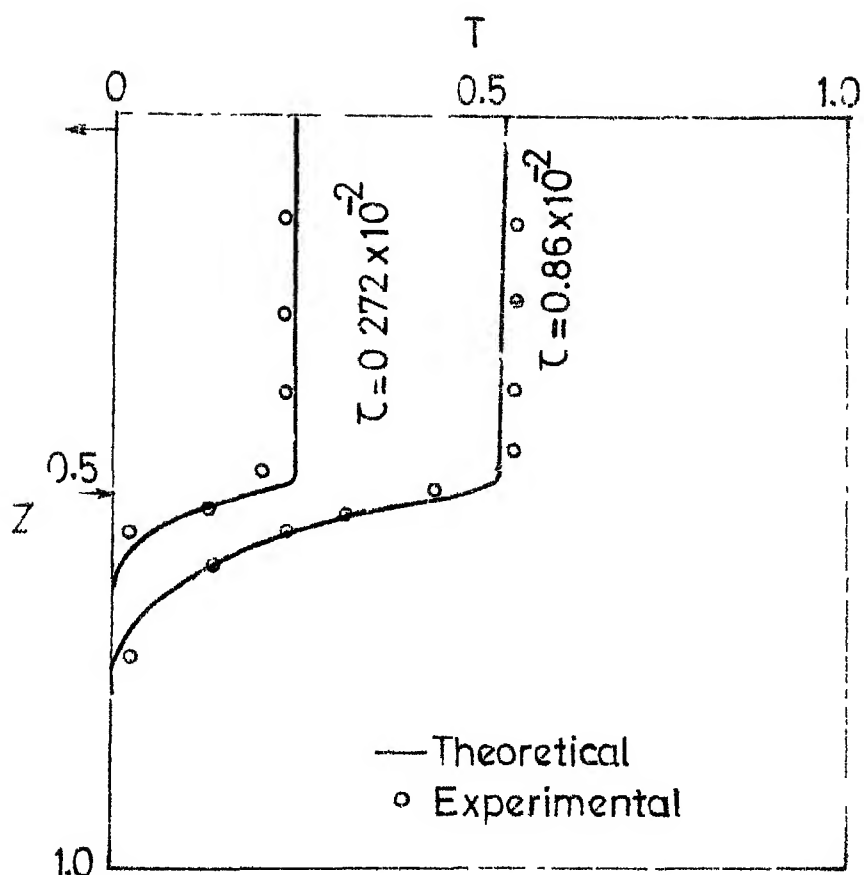


FIG. 3.13: Comparison of prediction of steady-state free-surface elevation versus time for a circular water body with the laboratory solution located in the center unit cell, respectively.

$$(Re = 2,500; \rho_1 = 6.675 \times 10^{-3} \text{ kg/m}^3; \eta_0 = 1.03 \text{ m};$$

$$\gamma = 0.1543 \text{ m}^3; \alpha_0 = 1.03 \text{ m}^2).$$

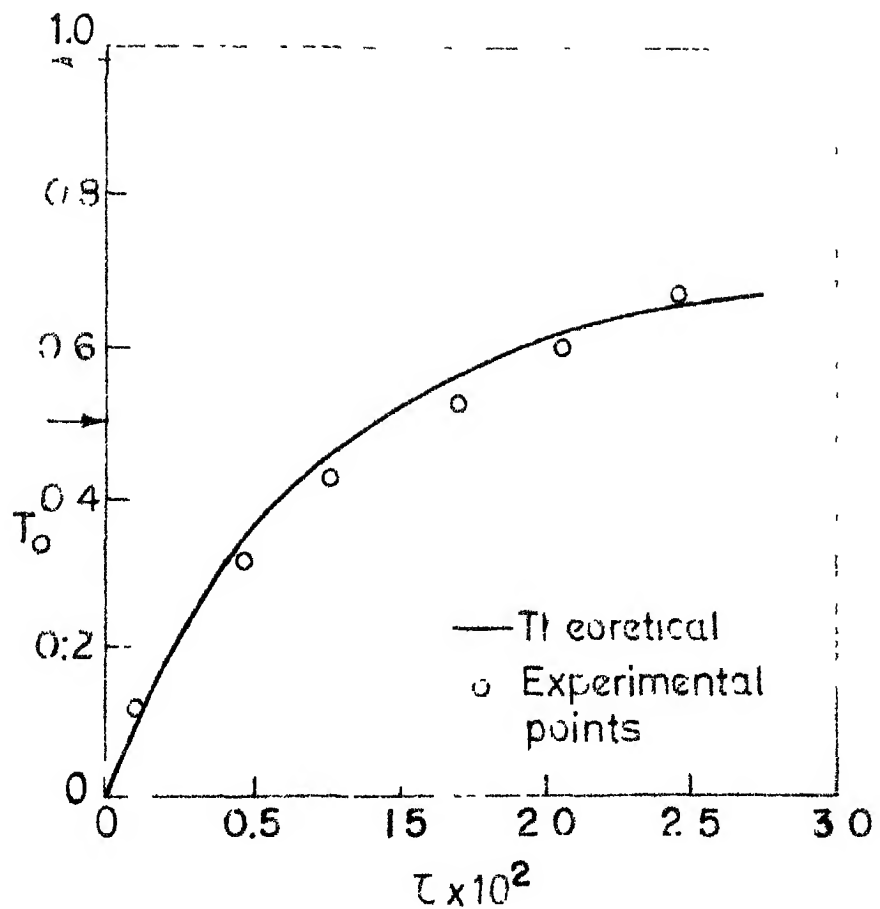


Fig. 3.14 Comparison of predicted and experimental transients outside an open cavity in an enclosed water body under free convection flow located at the center of the cavity top respectively
 $(Re = 1,500; \alpha_s = 0.95 \times 10^{-5} \text{ K}^3/\text{Watt};$
 $V = 0.1646 \text{ m}^3; h = 1.1 \text{ J/m}^2 \text{ }^\circ\text{C};$
 $A_g = 1.6 \text{ m}^2).$

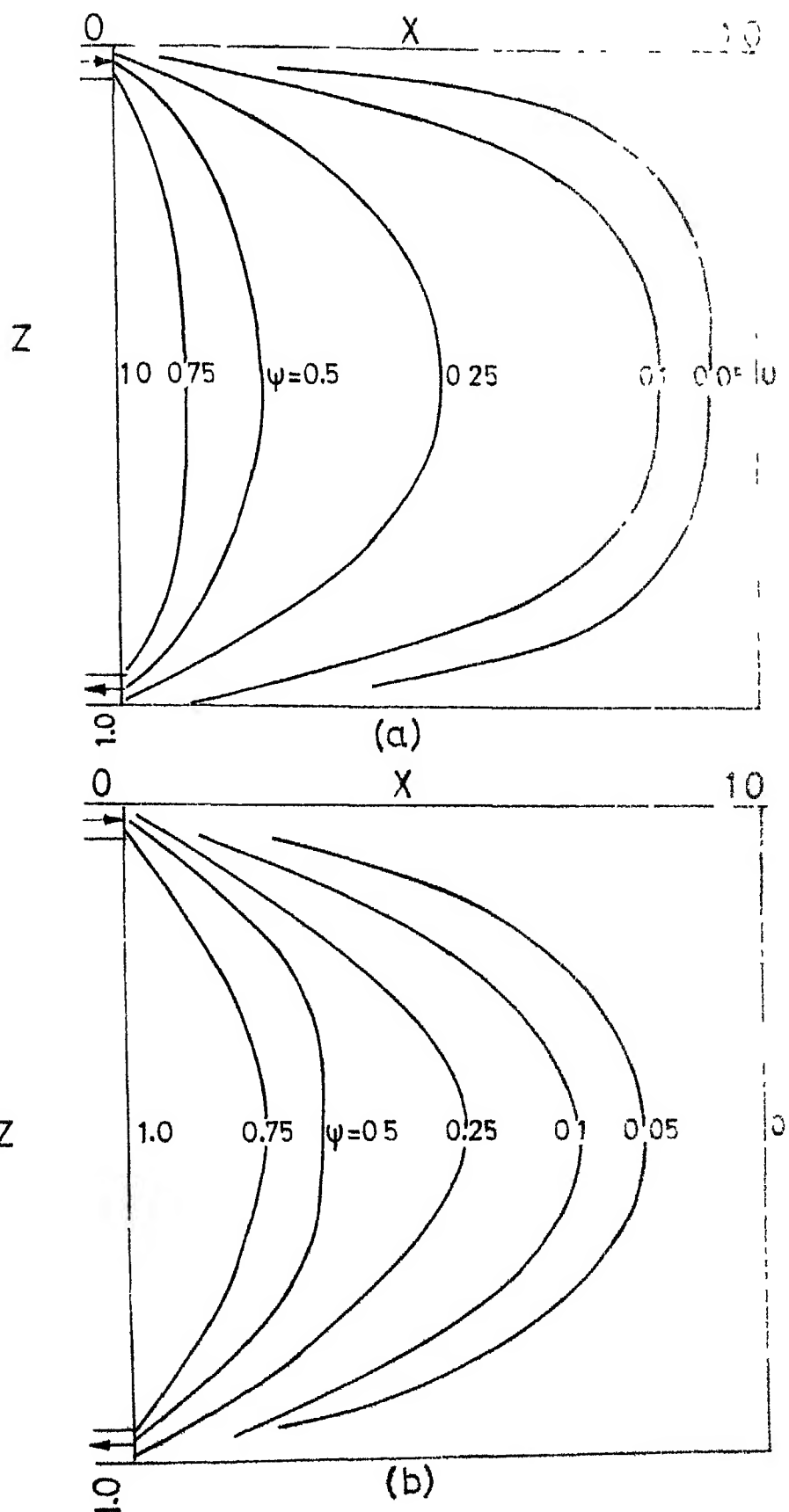


Fig. 3.15 Flow pattern in two-dimentional channel flow, with obstacle and subjected to creeping flow on one side of an enclosed water body,
(a) inviscid flow (b) creeping flow

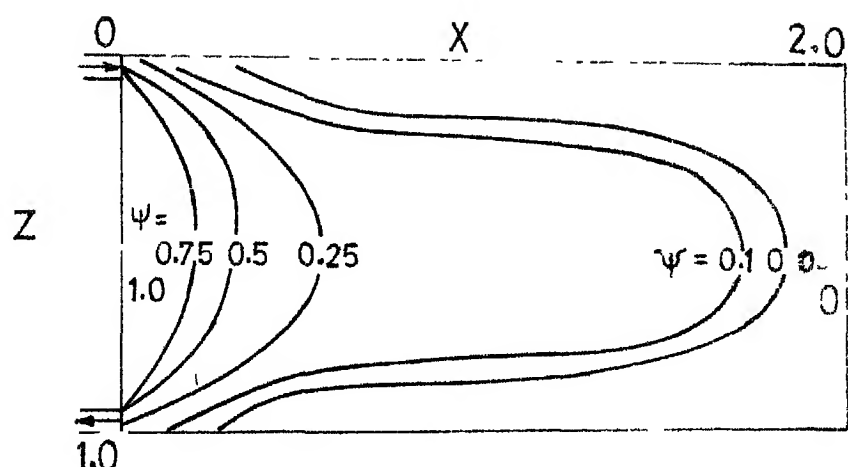


Fig. 3.16 Streamlines in a two-dimensional vertical creeping flow with intake and outfall located at $Z=0$ on the side of the water body.

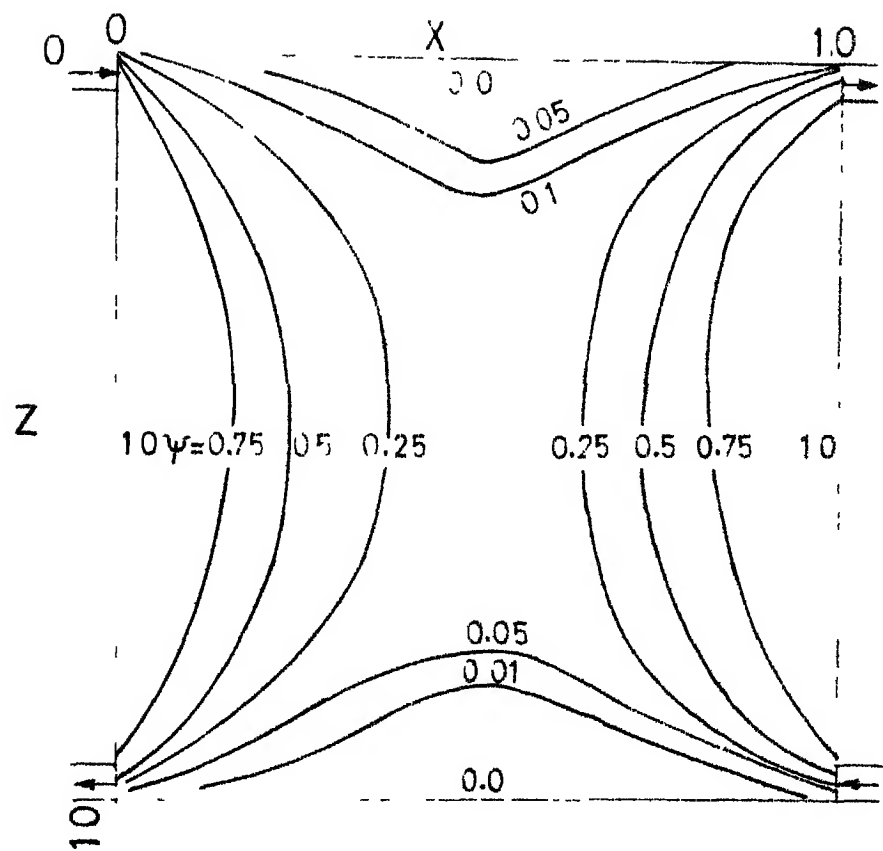


Fig. 3.17 Vertical flow due to an elliptical two flow circuit. This can be used to indicate directions of entry and exit flow.

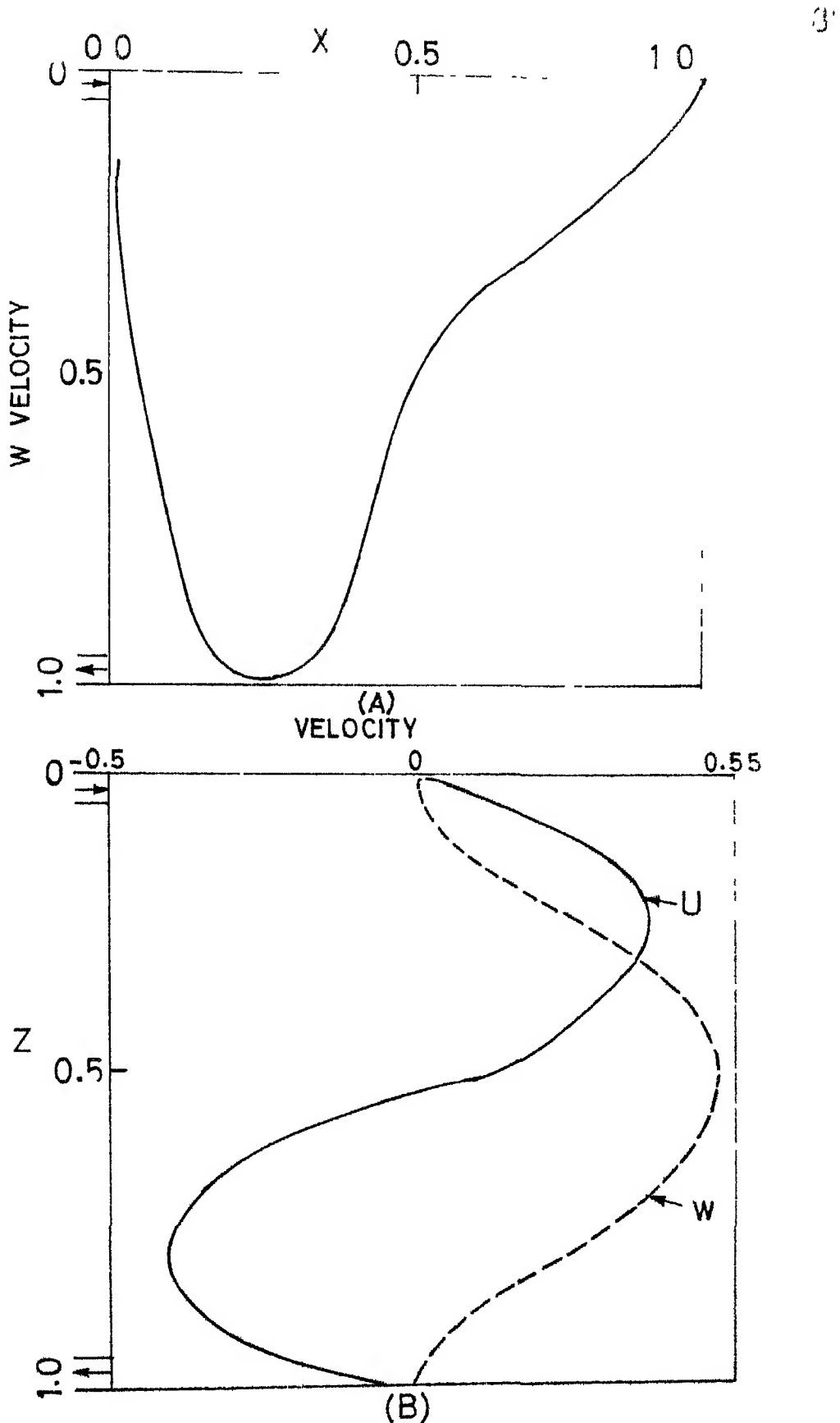
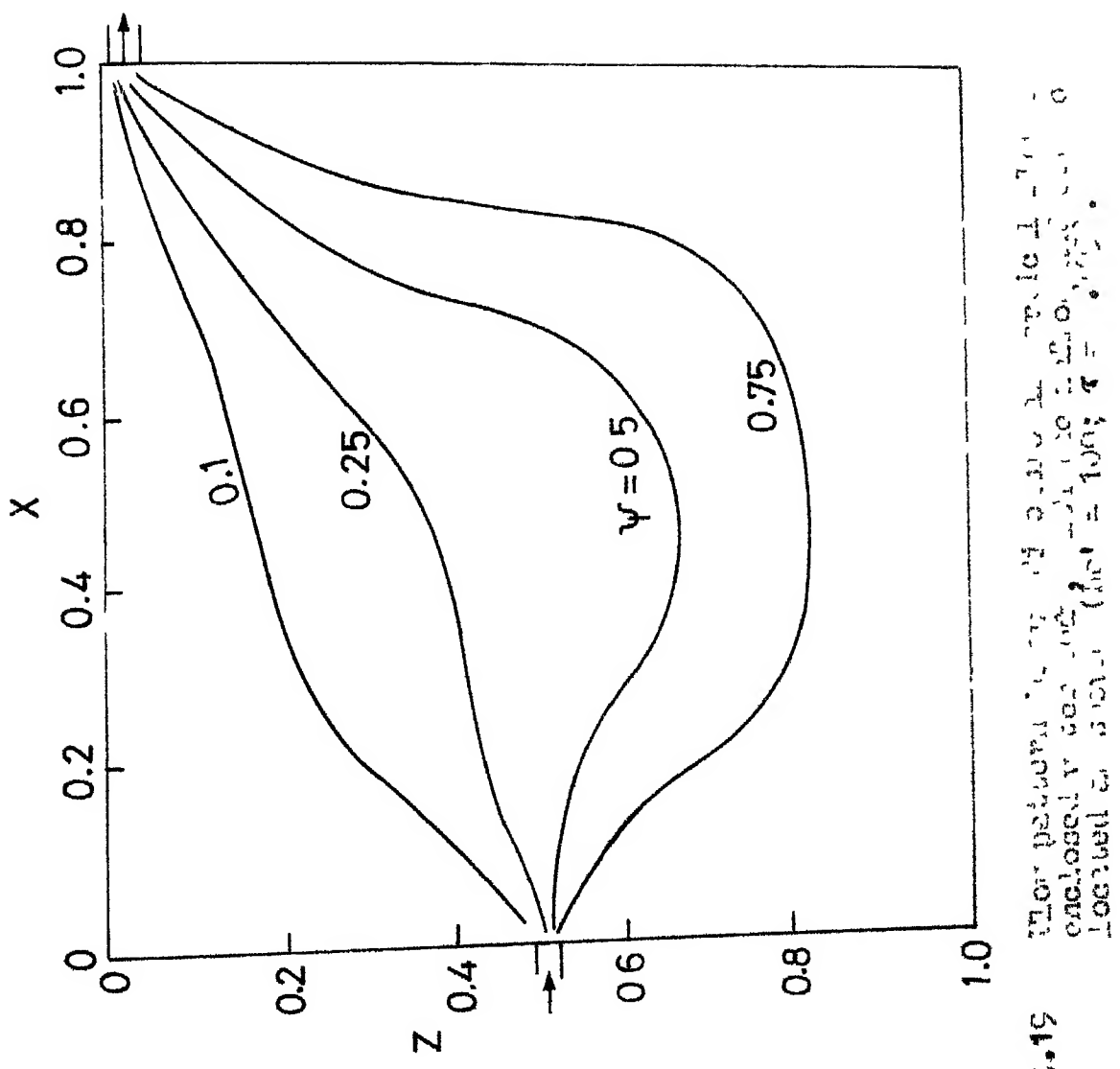
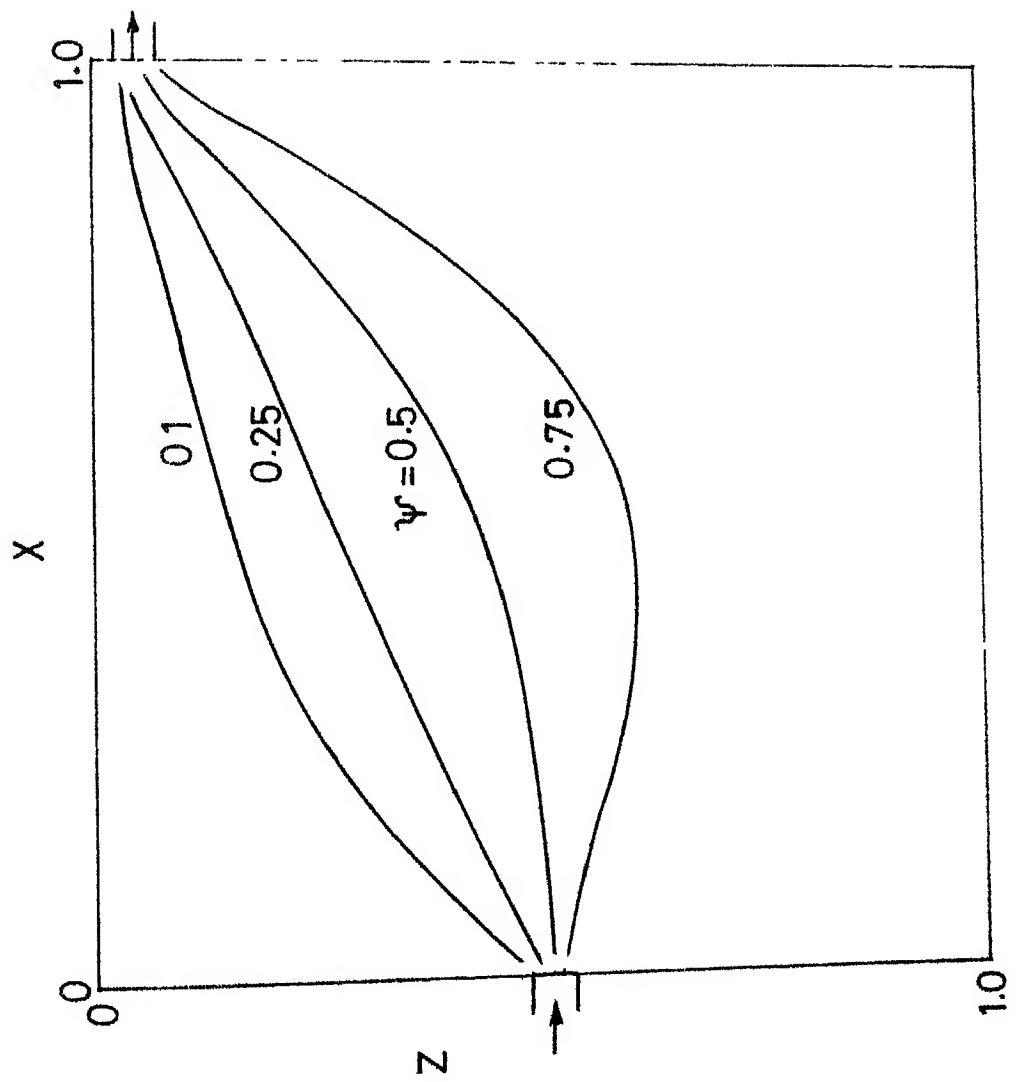
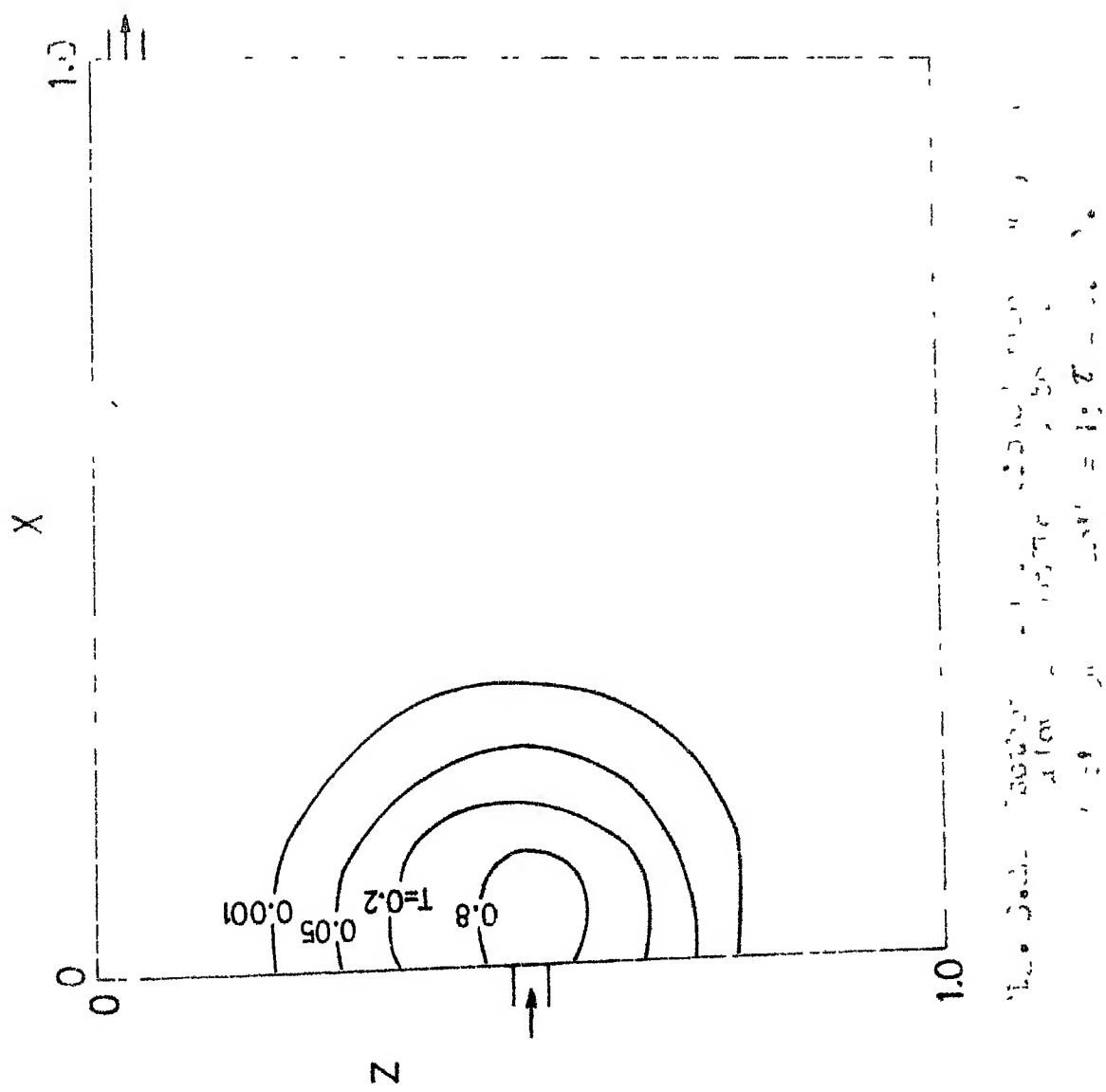


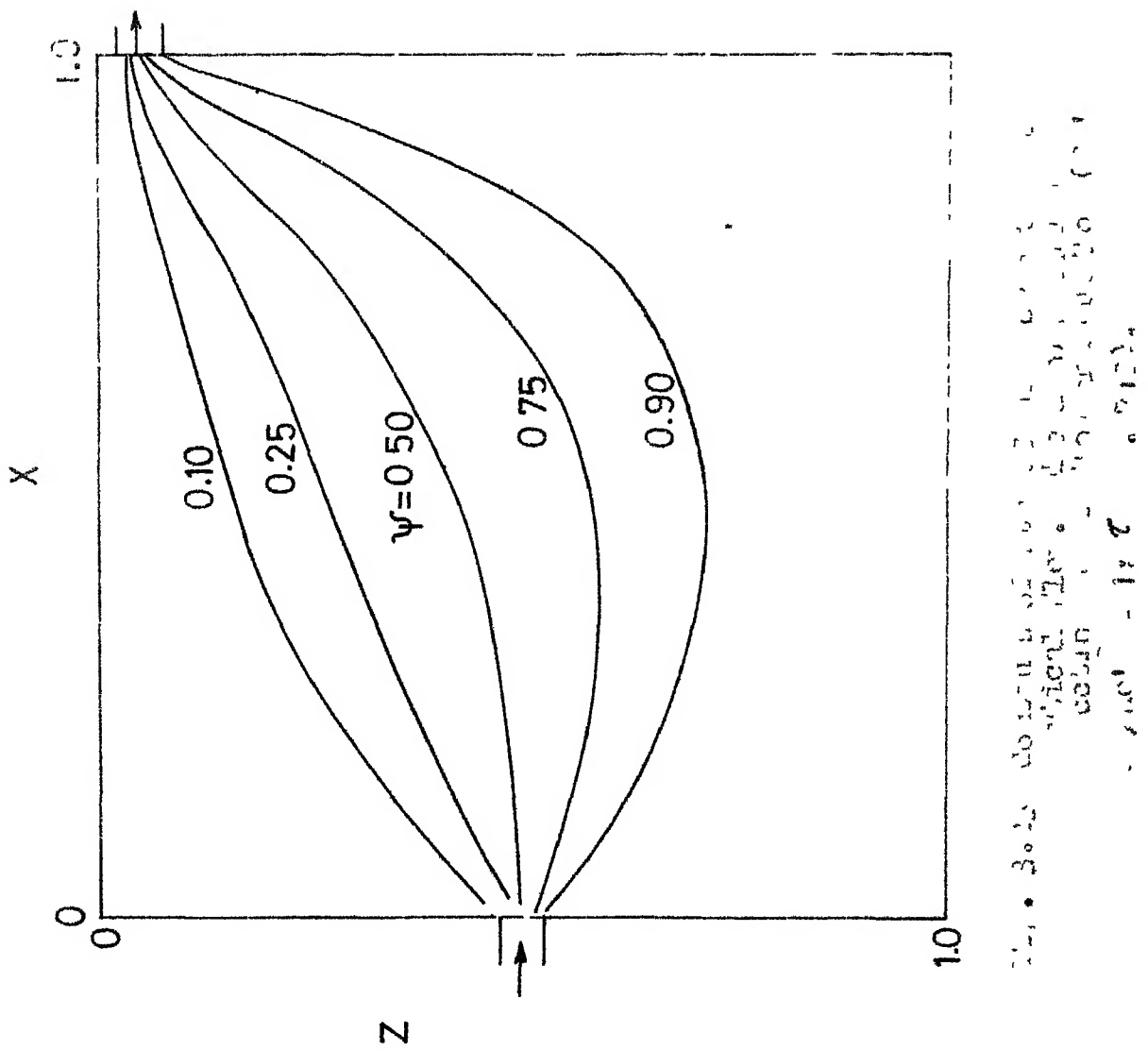
FIG. 3.18 Velocity distribution in die central plane (a) Z plane (b) X plane.

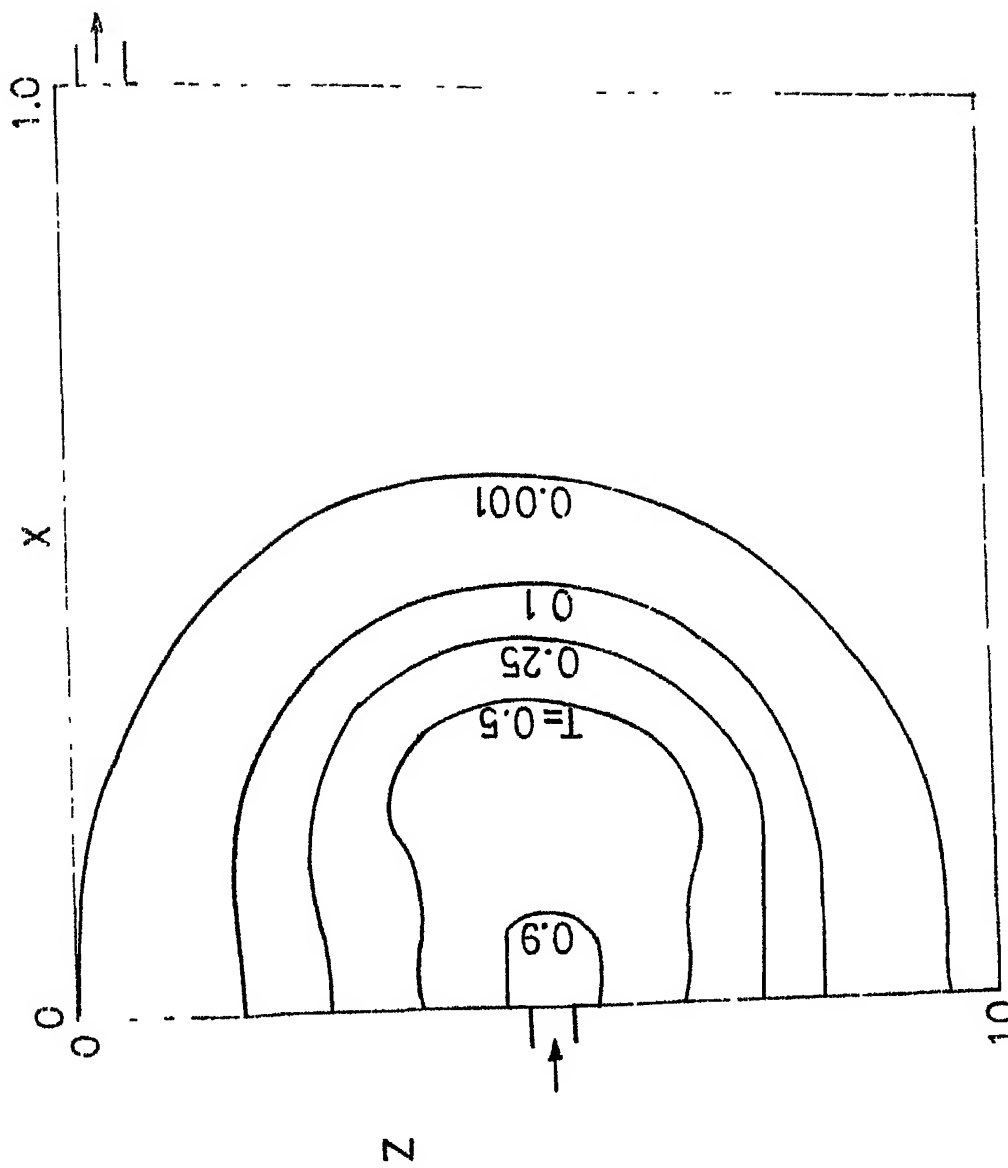


6









62232

26/4/81
8-18/4/81

Date Slip 62232

ie This book is to be returned on the
date last stamped

CD 6729

ME-1977-D-GIUPTRA